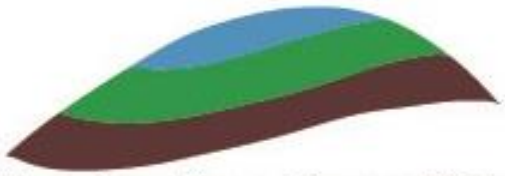

Third Australian Regolith Geoscientists Association Conference

Proceedings

Bunbury, WA
6-7th February 2014

Editor: V.N.L. Wong

Australian Regolith Geoscientists Association

The Australian Regolith Geoscientists Association Inc. (ARGA) is a not-for-profit learned association of regolith practitioners throughout Australia. The Association was set up to to provide a mechanism through which people interested in regolith science could keep in touch and share their experiences via newsletters, email, the internet and an annual conference.

The objects of the association are to further the study of regolith geoscience and allied disciplines by:

a. Facilitating the exchange of information among members of the association, and, in general, all those interested in regolith science;
b. Stimulating interest in regolith geoscience;
c. Encouraging the practical applications of regolith geoscience research.

How to join ARGA

All those having an interest in the objectives of the Association are eligible to become members. All who have attended a Biennial Conference of the Association become members for the next four years. Alternatively, you can join the Society by contacting the Secretary, explaining your interest and paying $1 per year.

ARGA Committee

President: David Gray
Past President: Lisa Worrall
Secretary: Matilda Thomas
Treasurer: John Keeling
Conference Organiser: Vanessa Wong
Student Representative: Stephanie McLennan
Jon Clarke
Nathan Reid
Ian Roach
Anna Petts

Website: http://regolith.org.au

Program

Wednesday 5th February
Joint Field Trip with ACMS

Thursday 6th February			
8.30	**Registration**		
Chair: David Gray			
9.00	David Gray	Welcome and opening	
9.10	Bradley Degens	Keynote: Managing water resources around regolith acidity hazards in southern WA – translating science for management	6
9.45	Alie Cowood	Controls on wetland hydrology in southwest NSW: observations in areas with differing regolith geology	8
10.05	Margaret Sweeney	Characterising the weathering of Jurassic dolerites in areas subject to land salinisation in North-East Tasmania	11
10.30	Leah Moore	Enhancing the hydrogeological landscape (HGL) characterisation of the Greater Launceston area (GLA) through better understanding of dolerite weathering, stream water properties and a revised landscape evolution model	13
10.55	**Morning tea**		
Chair: Matilda Thomas			
11.25	Andreas Scheib	Application of passive seismic to estimate cover thickness in greenfields areas of Western Australia	16
11.50	Matthew Cracknell	Unsupervised clustering of continental-scale geophysical and geochemical data using Self-Organising Maps	20
12.10	Nadir de Souza Kovacs	Regolith-landform distribution and composition on the West Kimberley Plateau: mapping by interpretation of geophysical and remotely sensed data	25
12.35	Alexandra Possingham	Waking up Sleeping data – Development of a geodatabase of historical remote sensing data	29
1.00	**Lunch**		
Chair: Nathan Reid			
2.00	Matilda Thomas	Validating the Australian ASTER geoscience maps using the National Geochemical Survey of Australia surface regolith samples	32
2.25	Thomas Cudahy	Validating the Australian ASTER geoscience maps using the National Geochemical Survey of Australia surface regolith samples	32
2.50	Thomas Cudahy	Validating the Australian ASTER geoscience maps using the National Geochemical Survey of Australia surface regolith samples	32
3.15	**Afternoon Tea**		
3.45	Drinks + ARGA AGM		
6.30 -	Conference Dinner	Noovoh Backbeach Restaurant After dinner speaker: Charles Butt	

Friday 7th February			
Chair: John Keeling			
9.00	Paul Morris	Keynote: Regolith and regolith geochemistry in several dimensions	35
9.35	Stephanie McLennan	The Loxton-Parilla Sands of the Western Murray Basin – From Macro to Micro Scale	39
10.00	David Gray	Hydrogeochemistry and other “aqueous phase” media in exploration	42
10.25	Tony Bernardi	Regolith influences on surface water and groundwater composition at the Baldry dryland salinity management site, central west NSW	46
10.50	**Morning Tea**		
Chair: Vanessa Wong			
11.20	Carmen Krapf	Unravelling the regolith history and landscape evolution of the Eastern Musgrave, South Australia	49
11.45	Dan Clark	Rates of seismogenic landscape change in intraplate Australia	51
12.10	Robert Thorne	Nickel laterites formed from the weathering of Tethyan ophiolites	55
12.35	Matilda Thomas	Unlocking the Southern Thomson’s hidden mineral resource potential	59
1.00	**Lunch**		
Chair: Leah Moore			
2.00	John Keeling	Provenance of zircon in high-zirconium heavy mineral sand deposits of the Eucla Basin, southern Australia	60
2.25	Nathan Reid	Biomineralisation in the sulfur hyperaccumulator *Acacia bivenosa*	63
2.50	Vanessa Wong	Forming an artificial soil from waste materials for mine site rehabilitation	66
3.15	**Afternoon Tea**		
Chair: Lisa Worrall			
3.45	Student Prize Presentation: The Keith Scott Memorial Award		
3.55	Discussion:	Future directions for regolith science	

Saturday 8th February	
7.00	Bus transport to Perth Airport and then Perth CBD. Depart Lord Forrest Hotel

Managing water resources around regolith acidity hazards in southern WA – translating science for management

B.P. Degens

Department of Water, PO Box K822, Perth WA 6892

Understanding of regolith acidity hazards has greatly increased during the last decade largely driven by concern about impacts of acidic water discharge on water quality and aquatic ecosystems. Management of water resources has mostly focused on acidity sources and mobility but is limited by viable options for dealing with regolith hazards at both local and landscape scales.

Two types of regolith acidity are reviewed from the perspective of how investigations of these have been translated for water resource management and the most limiting gaps. This comprises a decade of acidic saline groundwater investigations in the weathered geology of the WA Wheatbelt and acid sulfate soils in upland coastal sedimentary formations.

Acid sulfate soils (ASS) are a widespread acidity hazard in coastal regions of WA where investigations have focused on defining the hazard. Mapping of ASS has been completed at broad scales and has been important in underpinning identification and management of the soils during urban and industrial land development. In groundwater management, ASS information from site investigations is increasingly used as proxy benchmarks for environmental water requirements. However, the extensive coupling between the hazard soils and shallow groundwater systems presents significant challenges for water resource managers in a drying climate.

Mapping and recent investigations of ASS risk indicate that there are extensive areas of low sulfide content, low buffer capacity sands in close proximity to water-tables in WA's groundwater supply areas (Degens & Wallace-Bell 2009; Prakongkep et al. 2012; Singh et al. 2012b). Extensive areas of ASS occur on Gnangara Mound, Perth's main public and private water supply, where water-tables have declined by 1 to >7 m over several decades due declining rainfall, pumping of groundwater and plantations. This decline has clearly triggered oxidation of ASS and generation of acidity, but the extent has been difficult to characterise because of the area involved (over 1000 km^2). Some wetlands have acidified (Sommer & Horwitz 2009) and regional hydrochemical investigations provide an indication of the extent of groundwater acidification influenced by ASS oxidation (e.g. Clohessy et al. 2013) – highlighting a problem covering 100's km^2. Research indicates that oxidation of the sulfide minerals in the sandy formations can be rapid with limited buffering and mitigation processes (Salmon et al. In Press; Singh et al. 2012a). However, the problem is compounded by a lack of viable mitigation and remediation options relevant to the scales at which the problem occurs.

Groundwater managers have been left with little guidance on appropriate management responses apart from restoring historic groundwater levels as soon as practicable. This may take some decades for regional groundwater systems during a time of declining rainfall – if all. An interim regional scale risk assessment may provide a framework for prioritising risk by management areas, but this requires workable management responses when restoring groundwater levels is unachievable.

The second area of regolith acidity concerns discharge of saline acidic groundwater in the WA Wheatbelt. Use of groundwater drains to manage rising saline groundwater in the Wheatbelt has inadvertently revealed an acidity hazard previously unrecognised in salinity management (Degens et al. 2012). Regional surveys identified extensive areas where saline groundwater contained low pH and dissolved metals (Degens & Shand 2010) – including some geochemical anomalies that have since led to discovery of ore bodies. Soil chemical and mineralogical assessments confirmed that conditions similar to those of ASS formed where the acidic groundwater discharged to floodways and lakes (Shand & Degens 2009). The sediments in these environments also contained extremophile organisms with recent bio-prospecting finding species of salt-tolerant microorganisms suitable for sulfide ore bioleaching (McSweeney et al. 2013). Research found acidic sediments had been forming for some time in primary and secondary salinised floodways and lakes (Degens et al. 2010) and that the changes in hydrology with land clearing was also a significant factor driving rejuvenated discharge (Degens et al. 2012). However, it was also recognised that formation of

acidified aquatic environments would be accelerated by unmanaged discharge of acidic waters from groundwater drains (Degens et al. 2012).

Broad understanding of the acidic groundwater issue has focused management on identifying and mitigating acidic drainage discharge (including treatment) to avoid acidification of waterways, rather than preventing drainage of the groundwater. This was possible without full understanding of the origin of the acidity or full understanding of behaviour in semi-arid saline environments. Subsequent work has focused on assessing and adapting practical treatment options (Degens 2009) and criteria for assessing acidic groundwater hazards (Degens 2013). These findings have gradually been integrated into the regulation and management of groundwater drainage and informed assessments of alternative water supplies involving desalination of groundwater.

Greater understanding of acidity hazards has set the foundation for advice on management of risks to water resources, but a common deficiency is practical management options at scales where this is applied. This has arisen partly because of an over focus on defining hazards at the expense of options that would empower managers to take early action. While there are risks with early action, experience shows that these are best mitigated by on-going research while actions are carried out. Solutions that recommend avoiding disturbance of regolith acidity are of little use when acidification has well progressed, occurs at landscape scales and is influenced by changing hydrology.

References

Clohessy S., Appleyard S. and Vogwill R. 2013. Groundwater acidification near the water table of the Superficial aquifer, Gnangara Mound, Swan Coastal Plain, Western Australia. *Applied Geochemistry* **36**, 140-152.

Degens B.P. 2009. *Proposed Guidelines for Treating Acidic Drain Water in the Avon Catchment, Western Australia: Adapting Acid Mine Drainage Treatment Systems for Saline Acidic Drains*. Salinity and Land Use Impacts Series, **Report No. SLUI 54**, Department of Water, Perth.

Degens B.P. 2013. *Acidic water discharge criteria for saline aquatic ecosystems in the WA Wheatbelt – a technical discussion paper*, Salinity and land use impacts series, **Report no. SLUI 65**, Department of Water, 30p.

Degens B.P., Fitzpatrick R.W. and Raven M.D., 2010. Hydric halitic sulfuric soils in secondary salinised landscapes of Southwest Western Australia. *In*: Gilkes R.J., Prakongkep, N. (Eds.). *Proceedings of 19th World Congress of Soil Science – Soil Solutions for a Changing World*. Brisbane, Australia. Working Group 3.1, International Union of, Soil Science, pp 56–59.

Degens B.P., Muirden P.D., Kelly B. and Allen M. (2012). Acidification of salinised waterways by saline groundwater discharge in south-western Australia. *Journal of Hydrology* **470-471**,111-123.

Degens B. & Shand P., 2010. Assessment of Acidic Saline Groundwater Hazard in the Western Australian Wheatbelt: Yarra Yarra, Blackwood and South Coast. CSIRO, Water for a Healthy Country National Research Flagship, Adelaide.

Degens B & Wallace-Bell P 2009. *Acid sulfate soil survey of shallow regolith on the Scott Coastal Plain*, Department of Water, Government of Western Australia, Hydrogeological record series, **Report no. HG24**.

McSweeney NJ, Rea S, Siebert H-M, Collinson DM, Degens B, Gray DJ, Wylie J, Watling HR and Kaksonen AH, 2013. Bioprospecting and adaptation of salt-tolerant bioleaching microorganisms. CSIRO, Minerals Down Under Flagship, Perth. **Report EP1310587.**

Prakongkep N., Gilkes R.J., Singh B. and Wong S. 2012. Pyrite and other sulphur minerals in giant aquic spodosols, Western Australia. *Geoderma* **181(182)**, 78–90.

Salmon S.U., Rate A.W., Rengel Z., Appleyard S., Prommer, H. and Hinz, C. In Press. Reactive transport controls on sandy acid sulphate soils and impacts on shallow groundwater quality. *Water Resources Research*.

Singh B., Pal Y. and Wong S. 2012a. *Experimental oxidation of Bassendean sands in soil columns.* Department of Environment and Conservation, Government of Western Australia.

Singh B., Pal Y., Clohessy S., & Wong S. 2012b. *Acid Sulfate Soil Survey in Perth Metropolitan Region, Swan Coastal Plain WA.* Department of Environment and Conservation, Government of Western Australia.

Sommer B. & Horwitz P 2009. Macroinvertebrate cycles of decline and recovery in Swan Coastal Plain (Western Australia) wetlands affected by drought-induced acidification. *Hydrobiologia* **624**,191–203.

Controls on wetland hydrology in southwest NSW: observations in areas with differing regolith geology

Alie Cowood and Leah Moore

Dryland Salinity Hazard Mitigation Program (DSHMP), University of Canberra, ACT 2601

Upland freshwater wetlands are formed in low points and depressions in the landscape that allow surface water to accumulate and/or groundwater to emerge. Wetlands have a major role in the ecosystem as they: support a broad range of aquatic and terrestrial biota, provide drought refuge; and, provide a range of variably quantifiable ecosystem services (Chen & Lu 2003; Zedler 2000; Mitsch & Gosselink 2000). Because of their significance and complexity, it is useful to understand and model wetlands based on their landscape setting (Zedler 2000), but the hydrogeological mechanisms allowing water to accumulate in wetlands in particular parts of the landscape is not well understood. Conceptual models for fluid flow and mobilization of solutes in a range of landscapes across the southern tablelands of NSW (NSW ST) (Figure 1) have been developed as part of a Hydrogeological Landscape (HGL) analysis (Wilford *et al.* 2010; Jenkins *et al.* 2010; Cowood 2013).

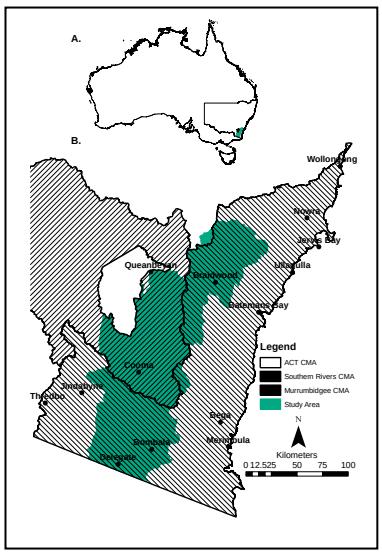

Figure 1. A. Location of the study area in relation to NSW and the ACT, Australia. B. Extent of the study area within the Southern Rivers, Murrumbidgee and Australian Capital Territory Catchment Management Authority regions

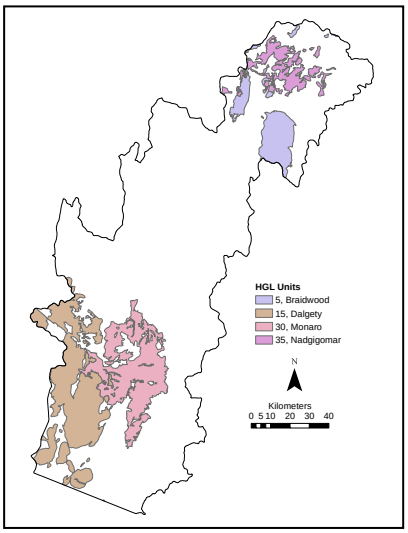

Figure 2. The four HGLs chosen for the detailed assessment within the Southern Tablelands study area: Northern: Braidwood and Nadgigomar.; Southern: Monaro and Dalgety

The premise is that the HGL framework could provide the basis for a regionalised hydrological wetland classification similar to those suggested in international studies (Winter 1992; 2001; Brinson 1993; Semeniuk and Semeniuk 1995; 1997), with HGL units utilised as representations of geomorphic setting. The HGL units that will be studied in detail include northern units (Braidwood and Nadgigomar in the Shoalhaven area (Figure 3) and southern units (Monaro and Dalgety) in the Monaro area (Figure 4).

The Braidwood and Dalgety HGL units are developed over jointed and faulted Siluro-Devonian granitic rocks, but regolith materials are distributed differently (contrasting regolith thickness) within areas and between the two areas, and hence the proposed fluid flow pathways and hydrogeological setting for wetlands are different. The Monaro HGL unit is developed over Paleogene basaltic volcanic rocks dominated by a layered lava flow sequence with discontinuous duricrusts and paleosols preserved between flow units. Wetlands in this area form as a result of the emergence of water at breaks in slope, in areas of permeability contrast and as ephemeral features

on low relief surfaces. The Nadgigomar HGL is developed on a Cainozoic paleo-Shaolhaven River alluvial sequence, with alternating sands and gravels and localized bedding-parallel (Fe/Si) duricrust formation. Wetlands in this setting are typically formed due to perching on impermeable layers, or as ephemeral surface systems.

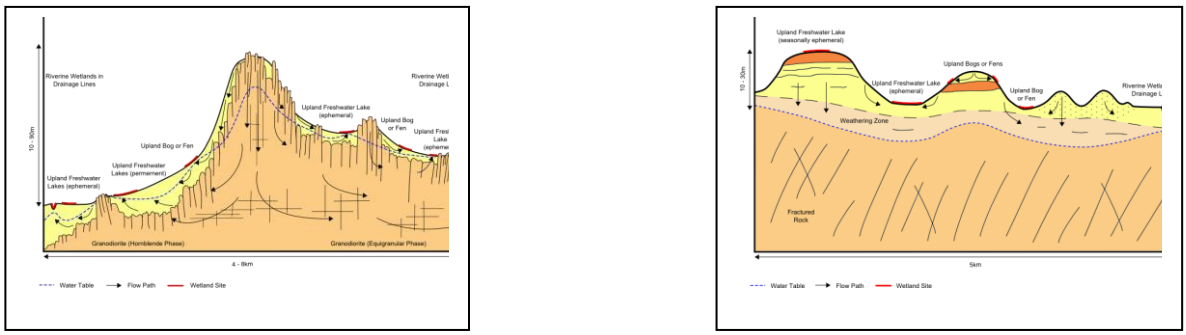

Figure 3. Conceptual model of the Braidwood HGL developed on Siluro-Devonian granitic rocks, and the Nadgigomar HGL developed on Cainozoic alluvial sediments, in the Shoalhaven area, south west NSW.

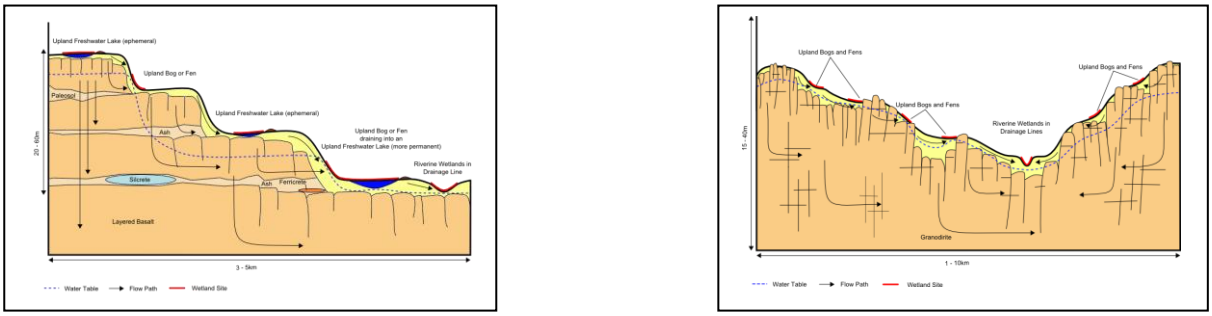

Figure 4. Conceptual model of the Monaro HGL developed on Paleogene basaltic volcanic rocks (lavas), and the Dalgety HGL developed on Siluro-Devonian granitic rocks, in the Monaro area, south west NSW.

The preliminary findings of a biophysical analysis (e.g. geology, soils, vegetation, geomorphology, regolith thickness, meterological data) in selected regions of the NSW ST (Figure 2) are reported here. This work is designed to field-proof the HGL conceptual models that have already been developed. This ensures that the hydrogeological framework can be confidently used to contextualize wetland setting. Using the HGL framework in this manner will ultimately allow scenario-based interpretation of the impacts of likely local climate and land use change with respect to wetlands (Carpenter *et al.* 1992). In addition, characterisation of the geology and regolith materials (including soils) will provide essential data for a wetland water budget analysis that will be conducted from 2014.

Preliminary soil descriptions (e.g. Munsell colour, mottles, soil texture, presence of gravel, soil structure (ped formation), soil fabric, consistence, Fe/Mn nodules, organic material, $CaCO_3$, soil pH as per McDonald *et al.* 1998) have been compiled for the Shoalhaven area as part of the initial phase of this study. Although there is slightly higher rainfall in the Braidwood area than the Nadgigomar area, this difference is not significant (800-900mm). Land use in both areas is grazing of cattle and sheep on modified and native grass cover. Over the 2013/2014 sampling season the wetlands on the Braidwood HGL were full, but the Nadgigomar wetlands were dry. Although sandy

soils occur on both HGL's, in general the Braidwood Back Creek site has higher soil clay content and sub-cropping granite is present in the shallow subsurface. The Nadgigomar site has sandier soils, and wetlands form in localised areas as perched system, each with a relatively small catchment area. Wetlands in the Braidwood HGL area are more persistent than in the contrasting hydrogeological setting to the north. Biophysical observations allow refinement of the HGL models and development for explanations regarding the location and sensitivity of wetlands on the basis of their hydrogeological setting.

References

Carpenter, S.R., Fisher S.G., Grimm, N.B., and Kitchell. J.F. (1992) Global change and freshwater ecosystems. Annual Review *Ecol. Syste.* 1992. 23: 119-139.

Chen, Y., and Lu, X. (2003) The wetland function and research tendency of wetland science. *Wetland Science* 2003-01.

Cowood, A. (unpublished) Wetland conservation in the face of climate change integration of wetlands into the hydrogeological landscapes of the southern tablelands.

DeBano, L.F. (1971) The Effect of Hydrophobic Substances on Water Movement in Soil during Infiltration. *Soil Science Society of America Journal* Vol. 35 No. 2, p. 340-343.

Faulkner, S.P., and Richardson, C.J. (1989) Physical and Chemical Characteristics of Freshwater wetland soils. Chapter 4 of *Constructed Wetlands for Wastewater Treatment: Municipal, Industrial and Agricultural.* Florida: Lewis Publishers.

Jenkins, B., Nicholson, A., Wooldridge, A., Moore, L., Harvey, K., Nowakowski, A., and Cook, W. (2010) Hydrogeological landscapes – an expert system for salinity management. 2010 19th World Congress of Soil Science, *Soil Solutions for a Changing World* 1 – 6 August 2010, Brisbane, Australia

McDonald, R.C., Isbell, R.F., Speight, J.G., Walker, J., and Hopkins, M.S. (1998) *Australian Soil and Land Survey Field Handbook Second Edition*. Department of Primary Industries and Energy and CSIRO Australia.

Mitsch, W.J. & Gosselink, J.G. (2000) The value of wetlands: importance of scale and landscape setting. *Ecological Economics* 35 (200), p. 25-33.

CSIRO Division of Soils (1966) *The soils of Australia.* Year Book Australia No. 52 1966. Australian Bureau of Statistics.

Wilford, J., Nicholson, A., and Summerell, G., (2010) Hydrogeological-Landscapes system: a framework for managing water resources. *AusGeo News* March 2010 Issue No. 97.

Zedler, J.B. (2000) Progress in wetland restoration ecology. *Tree* vol. 15, No. 10 October 2000.

Characterising the weathering of Jurassic dolerites in areas subject to land salinisation in North-East Tasmania.

Margaret Sweeney[1] and Leah Moore[2]

[1]Dryland Salinity Hazard Mitigation Program, Institute for Applied Ecology, University of Canberra
Margi.Sweeney@canberra.edu.au
[2]Dryland Salinity Hazard Mitigation Program, Institute for Applied Ecology, University of Canberra
Leah.Moore@canberra.edu.au

Salt occurs naturally in Australian landscapes. Some salts are the result of rock weathering or are derived from marine sediments or wind-blown dust but in Tasmania most originate from salt dissolved in rainfall that is concentrated during evaporation. The volume of salts deposited over North-east Tasmania from precipitation exceeds 85 kg/ha/year (Dell 2000, Kidd 2003). Over thousands of years, salt can accumulate in regolith and groundwater. The concentration of salts in the landscape is not evenly distributed and salinity tends to occur in drier and flatter parts of Tasmania because there is not sufficient rain to flush the salts out of the landscape. Although salinity occurs naturally, changes in land use and vegetation due to agriculture, forestry practices and urbanisation can accelerate salinity effects leading to land degradation and potentially threatening built and natural assets.

The dominant lithology of the salt affected regions in Tasmania is dolerite with some paleo-lacustrine and estuarine sedimentary rocks. The weathering of Tasmanian dolerites, sampled from fresh corestones, weathering rinds and sequentially through the soil horizon, at two locations (Woodbury Quarry and Breadalbane, Figure 1), has been examined petrographically and geochemically. Dolerite breaks down to form secondary minerals including smectite and kaolinite clays and Fe-bearing sesquioxides. Bicarbonate fluids are typically associated with dolerite weathering.

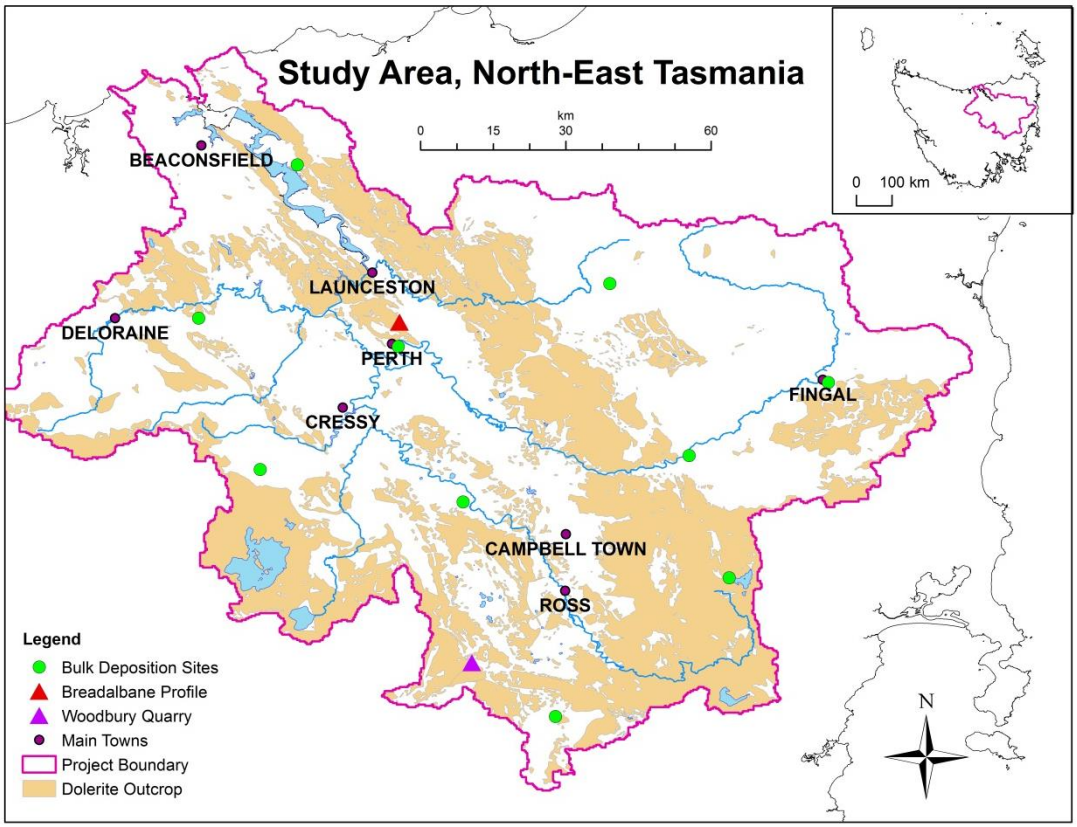

Figure 1: Location map of the study area indicating regolith profile locations (Breadalbane and Woodbury Quarry), extent of dolerite (Mineral Resources Tasmania 2011) and location of bulk deposition collector sites. The study area was selected to be all of the catchments where surface waters eventually flow into the Tamar Estuary, which encompasses the majority of the northern *National Action Plan for Salinity and Water Quality 'priority area'* (National Land and Water Resources Audit 2000) and most of the severely salinized land in Tasmania (Bastick and Lynch 2003).

In the Breadalbane regolith profile, the $EC_{1:5}$ increases with weathering to a maximum 4.9 dS/m and then decreases in the pedogenic zone. This confirms field observations that deeply weathered dolerite can serve as a significant store for salt in the landscape. The $pH_{1:5}$ decreases as the samples weather and increases in the pedogenic zone. Clay content increases with distance from fresh corestones in both profiles (sandy clay loam to heavy clay), and this is also reflected in the density (2.6-1.3 gm/cm^3) and loss on ignition (1.3-13.3 wt%). The patterns for Na are complicated as it is enriched through NaCl accession and removed during the weathering of plagioclase. The net enrichment of Cl (up to 5239 ppm) implies decoupling of Cl from Na during weathering. Potassium, Ca and Sr are mobilised from the profile as plagioclase weathers, and silica is progressively lost from the profile with the weathering of silicate phases. Iron is initially mobilised with the weathering of pyroxene and mafic accessory minerals, but is then fixed in the weathering profile as Fe-oxides (hematite, goethite) in veinlets and in association with secondary clays. Pedogenic processes mobilise iron near the land surface. Elements including Nb, Zr and Ti partition in resistant accessory phases like zircon and remain immobile during weathering. Ongoing X-Ray diffraction and microprobe analysis will further characterise the regolith materials that comprise the salt stores in the landscape.

Water sampling and analysis is necessary to monitor which ions present in the landscape are derived from the regolith materials and determine the species and likely source of other ions (e.g. sourced from salt accession). Studies of the flux of oceanic aerosols in Australia indicate that salt derived from the sea can be deposited several hundred kilometres from the coast, (Keywood et al. 1997, Cresswell 2005, Biggs 2006, Guan et al. 2010). In North-east Tasmania there is little information on the source, or spatial and seasonal variation of salt in precipitation. Furthermore, the continental-scale ion accession models cannot easily be adapted for Tasmania, as not only is the state more mountainous, but the rains come from several directions. Analysis of rainwater chemistry, (from an array of bulk deposition collectors) to determine the patterns and volumes of salt deposition from atmospheric aerosols, will allow more accurate quantification of the salt flux in North-east Tasmania.

By exploring the complex interactions of biophysical parameters such as rainfall, soil, geology, vegetation and hydrology, the study area can be divided into Hydrogeological Landscape (HGL) units (Moore et al. 2012). Preparation of a HGL characterisation for the study area and development of a landscape evolution model will provide an understanding of how regolith materials are distributed in the landscape, how and where salt is stored and how water moves through or over the materials. Linking this information with the regional structural geology and geomorphology will allow evaluation of how and why salt manifests in certain parts of the landscape. Fluid movement is intimately associated with structures in basement rocks, so understanding the extent and location of faults, the shape of the dolerite sills, and the jointing patterns in the dolerite (the underlying plumbing) will contribute insight into salt mobility. This multi-disciplinary analysis will provide a framework to assist natural resource managers to identify management priorities in North-east Tasmania and in other dolerite (or basalt) dominated landscapes.

References

BASTICK C. & LYNCH S. 2003 Extent and Impacts of Dryland Salinity in Tasmania.: Department of Primary Industries, Water and Environment, Tasmania.

BIGGS A. J. W. 2006 Rainfall salt accessions in the Queensland Murray–Darling Basin, *Soil Research,* vol. 44, no. 6, pp. 637-645.

CRESSWELL R. G. 2005 Chloride dynamics across Australia, *Geophysical Research Abstracts,* vol. 7, no. 02199.

DELL M. 2000 Hydrogeological setting for areas subject to soil salinity in Tasmania. . Tasmanian Geological Survey Record

GUAN H.*, et al.* 2010 Factors influencing chloride deposition in a coastal hilly area and application to chloride deposition mapping, *Hydrology and Earth System Sciences,* vol. 14, no. 5, p. 801.

KEYWOOD M. D.*, et al.* 1997 The accession of chloride to the western half of the Australian continent, *Australian Journal of Soil Research,* vol. 35, no. 5, pp. 1177-1189.

KIDD D. B. 2003 Land Degradation and Salinity Risk Investigation in the Tunbridge District, Tasmanian Midlands. Tasmania, Australia.: Department of Primary Industries, Water and Environment.

MINERAL RESOURCES TASMANIA 2011 Digital Geological Atlas 1:250,000 Scale Series. Digital Geology Data. Mineral Resources Tasmania.

MOORE C. L.*, et al.* 2012 Controls on salt storage and urban/peri-urban land salinisation in the Greater Launceston Area: Preliminary hydrogeological landscape characterization. Soils Solutions for Diverse Landscapes: Soils and Land Degradation. Proceedings of the Joint Soil Science Australia (SSA) and the New Zealand Society of Soil Science (NZSSS) Conference. Hobart.

NATIONAL LAND AND WATER RESOURCES AUDIT 2000 Australian Dryland Salinity Assessment 2000. Extent, impacts, processes, monitoring and management options. Canberra: National Heritage Trust. Commonwealth of Australia.

Enhancing the hydrogeological landscape (HGL) characterisation of the Greater Launceston area (GLA) through better understanding of dolerite weathering, stream water properties and a revised landscape evolution model.

[1]Leah Moore, [2]Allan Nicholson, [3]Wayne Cook and [1]Margaret Sweeney

[1]Dryland Salinity Hazard Mitigation Program, University of Canberra, ACT 2601
[2]NSW Office of Environment and Heritage, P.O. Box 123, Wellington, NSW 2820
[3]NSW Department of Primary Industries, P.O. Box 733, Queanbeyan, NSW 2620

In the Greater Launceston Area (GLA) in northern Tasmania there is a widespread urban salinity problem, with severe impacts to urban/peri-urban infrastructure in localised parts of the landscape (Figure 1). Earlier studies (Moore et al. 2013) revealed that salinity patterns in the landscape (elevated flux to waterways; salt efflourescence at the land surface; Figure 2) could be related to: the underlying rock type, the thickness of regolith materials and hence the volume of the salt store, the landforms present and the amount of water passing over and through the landscape. More specifically, salinisation in the GLA typically impacts localised areas on: deeply weathered Jurassic dolerite (Figure 3); moderately to deeply weathered bedded paleo-estuarine sediments of the Paleogene Tamar/Esk River system (Figure 4); some Quaternary terrace deposits along the Tamar and Esk Rivers; and some Holocene estuarine sediments (Moore et al. 2013).

This research is significant because salinity damage in the GLA includes: etching and rotting of brickwork; 'rising damp' in masonry walls; fracturing and flaking of pavements and roads; salt efflorescence as a 'tide mark' on some brick and concrete walls; blistering of paintwork; formation of scalds in grassy areas; presence of salt tolerant species in water courses; and, acid and saline chemistries in some natural waters (Figure 2). This salinity hazard constitutes a major economic and planning consideration for local land holders and councils.

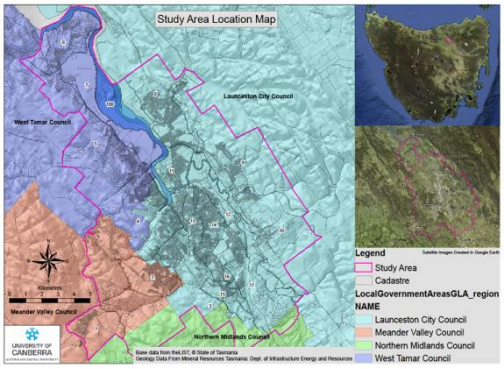

Figure 1. Location of the Greater Launceston Area (GLA) study in northern Tasmania

Figure 2. Etching of brickwork due to salt damage and salt efflorescence in the Hadspen HGL area, northern Tasmania

This paper details information compiled as a result of three recent studies: characterisation of northern Tasmania Jurassic dolerite weathering (Sweeney et al. 2014 this volume), monthly rapid stream surveys across the GLA, and a comprehensive study of Tamar Valley geomorphology as part of a landslide susceptibility mapping initiative conducted by Mineral Resources Tasmania (MRT)(Mazengarb et al. 2014).

Commonly assumptions made about dolerite weathering in Tasmania are based on studies from elsewhere, and from studies of basalt weathering (e.g. Eggleton 1987, Moore 1996). In northern Tasmania a targeted study of dolerite weathering is being conducted in part due to recognition that deeply weathered profiles on Jurassic dolerite are more widespread that previously mapped, and that regolith materials developed over this substrate have the capacity to store salt adsorbed onto and within the structure of secondary phases as well as in pore spaces (Sweeney et al. 2014 this

volume). Secondary mineralogy on dolerite typically includes formation of Fe/Ca smectite phases (e.g. nontronite, saponite) and Fe-Ti oxides/sesquioxides (e.g. hematite, goethite) with some primary phases (e.g. Ca-plagioclase feldspar, augite) weathering through to a suite dominated by kaolinite clay and Fe-Ti oxides/sesquioxides. Deeply weathered profiles in the GLA have weathered to the kaolinite-clay dominant mineralogy and in places there are gibbsite/beidellite/hematite/goethite bauxites developed. In the GLA most existing salinity mapping emphasised salt manifestation over paleo-estuarine sediments of the Paleogene Tamar/Esk River system, so incorporation of deeply weathered Jurassic dolerite materials into the salt budget considerably augments the estimated potential hazard.

Figure 3. An example of Jurassic dolerite with a thick regolith profile. The dolerite has been weathered along joints to form spheroidal corestones in a clay-rich matrix. These regolith materials are increasingly recognised as one of the major salt stores in the GLA

Figure 4. Deeply weathered Paleogene paleo-estuarine and paleo-lacustrine sediments showing secondary weathering features including formation of ferruginised layers (ironstone). These regolith materials have been recognised as one of the major salt stores in the GLA

Rapid stream surveys provide a snapshot of stream electrical conductivity (EC) over the whole study area at regular intervals (monthly) allowing a broad evaluation of salt flux patterns in surfaces waters. Higher EC readings were obtained from selected streams: in the West Riverside area (1.11 to 1.86 dS/m), Alanvale area (0.40 to 0.55 dS/m), and elevated parts of the Ravenswood area (0.37 to 0.49 dS/m), draining deeply weathered dolerite profiles; the Prospect Vale area (0.49 dS/m), on a naturally partially-dammed system overlying deeply weathered Paleogene paleo-estuarine sediments; and the East Launceston (0.51 to 0.67 dS/m), Norwood (0.66 to 0.82 dS/m) West Kings Meadow (1.16 dS/m) and Legana areas (0.52 dS/m), overlying deeply weathered Paleogene paleo-estuarine sediments. Lower values were measured in the Trevallyn area (0.0 to 0.10 dS/m) an up-faulted dolerite block with thinner regolith cover, the Saint Leonards area (0.02 to 0.03 dS/m) moderately weathered, higher relief dolerite, and the lower parts of the Ravenswood area (0.02 to 0.03 dS/m) in incised streams flowing over a rocky dolerite substrate. The patterns of stream EC reflect the nature of the regolith materials the streams drain, and match mapped patterns for distribution of deeply weathered Jurassic dolerite and moderately to deeply weathered bedded paleo-estuarine sediments of the Paleogene Tamar/Esk River system.

Preparation of a series of landslide susceptibility maps in the Tamar region included detailed mapping of geomorphic features of this landscape (Mazengarb et al. 2014). This mapping is a significant recent compilation of observed geomorphic information enabling development of a more comprehensive and consistent landscape evolution model that builds on existing knowledge. This model describes the influence of a progressively incising river system (North Esk, South Esk and Tamar rivers) in response to episodic lowering of the local base level, with multiple episodes of valley widening as the river system stabilised after incision. Successive lowering events dissected earlier landforms, but locally remnant surfaces are preserved that represent former fluvial plain and terrace features. These processes were partially controlled by the structural configuration and contrasting resistance of the underlying lithologies, influencing the planform geometries of the rivers through time, and consequently the potential to preserve paleo-fluvial features. Because the Tamar River is an estuarine system, some of the lowermost preserved surfaces are likely to reflect marine processes (e.g. surfaces at 5-7m and 10-12m above sea level). Although this mapping was

conducted independently of the hydrogeological landscape (HGL) characterisation research in the GLA, the areas identified as having elevated salinity hazard typically correlate well with newly mapped remnant surfaces in this landscape.

Gaining a more comprehensive understanding of northern Tasmanian Jurassic dolerite weathering processes, stream EC patterns across the study area, and the landscape evolution history in the Tamar allows development of an increasingly rigorous evidence-based management framework to enable key stakeholders to identify relative salinity hazard and risk, and to prioritise works appropriately.

References

Eggleton R.A.C., Foudoulis C. Varkevisser D. 1987. The weathering of basalt: changes in bulk chemistry and mineralogy. Clays and Clay Mineralogy, v35, p161-169.

Moore L. 1996 Processes of chemical weathering of selected Cainozoic eastern Australian basalts. Unpublished thesis, Australian National University, pp 352.

Moore L., Sweeney M, Nicholson A. and Cook W. 2012. Controls on salt storage and urban/peri-urban land salinisation in the Greater Launceston Area: Preliminary hydrogeological landscape characterisation. Soil Solutions for Diverse Landscapes. Soil Science Australia – New Zealand Soils Science Society, Hobart: Tasmania

Stevenson M.D. and Mazengarb C. 2013. Windermere Map 2 – Geomorphology. Tasmanian Landslide Map Series. Mineral Resources Tasmania, Department of Infrastructure, Energy and Resources, Hobart:TasmaniaSweeney M. & Moore L. 2014. Characterising the weathering of Jurassic dolerites in areas subject to land salinity in North-East Tasmania. Australian Regolith Geoscientists Association Conference 2014, Bunbury:Australia.

Application of passive seismic to estimate cover thickness in greenfields areas of Western Australia

A.J Scheib and P.M. Morris

Geological Survey of Western Australia, 100 Plain Street, East Perth WA 6004

Introduction

The decline in exploration success is in large part due to the difficulty of exploring beneath the regolith and sedimentary basins that cover some 80% of the Australian landmass. Future exploration will need to expand into greenfields areas, but it is hampered by the extent of regolith and sedimentary cover. In these areas knowing the thickness of cover is essential to explore effectively. Depth information from drilling is often sparsely distributed, non-existent, or in the case of deep regional seismic, imprecise. Passive seismic offers an alternative. Passive seismic method is a rapid, low-cost, and non-invasive technique that has been successfully applied to estimate the thickness of sedimentary cover in North America (Lane *et al*. 2008), Spain (Delgado *et al*. 2000), and Germany (Parolai *et al*. 2002; Ibs-von Seht & Wohlenberg 1999). The Geological Survey of Western Australia recently acquired the passive seismic system Tromino® (Figure 1a, e) to test its suitability to estimate cover thicknesses in greenfields areas of Western Australia. Results and interpretations from two trial surveys in the Gunbarrel and the eastern Eucla Basins (Figure 2a) are presented below.

The passive seismic methodology

Passive seismic does not require a controlled seismic source and records the ambient noise (or vibration) caused by wind, waves, and distant anthropogenic activities which are present in the subsurface commonly at low frequencies <10 Hz. The Tromino® (Figure 1a) is a broad-band seismometer that is attached to the ground using three ~6 cm long spikes. It was set to record two horizontal (E-W, N-S) and the vertical spectral components of the ambient noise over 20 min and up to 128 Hz (Figure 2a). For the analysis, the system applies the H/V method, also referred to as the Nakamura technique (Nakamura 1989), which calculates the spectral ratio of the averaged horizontal (H) to vertical (V) components to determine the site resonance frequency (fz) of the subsurface (Figure 4b). A peak in the resulting H/V spectrum (Figure 2b) indicates an acoustic impedance caused by, for example, a change in rock type. In a simple two-layer model (Figure 2c) this acoustic impedance relates to the boundary between the regolith cover and basement.

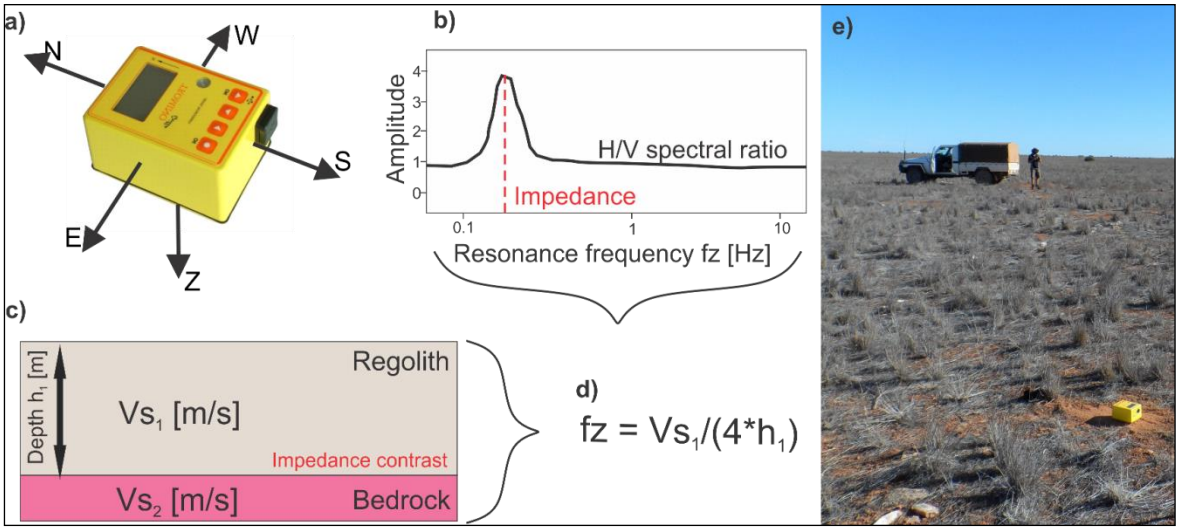

Figure 1 Schematic diagram of the acquisition and analysis of passive seismic data; a) the Tromino®, a three-component, broadband seismometer; b) a simplified horizontal to vertical (H/V) spectral ratio plot calculated for each acquisition; a peak indicates an impedance at depth and corresponds to a certain resonance frequency (fz); c) cartoon of a simple two layer regolith-bedrock system with an impedance at depth h_1; d) equation relating the resonance frequency (fz) to the shear-wave velocity (Vs_1) and depth (h_1) of the impedance; e) photo of site MAD002 near Haig, Eucla Basin.

The resonance frequency derived from a peak in the spectrum is related to two parameters of the layer above the impedance: the thickness (h) and the shear-wave velocity (Vs). The relationship between these two parameters is expressed by the equation shown in Figure 1d and forms the backbone of the analysis of the H/V spectra. It is essential to know either the thickness or shear-wave velocity of the site in order to interpret the results. In this study, this is achieved by deriving shear-wave velocity values at drill holes where the thickness of regolith or sedimentary cover is known. The resulting value can then be applied to the remaining H/V data assuming a uniform stratigraphy across the area.

Study areas

Two passive seismic surveys were carried out across the Eucla and Gunbarrel Basins (Figure 2a). Both of these basins have a thick cover of regolith and sedimentary rock over crystalline basement. In the Eucla Basin, a total of 35 measurements were taken at intervals of approximately 10 km within a corridor along the Transline between Haig and Forrest (Figure 2b). Here, the thickness of Phanerozoic sedimentary cover over crystalline basement varies between 200 and 400 m, with a general decrease in thickness to the north. The sedimentary succession comprises variably consolidated sedimentary rocks of Permain to Eocene age. Regolith in the Eucla Basin is largely non-existent, with only a thin veneer of soil covering the Nullarbor limestone.
At Mulga Rock in the Gunbarrel Basin, a total of 89 measurements are located along one main and two smaller SE-NW trending traverses at an average spacing of 1 km (Figure 2c). The main traverse corresponds to the PNC Baseline that crosses the Gunbarrel Basin and covers the margin of the southeast Yilgarn Craton and east Albany-Fraser Orogen. The area is dominated by several metres of sandplain which in turn covers Cenozoic sediments that can be up to 100 m thick. The Gunbarrel Basin is characterized by a deep trough filled with predominantly Permian glacigenic sedimentary rocks that can reach thicknesses in excess of 600 m.

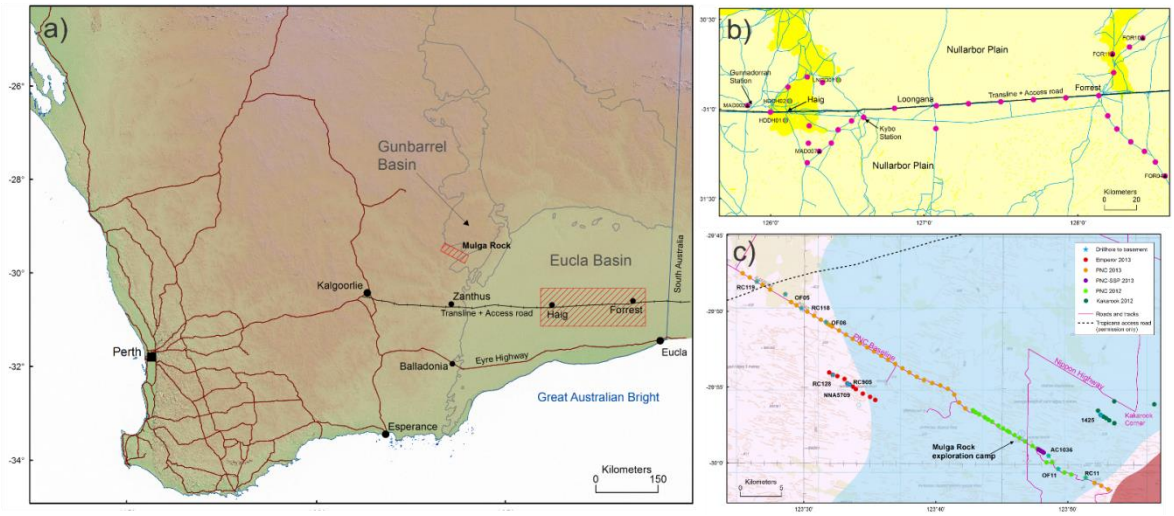

Figure 2 a) Map of southern Western Australia showing the two study areas in the Gunbarrel Basin (at Mulga Rock) and the Eucla Basin; b) locations of 35 passive seismic acquisition sites in the Eucla Basin between Haig and Forrest; black triangles indicate recent GSWA drill sites and green diamonds are sites of existing deep drill holes that reached crystalline basement; light yellow indicates exposed limestone and darker yellow thin sandplain deposits; c) Locations of 89 passive seismic acquisition sites across the southern Gunbarrel Basin, green and orange dots correspond to the PNC Baseline, red dots to the Emperor traverse and dark green dots to Kakarook Corner; blue stars indicate locations where drill holes reached crystalline basement; light blue area indicates the extent of Permian sedimentary rocks of the Gunbarrel Basin.

Results

Figures 3a-c and 4a-b display a selection of H/V spectra acquired at sites in the Gunbarrel and Eucla Basin, respectively. Across both areas most acquisitions have distinct peaks of ratio amplitudes >2 indicating an impedance at depth. The peak location along the x-axis in the H/V spectrum provides the site resonance frequency (fz) for the subsurface above the impedance. These are shown in Figures 3d and 4c in cross section. To convert the resonance frequency values into a depth to the impedance, the shear-wave velocity (Vs) is essential, which can be derived from resonance frequency values at sites where depth data, in particular to basement, is known. The

shear wave velocity can then be applied to passive seismic data from neighbouring acquisition sites to derive depth estimates.
Along the PNC Baseline and Emperor traverse, the derived shear-wave velocity values vary from 410 to 590 m/s for sites beyond the Gunbarrel Basin and with resonance frequency values >1.2 Hz. Sites directly over the Gunbarrel Basin correspond to resonance frequencies from 0.4 to 1.2 Hz and have an increased shear-wave velocity value of 1240 m/s. As no drill hole within the Gunbarrel Basin intercepted basement, the increased shear-wave velocity value was derived from rheological analysis of five core plugs taken from 35 m of core from the Empress 1A borehole in the Gunbarrel Basin and reflects a bulk value for Permian strata. The difference in velocities is also reflected in the H/V spectra where measurements over the basin have noticeably stronger and more pronounced peaks; likely a reflection of a stronger impedance related to a proposed unconformity between the basement and overlying Permian sedimentary rocks.
Figure 4c displays the resonance frequency values derived from peaks in the H/V spectra of sites in the Eucla Basin. Here, the resonance frequency values largely range from 0.6 to 0.4 Hz and correspond to the deepest impedance detected by the Tromino®. The resonance frequencies recorded at six drill holes are plotted against the depth to basement data in Figure 4d and shows a strong correlation between the two, which is emphasized by an R^2 of 0.93 for a fitted power-law regression model. In contrast to the interpretation of data from the Gunbarrel Basin, resonance frequencies from the Eucla Basin were converted to depth estimates using the equation in Figure 4d. This approach has also been used by Parolai *et al.* (2002) and Ibs-von Seht & Wohlenberg (1999) and can be applied because of a largely uniform stratigraphy across the Eucla Basin. This approach allows for a simple and direct conversion of the resonance frequency values from the remaining sites into cover thickness estimates without the need to derive a shear-wave velocity.

Derived cover thickness estimates

Based on the above results the derived thickness, models for the Gunbarrel and Eucla Basins are displayed in Figures 3e and 4e, respectively. For the Gunbarrel Basin, the estimated cover thicknesses are displayed for sites along the PNC Baseline and Emperor Traverse (Figure 3e), and range from ~50 m to >700 m. The distribution clearly outlines a trough-like shape where the thickness of sedimentary cover gradually decreases to the northwest. To the southeast, the data detects the Cundeelee Fault Zone in remarkable detail (Figure 3e). Here, the edge of the basin is marked by a drop of nearly 400 m over a distance of less than 500 m. These estimates are the first quantitative depth to basement values for the main part of the basin, as drill data are absent.

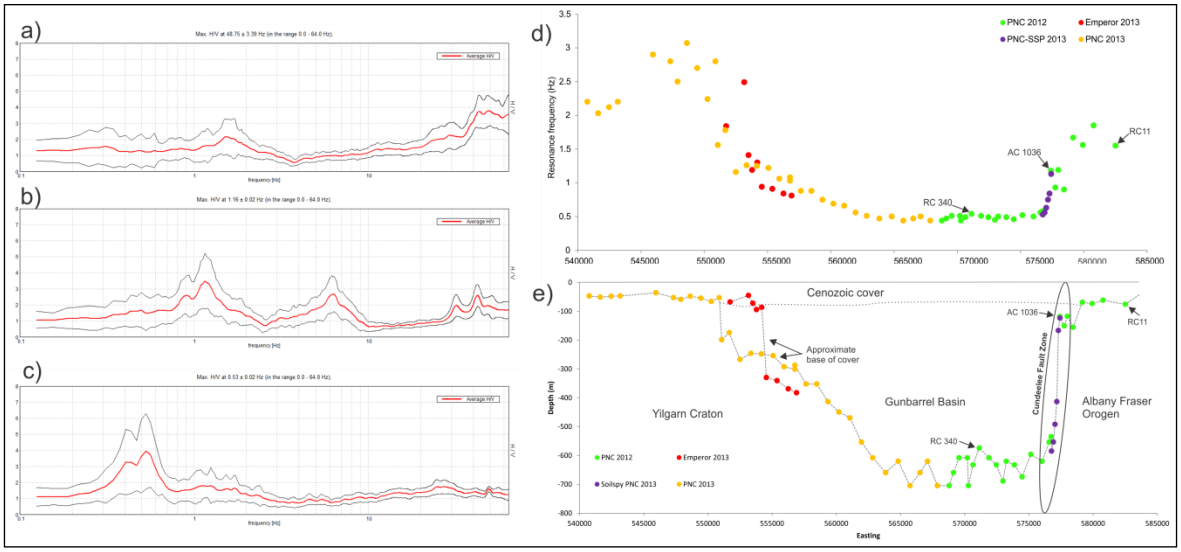

Figure 3 Selection of H/V spectral ratio plots for sites a) RC11, b) AC1036 and c) RC340; d) distribution of site resonance frequencies (fz) of lowest peaks in 89 H/V spectra of sites along the PNC Baseline and Emperor Traverse; e) derived depth to basement estimates.

For the Eucla Basin, estimates of cover thickness range from 200 to 400 m (Figure 4e) indicating a gently undulating basement topography. These thickness values are much smaller than those derived for similar resonance frequencies measured in the Gunbarrel Basin. This is due to lower shear-wave velocities of the partly unconsolidated sedimentary rocks between the basement and

the Cenozoic limestone at the surface in the Eucla Basin. Based on the regression model, the average shear-wave velocity values for the sedimentary strata in the Eucla Basin are low and increase with depth from 560 to 740 m/s. Furthermore, an initial, in-the-field estimate of 350 m for MAD002, based on a resonance frequency of 0.44 Hz and a shear-wave velocity of 620 m/s, was later confirmed after drilling to be 383 m. This translates into an error of prediction of <10%. Our estimates also correspond well with results from a regression model developed by Parolai *et al*. (2009; Figure 4e) for Tertiary to Quaternary sedimentary cover in Germany.

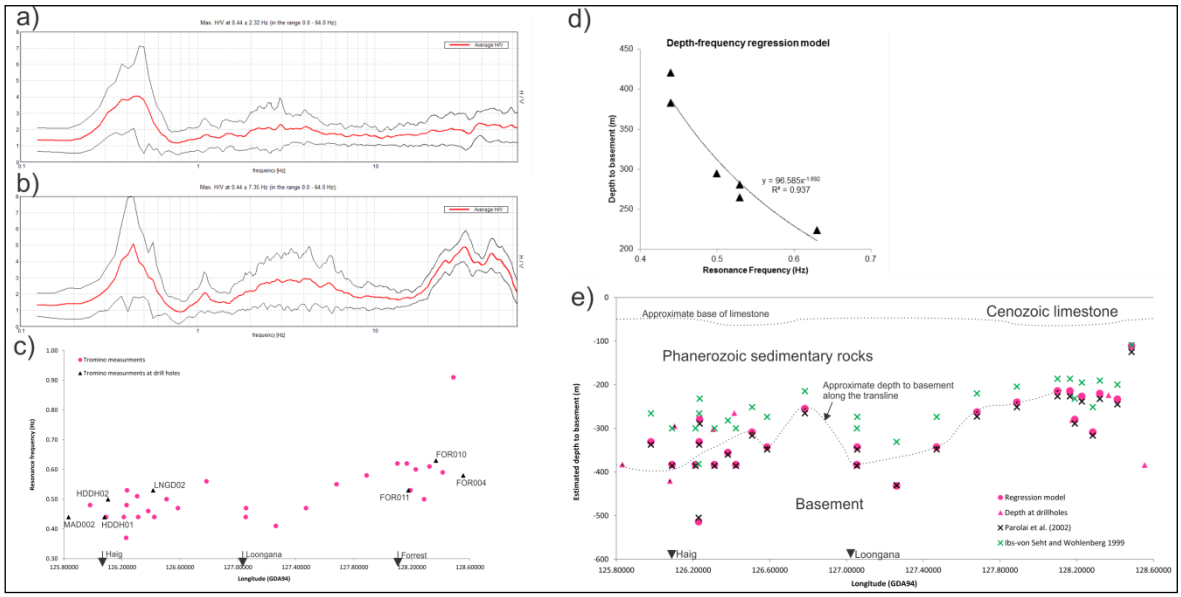

Figure 4 Selection of H/V spectral ratio plots for sites a) MAD002 and b) EUC02; c) distribution of sites resonance frequencies (fz) of lowest peaks in 35 H/V spectra from sites between Haig and Forrest; d) bivariate plot of fz values and corresponding depth to basement data at drill sites and regression model; e) derived depth to basement estimates (pink dots) based on model in d), green and black crosses are results derived from conversion models published by Parolai et al. (2002) and Ibs-von Seht & Wohlenberg (1999).

Conclusion

Passive seismic data from the Gunbarrel and Eucla Basins provide reliable cover thickness estimates ranging from only 5 m of regolith to >700 m of botet alh regolith and sedimentary rock cover. Furthermore, the application of a regression model is a quick and robust approach to derive estimates for thickness cover directly from passive seismic data. In case of the survey at Mulga Rock, passive seismic data provided the first quantitative depth to basement values for this part of the basin. The results indicate that the application of passive seismic surveys can provide invaluable information on the cover thickness for on-going and future exploration efforts in greenfields areas. This information will be particularly useful for planning drilling campaigns, but also for geochemical surveys and the interpretation of their results. Ultimately, a combination of regional geochemical mapping programmes and passive seismic surveys could enhance exploration in greenfields areas by providing data on both anomalous geochemical surface expression and estimates of cover thickness over basement at the same time.

References

Lane J.W., White E.A., Steele G.V. and Cannia J.C. 2008. Estimation of bedrock depth using the horizontal-to-vertical (H/V) ambient noise seismic method. *In:* Proceedings of 21st Symposium on the Application of Geophysics to Engineering and Environmental Problems, Philadelphia: Environmental and Engineering Geophysical Society, 1247-1259.

Delgado J., López Casado C., Estévez A., Giner J., Cuenca A. and Molina S. 2000. Mapping soft soils in the Segura river valley (SE Spain): a case study of microtremors as an exploration tool. *Journal of Applied Geophysics* **45**,19-32.

Parolai S., Borman P. and Milkereit C. 2002. New relationships between Vs, thickness of sediments, and resonance frequency calculated by the H/V ratio of seismic noise for the Cologne area (Germany). *Bulletin of the Seismological Society of America* **92**, 2521-2527.

Ibs-von Seht M. and Wohlenberg J. 1999. Microtremor measurements used to map thickness of soft sediments. *Bulletin of the Seismological Society of America* **89**, 250-259.

Nakamura Y. 1989. A method for dynamic characteristics estimation of subsurface using microtremor on the ground. Quarterly Reports of the Railway Technical Research Institute, Tokyo, **30:1**, 25-30.

Unsupervised clustering of continental-scale geophysical and geochemical data using Self-Organising Maps

M. J. Cracknell[1] and A. M. Reading[1]

[1]Centre of Excellence in Ore Deposits (CODES) and School of Earth Sciences, University of Tasmania, Private Bag 126, Hobart, Tasmania, 7001. M.J.Cracknell@utas.edu.au

Self-Organising Maps is a data-driven approach for exploring and analysing disparate, high-dimensional data. In this experiment Self-Organising Maps is used to cluster remotely sensed geophysical and geochemical data covering the Australian continent into geologically meaningful groups. Our analysis of SOM derived clusters indicates the Australian continent can be represented by five generalised geochronological domains. These geochronological domains contain a number of lithologies symbolising bedrock and regolith units with distinct characteristics.

Introduction

Self-Organising Maps (SOM, Kohonen, 1982; Kohonen, 2001) is an unsupervised clustering algorithm that is useful for data-driven analysis of high-dimensional multivariate data. SOM treats each sample as a *n*-dimensional (*n*D) vector in variable space and employs vector quantisation to project data in *n*D space onto a 2D map. SOM finds natural groups or clusters in data via an iterative two-stage process that (1) identifies input samples to the closest randomly seeded seed-nodes and (2) trains seed-nodes such that their values are adjusted to align more closely to associated samples. In this way, SOM links input data to trained seed-nodes (nodes – representing groups of similar samples) onto a 2D topologically relevant space. The topology between SOM nodes is preserved such that nodes that are close in *n*D space maintain their relative proximities on the 2D map. A U-matrix is commonly used to visualise the 2D topology of SOM nodes (Fraser and Dickson, 2007). SOM has seen recent use in a wide range of geophysical and geological data mining applications such as mapping lithologies from airborne geophysical and hyperspectral imagery (Bedini, 2009; Bedini, 2012; Carneiro *et al.*, 2012), exploring geochemical databases for interesting and significant features (Penn, 2005; Bierlein *et al.*, 2008) and identifying waveform patterns in seismic data (Langer *et al.*, 2009).

In this experiment, SOM is employed to cluster spatially distributed airborne geophysical and ASTER derived mineral abundance data over the Australian continent available from Geoscience Australia (http://www.ga.gov.au/). Input data were selected based on their quality and perceived relevance to the task of identifying continental-scale geological provinces. SOM nodes to be analysed are merged using a hierarchical dendrogram clustering method. The optimal number of merged SOM nodes was identified by assessing Xie-Beni Index (XBI) values for different numbers of merged SOM nodes. This method is outlined in Paasche and Eberle (2009) for identifying an optimal number of clusters generated using the fuzzy *c*-means algorithm. A visual assessment of topological relationship between merged SOM nodes was carried out using a U-matrix. An interpretation of the geological significance of merged SOM nodes was performed by comparing their spatial distributions to the Australian 1:1,000,000 national-scale geological map (Liu *et al.*, 2005).

Data

Data used in this study were obtained from Geoscience Australia. Table 1 lists the 12 datasets analysed and their sources. The Satellite ASTER geoscience map product layers (Cudahy *et al.* 2012) were selected based on their coverage and quality as reported by Cudahy (2012). Data were resampled to 5 km resolution and to common extent using bilinear interpolation. All log-normal distributed data were transformed to approximate a normal distribution using the natural logarithm. All data were scaled and centred to zero mean and unit variance. Samples with missing values were excluded from analysis.

Methods

The R programming language (available at http://cran.r-project.org/) was used to implement SOM (*kohonen* package, Wehrens and Buydens, 2007) and select an optimal number of merged SOM nodes (*clusterCrit* package, Desgraupes, 2012). Default *kohonen* package parameters were used to train SOM nodes, these are: number of iterations 100; initial search radius 2/3 the dimensions of *n*D variable space; linear search radius decrease; and percentage adjustment of seed-node properties from 0.05 to 0.01. A 20 × 20 hexagonal topology was used to initiate seed-nodes resulting in 400 trained SOM nodes. These SOM nodes were merged to a specified number by pruning a dendrogram representing SOM node similarity using a hierarchical partitioning method. The Ward's minimum variance method was use to merge SOM nodes in the dendrogram as this finds compact spherical groups of SOM nodes. An optimal number of SOM nodes was selected using the XBI (Xie and Beni, 1991) and conducted using a random subset of samples equal to ~ 40 % of the available data. Low XBI values indicate samples within SOM nodes form compact clusters.

Results

Figure 1 shows that 16–20 merged SOM nodes generate consistently low XBI values. The optimal number of natural clusters with which to represent the input data, i.e. 16, was taken as the minimum number of merged SOM nodes from this range of consistently low XBI values. Figure 2 shows the spatial distributions of the 16 merged SOM nodes across the Australian continent. Table 2 provides an interpretation of the geological significance of these merged SOM nodes. Five generalised geochronological domains have been identified from the SOM U-Matrix (Figure 2). Domain *a* contains quaternary surficial sediments, such as unconsolidated aeolian dune sands (clusters 1 and 5), sand, clay and gravel regolith (clusters 10 and 12). Domain *b* contains clay and alluvial materials derived from Mesozoic siliciclastic sandstones and mudstones (cluster 7), mafic volcanics and carbon rich rocks (cluster 11) and Cenozoic carbonate rocks and clay-rich sediments (cluster 6) in central and eastern Australia. Cluster 13 and possibly cluster 3 constitute felsic igneous and siliciclastic sedimentary rocks primarily located in and around the Lachlan fold-belt of eastern Australia (domain *c*). Proterozoic mafic igneous rocks and associated sedimentary rocks (domain *d*) are primarily identified in cluster 15. Clusters 2, 4 and 16 indicate Archean/Proterozoic metamorphic felsic igneous and metasedimentary rocks (domain *e*). Several merged SOM nodes are likely to represent artefacts from moisture in clouds and/or vegetation (cluster 3), noisy data (clusters 8, 9 and 14), organic carbon and vegetation in the tropics (cluster 11). These SOM nodes group on the right-hand side of the U-matrix.

Discussion and Conclusion

The analysis of merged SOM nodes indicates a number of meaningful geochronological domains have been identified across the Australian continent, i.e. Archean/Proterozoic, Palaeozoic, Mesozoic, Cenozoic and Quaternary terranes. These geochronological domains comprise multiple merged SOM nodes defining contrasting lithological units. For example, merged SOM nodes discriminate between felsic, mafic, quartz and clay/ferricrete dominated igneous and sedimentary lithologies. In addition, the multiple merged SOM nodes representing large regions of unconsolidated Quaternary sediments indicate differing characteristics of regolith materials such as source mineralogy, mode of transport and depositional environment. These observations suggest that the integration and meaningful analysing of geoscience data representing characteristics of surficial materials, i.e. Gamma-Ray Spectrometry and ASTER geoscience products, and those indicating the physical properties of bedrock, i.e. gravity and Total Magnetic Intensity, can be achieved using SOM. The unsupervised clustering method described in this study has identified interesting patterns in disparate geophysical and geochemical data and will generalise readily to other novel geoscience applications.

Acknowledgements

We thank Matilda Thomas and Richard Lane for their encouragement during the preparation of this manuscript. This product incorporates data that are (c) Commonwealth of Australia (Geoscience Australia) 2003. The Data have been used in the product with the permission of Geoscience

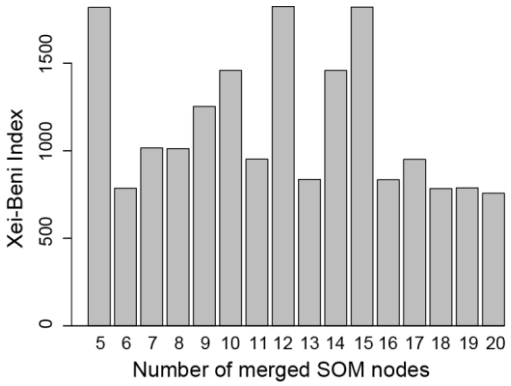

Figure 1: Xie-Beni Index results for 5–20 merged SOM nodes.

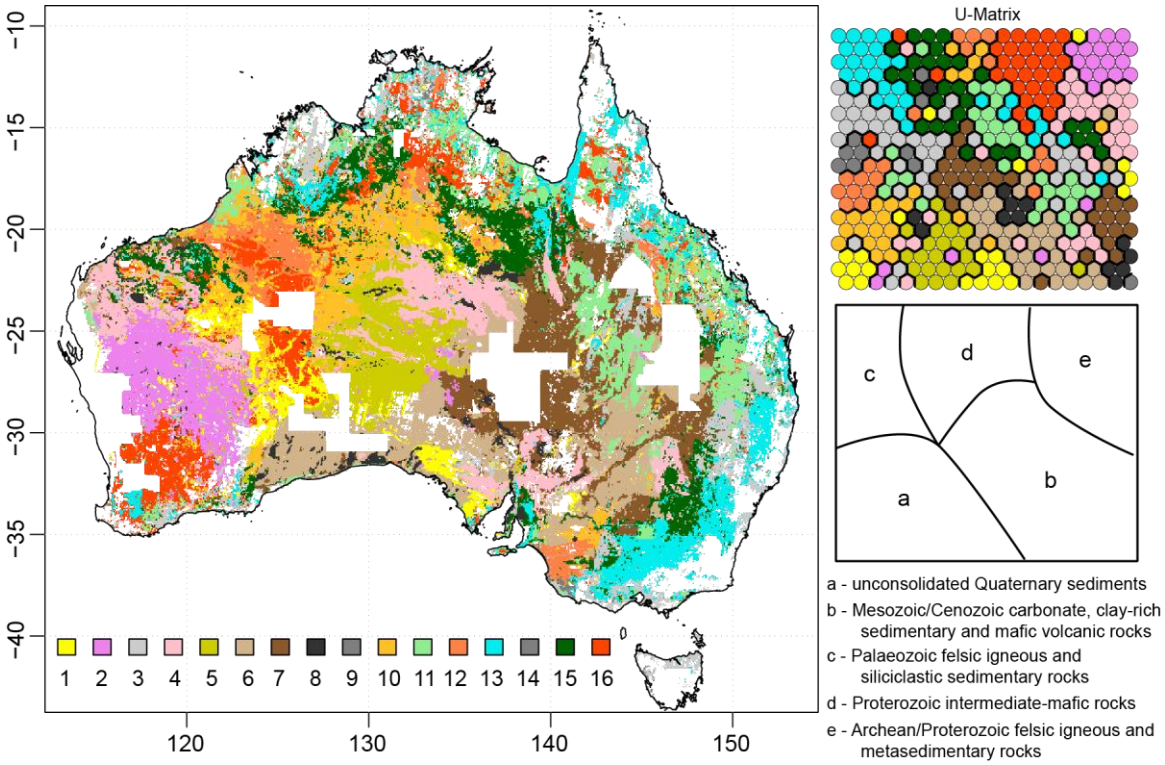

Figure 2: Spatial distributions of 16 merged SOM nodes across the Australian continent, colour coded U-Matrix and interpretations of the five generalised geochronological domains based on comparisons with the Australian 1:1,000,000 national-scale geological map (Liu *et al.*, 2005). See Table 2 for lithological interpretations of merged SOM nodes.

Table 1: Geoscience Australia datasets used in this study and data specific pre-processing methods.

Layer	Source	Pre-processing
Gravity (Bouguer anomaly corrected)	Australian National Gravity Database 0.5 Minute Onshore Gravity Grid[a]	-
Total Magnetic Intensity	5th Edition Total Magnetic Intensity Anomaly Grid of Australia[b]	-
K	The Radiometric Map of Australia[c]	$\log_e$ transform
Th	The Radiometric Map of Australia[c]	$\log_e$ transform
U	The Radiometric Map of Australia[c]	$\log_e$ transform
AlOH Group Content	National ASTER geoscience map product[d]	$\log_e$ transform
AlOH Group Composition	National ASTER geoscience map product[d]	-
Ferric Oxide Composition	National ASTER geoscience map product[d]	-
Ferric Oxide Content	National ASTER geoscience map product[d]	-
Ferrous Iron in MgOH	National ASTER geoscience map product[d]	-
Ferrous Iron Index	National ASTER geoscience map product[d]	-
MgOH Group Content	National ASTER geoscience map product[d]	$\log_e$ transform

NOTE – all data resampled to 5 km resolution using bilinear interpolation.
[a](Tracey et al., 2007), [b](Percival, 2010), [c](Minty et al., 2009), [d](Cudahy et al., 2012)

Table 2: Geological Era/Period and dominant lithologies of the 16 merged SOM nodes interpreted from comparisons with the Australian 1:1,000,000 national-scale geological map (Liu *et al.*, 2005).

	Era/Period	Lithologies	Comments
1	Quaternary	aeolian dune sands	
2	Archean	metamorphic felsic igneous rocks	northern Yilgarn Craton
3	?Palaeozoic	?felsic igneous and siliciclastic sedimentary rocks	?vegetation artefact in northern Australia
4	Proterozoic	metamorphosed felsic intrusive rocks, metasedimentary siliciclastic rocks	Gawler, Mt Isa, Broken Hill, Musgrave and northern Yilgarn Craton
5	Quaternary	unconsolidated sands	central Australia
6	Cenozoic/ Quaternary	limestone/calcareneous sands and muds	includes Eucla carbonate rocks
7	Late Cretaceous/Early Cenozoic – Quaternary	mudstones and associated unconsolidated channel and basin sediments	Darling and Euromunga Basins
8	-	-	small sample size, suspected artefact
9	-	-	small sample size, suspected artefact
10	?Quaternary	?regolith	located in central NT and western WA
11	?Cretaceous/ Quaternary	?carbon rich sedimentary and mafic igneous rocks	suspected artefacts in northern Australia
12	Cenozoic/ Quaternary	sand, clay and gravel regolith and/or dune sands	-
13	Palaeozoic	felsic igneous rocks and siliciclastic metasedimentary rocks	dominant cluster over the Lachlan and New England fold belts
14	-	-	small localised patches along coastline, suspected artefact
15	Proterozoic	mafic metavolcanics and metasedimentary rocks	associated with black soil in the MacArthur River Basin area, northern Lachlan fold belt
16	Archean/ Palaeoproterozoic/ ?Cenozoic	metamorphic felsic-intermediate igneous rocks, ferruginous duricrusts and sands	associated with cluster 11 in northern Australia

References

Bedini, E. 2009. Mapping lithology of the Sarfartoq carbonatite complex, southern West Greenland, using HyMap imaging spectrometer data. Remote Sensing of Environment, 113 (6), pp. 1208-1219.

Bedini, E. 2012. Mapping alteration minerals at Malmbjerg molybdenum deposit, central East Greenland, by Kohonen self-organizing maps and matched filter analysis of HyMap data. International Journal of Remote Sensing, 33 (4), pp. 939-961.

Bierlein, F. P., Fraser, S. J., Brown, W. M. & Lees, T. 2008. Advanced methodologies for the analysis of databases of mineral deposits and major faults. Australian Journal of Earth Sciences, 55 (1), pp. 79-99.

Carneiro, C. C., Fraser, S. J., Croacutesta, A. P., Silva, A. M. & Barros, C. E. M. 2012. Semiautomated geologic mapping using self-organizing maps and airborne geophysics in the Brazilian Amazon. Geophysics, 77 (4), pp. K17-K24.

Cudahy, T. *et al.* 2012. Satellite ASTER Geoscience Map of Australia. v1. CSIRO. Data Collection. DOI:10.4225/08/51400D6F7B335.

Cudahy, T.J., 2012. ASTER Geoscience Product Notes for Australia. Version 1, CSIRO ePublish Number. EP-30-07-12-44, 26 p. (2012).

Desgraupes, B. 2012. clusterCrit: Clustering Indices. R package version 1.0. [Online]. http://CRAN.R-project.org/package=clusterCrit.

Fraser, S. J. & Dickson, B. L. 2007. A new method for data integration and integrated data interpretation: Self-organising maps. In: 5th Decennial International Conference on Mineral Exploration, Expanded Abstracts, 2007. 907-910.

Kohonen, T. 1982. Self-organized formation of topologically correct feature maps. Biological Cybernetics, 43 (1), pp. 59-69.

Kohonen,, T. 2001. Self-organizing maps, Springer-Verlag, Berlin, p. 501.

Langer, H., Falsaperla, S., Masotti, M., Campanini, R., Spampinato, S. & Messina, A. 2009. Synopsis of supervised and unsupervised pattern classification techniques applied to volcanic tremor data at Mt Etna, Italy. Geophysical Journal International, 178 (2), pp. 1132-1144.

Liu, S. F., Raywond, O. L., Retter, A. J., Stanley, S. P. & Pervial, D. S. 2005. Surface Geology of Australia - 1:1,000,000, Tasmania - 2nd Edition [Digital Dataset] Canberra, ACT: Geoscience Australia. [Online]. http://www.ga.gov.au.

Minty, B., Franklin, R., Milligan, P., Richardson, L. M. & Wilford, J. 2009. The Radiometric Map of Australia. Exploration Geophysics, 40 (4), pp. 325-333.

Paasche, H. & Eberle, D. G. 2009. Rapid integration of large airborne geophysical data suites using a fuzzy partitioning cluster algorithm: a tool for geological mapping and mineral exploration targeting. Exploration Geophysics, 40 (3), pp. 277-287.

Penn, B. S. 2005. Using self-organizing maps to visualize high-dimensional data. Computers & Geosciences., 31 (5), pp. 531-544.

Percival, P. J. 2010. Index of Airborne Geophysical Surveys. Geoscience Australia. Australia, p. >.

Tracey, R., Bacchin, M. & Wynne, P. 2007. AAGD07: A new absolute gravity datum for Australian gravity and new standards for the Australian National Gravity Database. ASEG Extended Abstracts, 2007 (1), pp. 1-3.

Wehrens, R. & Buydens, L. M. C. 2007. Self- and Super-organising Maps in R: the kohonen package. Journal of Statistical Software, 21 (5), pp. 1-19.

Xie, X. L. & Beni, G. 1991. A validity measure for fuzzy clustering. IEEE Transactions on Pattern Analysis and Machine Intelligence, 13, pp. 841–847.

Regolith-landform distribution and composition on the West Kimberley Plateau: mapping by interpretation of geophysical and remotely sensed data

Nadir de Souza Kovacs

Geological Survey of Western Australia

A newly compiled 1:100 000-scale interpretive regolith-landform map layer of the northwest Kimberley region of Western Australia aims to provide a better understanding of the geological and landform development of the Kimberley region. This new map characterizes the regolith-landform of the Kimberley Plateau, its mineral composition and parent rock. It is the Geological Survey of Western Australia's (GSWA) contribution to the Kimberley Science and Conservation Strategy, a Western Australian state government science and conservation initiative. The Kimberley Science and Conservation Strategy area spans about 8 840 900 km^2, mostly on the West Kimberley Plateau. The complete regolith-landform map layer for the conservation area is available as part of the GSWA Kimberley Geological Information Series 2014 update.

The bedrock geology in the area consists of Paleoproterozoic granites and metamorphic rocks of the King Leopold Orogen, Paleoproterozoic sedimentary rocks and basalt of the Speewah and Kimberley Groups, Proterozoic Hart Dolerite, and Palaeozoic sedimentary rocks in the southern Yampi peninsula (Tyler, Hocking and Haines 2012; Fig. 1). The region is difficult to access, so mapping was completed primarily by remotely sensed data. Geophysical and satellite imagery were used to delineate and identify the landform types, as well as the regolith composition and parent rock. Where possible, ground observations verified and calibrated the imagery interpretation, together with reference to earlier bedrock geological mapping.

The map uses the regolith classification scheme developed by GSWA (2013) to code the regolith-landform units. In this scheme the primary code identifies the landform, the secondary code identifies the regolith composition, and the tertiary code the parent rock, or cement composition. The identification of the regolith landform and composition is from the interpretation of geophysical and remotely sensed data, calibrated by field checking. The primary landform code specifies the environment or process of formation of the regolith, and is determined mostly by using orthophotos, Google Earth imagery, Digital Elevation Models, and derived products. The composition (secondary code) and parent rock (tertiary code) are determined by concurrent interpretation of Landsat, radiometric, magnetic and ASTER images, verified with available bedrock geology from the existing 1:250 000 geological map coverage, and field observations from previously recorded field data.

In the present study, landforms (primary code) are classified as residual (R), exposed bedrock (X), colluvial (C), alluvial (A), coastal wave-dominated (B), or coastal tide dominated (T). The secondary codes specifying compositions are: ferruginous (f), mafic (m), quartzofeldspathic (g), quartz-rich (q), carbonate (k), mica (xi), black-soils or gilgai (cb), and aluminous/bauxite (xa). The tertiary codes specifying the major rock types in the area are: basalt (vb), sandstone (ss), granite (pg), dolerite (pl), dolomite (cd), and felsic volcanic (vf). The resultant map produced is a comprehensive record of the regolith-landform types and distribution on the West Kimberley Plateau, charting not only the landform type, but also identifying its main regolith composition and parent rock.

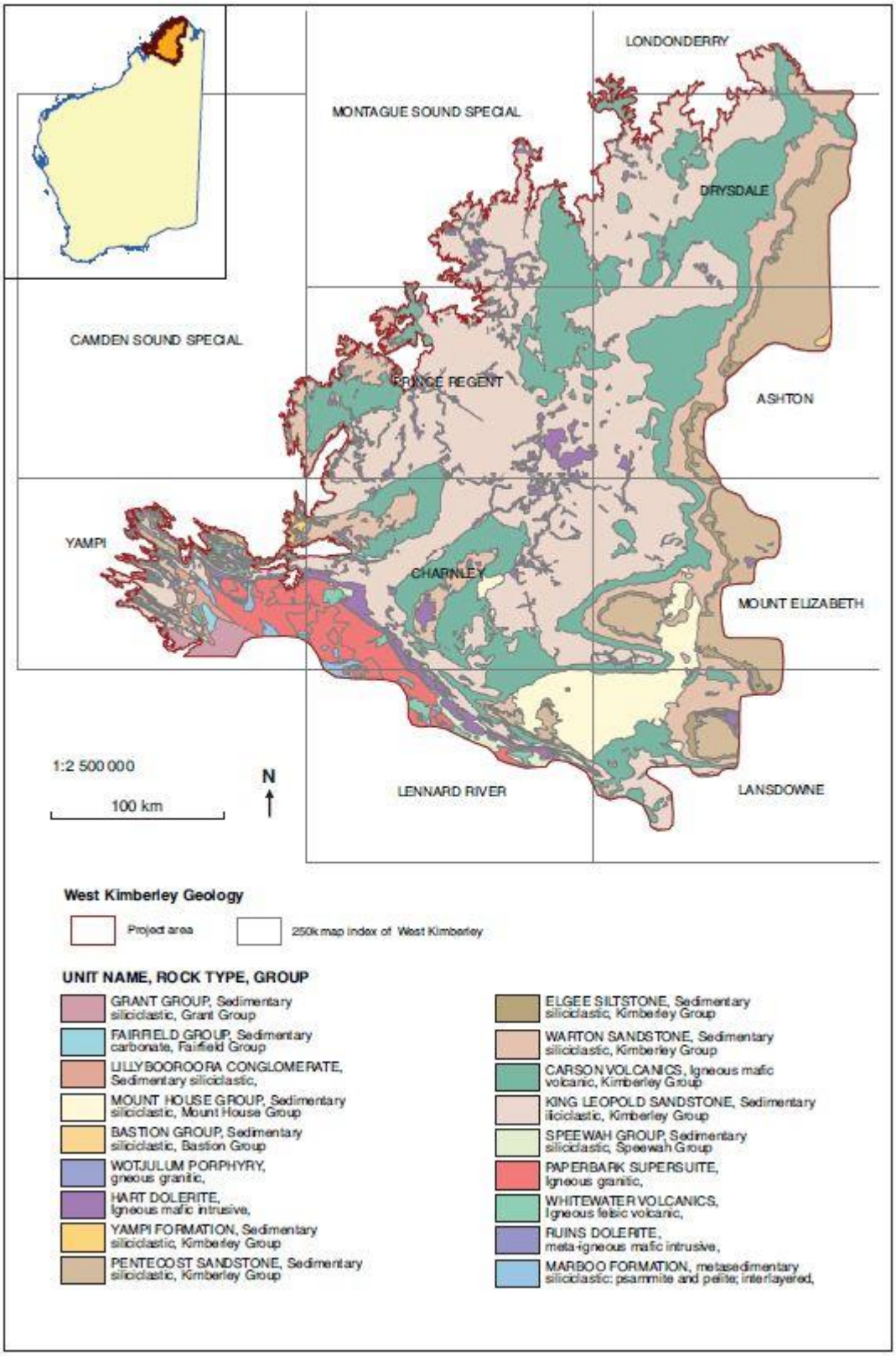

Figure1 shows a geological map of the West Kimberley and the location map for the Kimberley Science and Conservation Strategy project area.

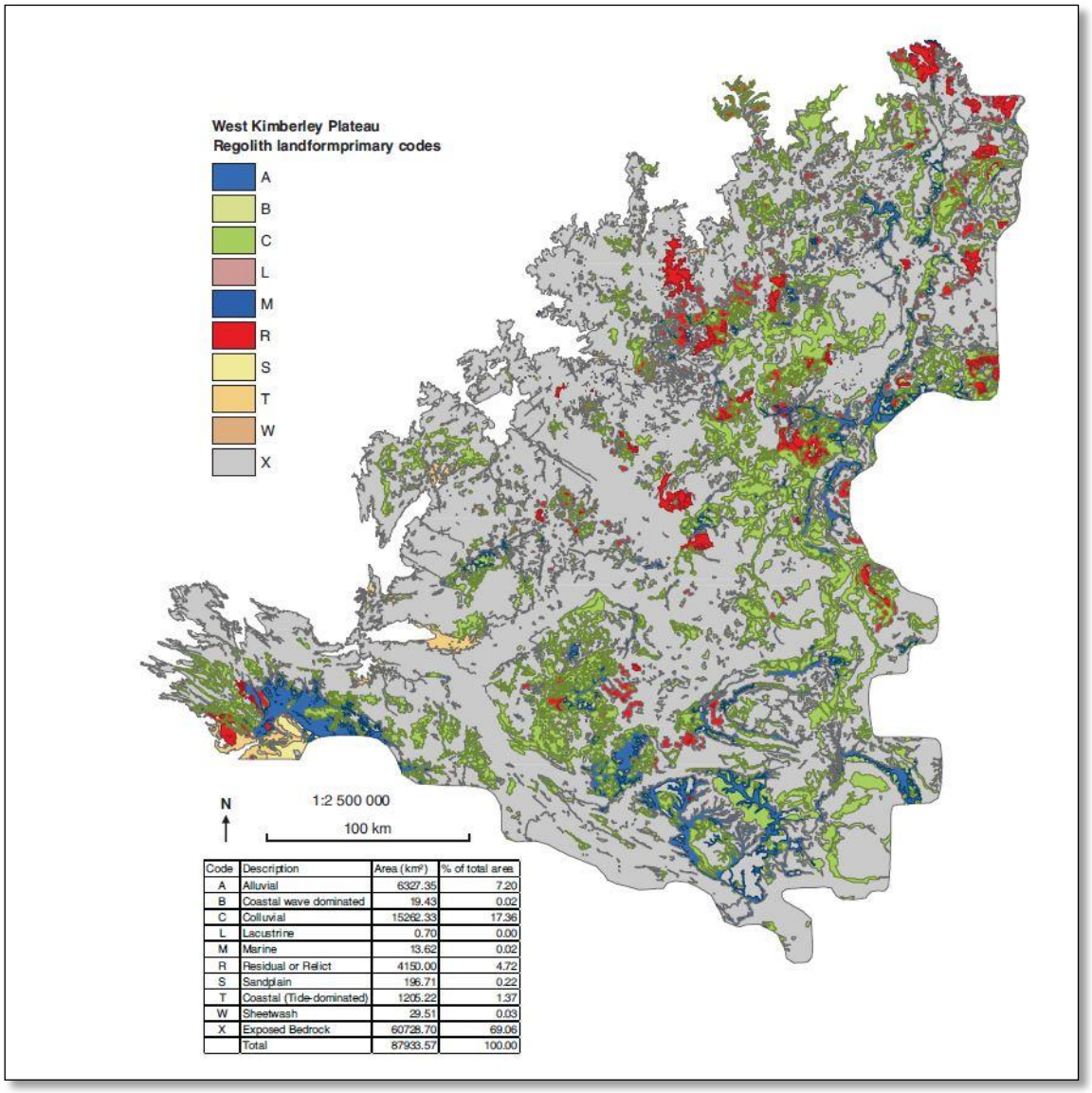

Code	Description	Area (km²)	% of total area
A	Alluvial	6327.35	7.20
B	Coastal wave dominated	19.43	0.02
C	Colluvial	15262.33	17.36
L	Lacustrine	0.70	0.00
M	Marine	13.62	0.02
R	Residual or Relict	4150.00	4.72
S	Sandplain	196.71	0.22
T	Coastal (Tide-dominated)	1205.22	1.37
W	Sheetwash	29.51	0.03
X	Exposed Bedrock	60728.70	69.06
	Total	87933.57	100.00

Figure 2. The regolith-landform map shows the distribution of exposed bedrock, the residual and depositional regolith-landform units on the West Kimberley Plateau.

Regolith-landform development in the West Kimberley reflects a combination of bedrock composition, structure, and chemical and physical weathering. Regolith covers approximately 30% of the mapped area (Fig. 2), and is related genetically to the underlying bedrock. It is notably more extensive and well developed on basalts of the Carson Volcanics, compared to either the Proterozoic sandstones on the plateau, or the Paleoproterozoic granitic rocks of the King Leopold Ranges. On the basalt, ferricrete and bauxite form the capping on mesas. Down slope, ferruginous pisolitic lateritic soils develop on the gently sloping terrain, and black soils on the alluvial plains. The regolith-landform developed on the Hart Dolerite is similar to the regolith-landform on the basalts, but to a lesser extent. Ferricrete caps some of the hills on dolerite outcrops to the northwest, and lateritic and black soils fill the narrow valleys formed by the weathering of the dolerite dykes.

The Proterozoic sandstones are the least weathered rocks on the mapped area, and form the higher terrain on the plateau. The regolith-landform which developed on the sandstone plateau consists of shallow residual sands on crests, and shallow, quartz-rich sandy alluvium and colluvium in drainage depressions. Rarely, ferruginous material, likely to be ferricrete, is found on the edge of sandstone outcrops next to basalt. The nature and origin of this material is yet to be determined. On the King Leopold Ranges, the granite weathers to proximal colluvium, composed of

quartzofeldspathic coarse-grained sand, and there is no evidence of residual units having developed on the granite. Extensive areas of mangrove and silty and sand tidal flats extend along the west coast of the Kimberley Plateau. These are not related to any particular rock type.

References

Geological Survey of Western Australia 2013. A revised classification system for regolith in Western Australia, and the recommended approach to regolith mapping. Geological Survey of Western Australia Record 2013/7, 26p.

Tyler I. M., Hocking R. M. & Haines P. W. 2012. Geological evolution of the Kimberley region of Western Australia. *Episodes: Geological newsletter: International Union of Geological Sciences*, 35, issue 1 March 2012 Geology in the Oceania Region – Special Issue for the 34 IGC, Brisbane, August 2012, 298 – 306p

Waking up Sleeping data – Development of a geodatabase of historical remote sensing data

Alexandra Possingham[1,2] , Mike Caccetta[3], Carsten Laukamp[3], Cindy Ong[3], Andrew Rodger[3]

1. Queesland University of Technology (QUT)
2. 2013/2014 Internship – Minerals Down Under Flagship and CSIRO Information Management & Technology
3. CSIRO Earth Science and Resource Engineering

Introduction

Increasing quantities of geophysical and spectroscopic remote sensing data are becoming available to the resources sector in the form of precompetitive data via online platforms offered by the federal, state and territory Geological Surveys. Recent discoveries made by the resources industry, using CSIRO's continental scale mineral maps of Australia have demonstrated the importance of such precompetitive data.

Over the course of many years numerous optical remote sensing datasets have been acquired by CSIRO from multi spectral and hyperspectral systems including: ASTER, OARS SWIPS/TIPS, Hyperion and Hymap. These datasets have been the basis of numerous successful studies (Cudahy et. al., 2005;Cudahy et.al., 2008; Caccetta, Collings & Cudahy.,2013) and both raw data and derived information products provide an invaluable source of information regarding surface and land cover composition. While these datasets have potential in a range of fields, including exploration, regolith mapping, and environmental land management these disparate datasets are not easily accessible or discoverable. The aim of this project is to synthesise and collate disseminated remote sensing datasets available in CSIRO's collection and archive them into a publically searchable geodatabase for reuse and preservation.

Approach

CSIRO's collection of optical remote sensing images contains 10,000's of datasets and equates to 10'sTb of data. In order to effectively collate and catalogue this extensive collection a systematic approach is required. A preliminary analysis of the collection was conducted and a curation workflow developed (Figure 1). The data curation approach adopted includes: archiving the collection to a web accessible data access portal and developing GIS-accessible layers. The GIS layers will describe, for example: image boundaries, data quality, flight conditions, acquisition system details, ownership and accessibility of the data. The collection will include radiance, reflectance and value-added products (such as mineral maps) where available.

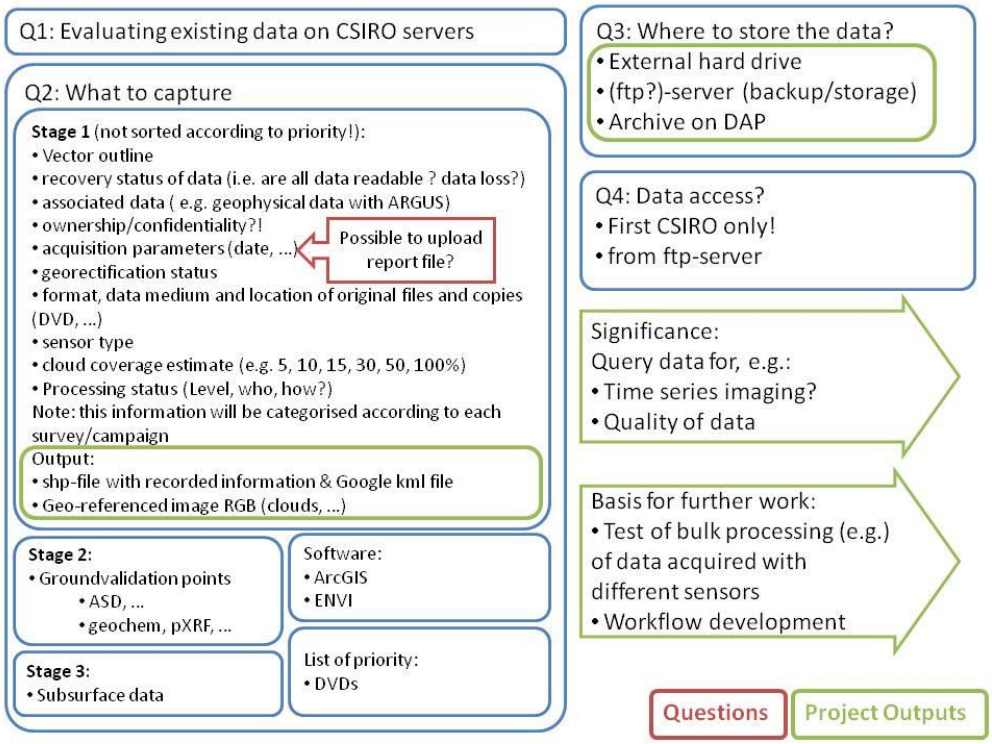

Figure 1: Demonstrates the approach taken to achieve the final product of a GIS Map with all available hyperspectral data - Waking up Sleeping data project work flow chart (Prepared by Laukamp, C).

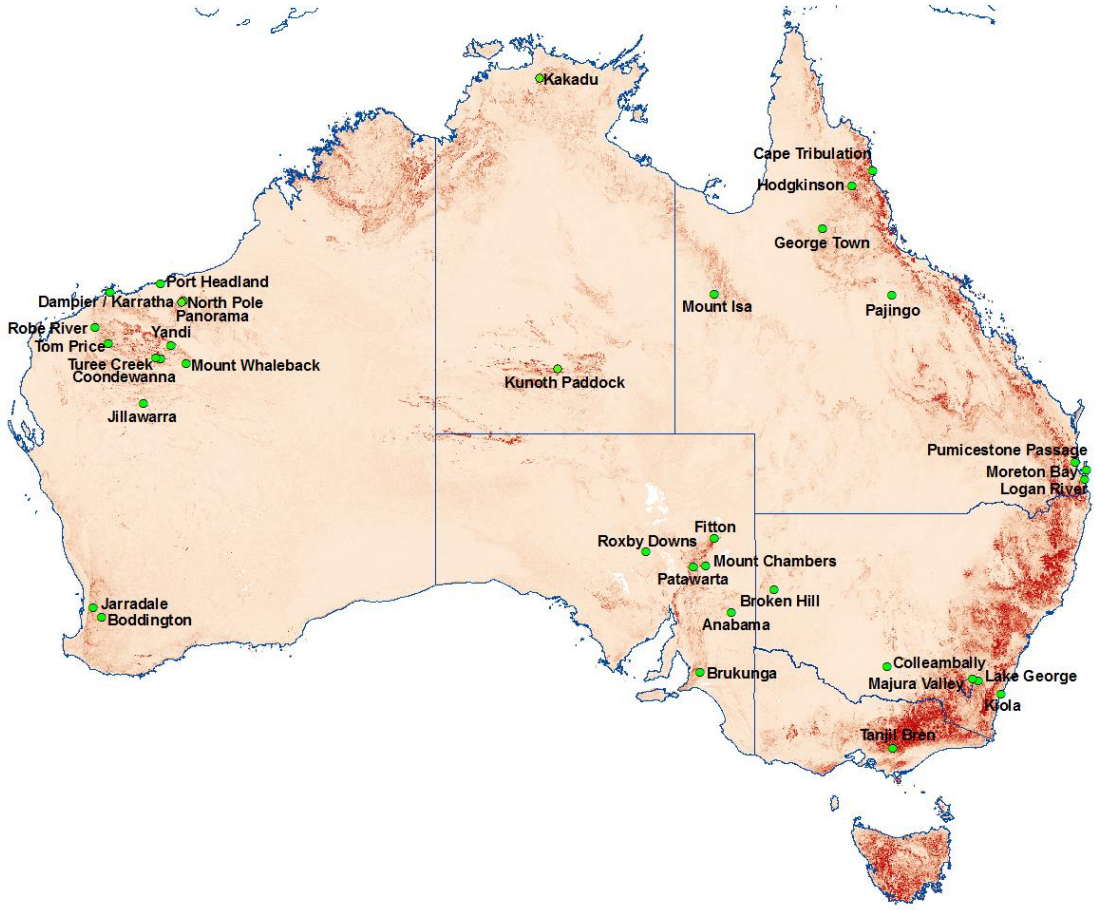

Figure 2: Locations of hyperspectral data used in the Waking up Sleeping data project overlain on SRTM elevation map (Gallant, J & Austin, J., 2012) and Geoscience Australia coast line and state boundary vectors (Geoscience Australia., 2010).

Discussion

Remote sensing methods such as hyperspectral sensing are non-invasive and highly efficient procedures for collecting mineral and regolith data. Remote sensing has the benefits of decreasing the environmental impact and the high costs of hands-on exploration. For example the database will be able to be used in many sectors, such as the resource sector in regards to exploration efficiency, land management, and environmental organisations in regards to determining the risk to biodiversity assets from mineral extraction (Butt *et al*., 2013). The hyperspectral database will also provide resources for the further development of Australian Regolith maps in regards to *in situ* and transported material (Cudahy *et al.*, 2005). These are just a few examples of how the database can be utilised as a practical commual tool which many sectors will benefit from and build on.

The resulting database would be beneficial not only to the resources sector, but also land management and environmental organisations concerned with planning and decision-making. Good land-use planning requires information about the likely costs and benefits of different actions in different places. The hyperspectral database can be used to assist land-use planning at regional, state and national scales. In any region, every parcel of land will have different potential benefits and/or potential impacts from a varity of land-use practices such as: agricullture, forestrsy, mining, conservation and urban development. Knowing the likely benefits and potential impacts of mining in any location will help us to weigh that option against the benefits of other land-use activities as well as help interested stake holders to determine where multiple-use is possible, for example mining and biodiversity conservation.

Acknowledgements

This is an internship project support by CSIRO's Minerals Down Under Flagship Program, Information Mangement and Technology (IM&T).

References

Butt, N., Beyer, H., Bennett, J., Biggs, D., Maggini, R., Mills, M., Renwick, A., Seabrook, L., Possingham, H., 2013. Biodiversity Risks from Fossil Fuel Extraction. Science 342, pp. 425-426.

Caccetta, M., Collings, S., & Cudahy, T., 2013. A calibration methodology for continental scale mapping using ASTER imagery . Remote Sensing of Environment 139, pp. 306-317.

Cocks, T., Jenssen, R., Stewart, A., Wilson, I., Shields, T., 1998. The Hymap Airborne Hyperspectral Sensor : The System, Calibration And Performance. In: *1st EARSEL Workshop on Imaging Spectroscopy*, pp. 37-42.

Cudahy, T., Caccetta, M., Cornelius, A., Hewson, R., Wells, M., Skwarnecki, M., Halley, S., Hausknecht, P., Mason, P., Quigley, M., 2005. Regolith, geology and alteration mineral maps from new generation airborne and satellite remote sensing technologies and Explanatory Notes for the Kalgoorlie-Kanowna 1:100,000 scale map sheet, remote sensing mineral maps. MERIWA Report No. 252, 114 pages.

Cudahy, T., Jones, M., Thomas, M., Laukamp, C., Caccetta, M., Hewson, R., Rodger, A., Verrall, M., 2008. Next Generation Mineral Mapping: Queensland airborne Hymap and satellite ASTER surveys 2006-2008. CSIRO report No. P2007/364, 161 pages.

Gallant, J., & Austin, J., 2012. *SRTM Grid Cell Area (3" resolution) derived from 3" SRTM DEM-S.* Retrieved December 13, 2013, from CSIRO Data Access Portal: http://dx.doi.org/10.4225/08/50AC89675E6DD

Geoscience Australia., 2010. Outline map of Australia (with state borders and capital city locations). Retrieved December 13, 2013, from Geoscience Australia: http://www.ga.gov.au/products/servlet/controller?event=GEOCAT_DETAILS&catno=61756

Validating the Australian ASTER geoscience maps using the National Geochemical Survey of Australia surface regolith samples

M. Thomas[1], T. Cudahy[2], P. de Caritat[1], C. Laukamp[2], I.C Lau[2], M. Caccetta[2], C. Ong[2], L. Ribeiro[3], and B. Pejcic[2]

[1]Geoscience Australia, Canberra, ACT, [2]CSIRO Earth Science and Resource Engineering, WA, [3]Sao Paulo State University, Sorocaba Campus, Brazil,

This collaborative project between Geoscience Australia (GA) and CSIRO aims to use physicochemical measurements, collected from surface overbank sediments as part of the National Geochemical Survey of Australia (NGSA) project, to help validate the ASTER multispectral geoscience maps of Australia. Both data sets have common information including that related to the surface abundance of silica, aluminium, iron, clay, sand and volatiles (including carbonate). The ASTER geoscience maps also provide spatial information about trends of mineral composition, which are potentially related to pH and oxidation state.

The ASTER mosaic and derived maps are made up of some ~3,500 60x60 km individual ASTER scenes, and represent the first continent-scale, public, web-accessible and GIS-compatible mineral group maps of their kind (Cudahy *et al.*, 2012, DOI. 10.4225/08/51400D6F7B335). In August 2012, 15 of these satellite-acquired mineral group products were released by a multi-agency collaboration, led by CSIRO, with GA and all the State and Territory geological surveys, with 2 additional products released subsequently. The products have applications ranging from mineral mapping and exploration, to soil-mapping, environmental monitoring and management, and agriculture (Cudahy *et al.*, 2010). An example of such an application is GA's pilot project characterising Australian salt lakes (Howard *et al.*, 2012. Thomas *et al.*, 2012). These products can also be utilised by regolith scientists for surface mineral group abundance and compositional information, to facilitate and improve mapping and characterisation of weathering, soil and geological boundaries, and chemistry.

The NGSA project was developed as part of GA's Onshore Energy Security Program 2006-2011, and was carried out in collaboration with all State and Territory geological surveys (www.ga.gov.au/ngsa). It delivered Australia's first national geochemical atlas (Caritat and Cooper, 2011), an underpinning geochemical database, and a series of reports and papers.

This new work aims to take spectroscopic measurements of the NGSA samples, as they represent a spatially extensive, roughly homogenous surface medium that is well suited to remote-sensing at the 30-90m pixel scale of the ASTER data. The study will combine ASTER data with other complementary datasets (e.g. terrain indices, gamma-ray radiometrics) to build statistical predictive models on surface regolith geochemistry. This investigation will assess the new products for geomorphic applications, particularly landscape analysis and characterisation. The current work builds upon the NGSA database by adding detailed spectral reflectance measurements across the 400 to 20000 nm wavelength region. Approximately 165 random samples of the 0-10 cm NGSA sample suite were selected for measurement of their reflectance and emission spectra before wavelength re-sampling to simulate the ASTER spectral band response.

Catchment outlet sediments (mostly similar to floodplain sediments) were sampled in 1186 catchments covering ~6.2 million km^2 or ~81% of the country (on average one sample per 5200 km^2). Samples were collected at two depths (0-10 cm and ~60-80 cm), each sieved to two grain size fractions (<2 mm fraction, and a <75 µm fraction) and analysed for total, aqua regia, and Mobile Metal Ion® element contents; other analyses (pH, electrical conductivity, grain size distribution, etc.) were also performed. Here bulk (unsieved) aliquots of the top samples were separated for reflectance spectroscopic analysis.

Reflectance spectra of powders were measured using a Bruker Vertex 70 Fourier transform infrared spectrometer equipped with an Integrating Sphere (A 562-G, Bruker). For analysis, powder samples were placed in a cup holder at the bottom of the Integrating Sphere. Infrared reflectance measurements were undertaken at room temperature and performed in the short-wave infrared (SWIR) and mid infrared (MIR) wavelength regions. The SWIR spectra were collected between

10000 cm^{-1} (1000 nm) and 3700 cm^{-1} (2700 nm) using an indium-gallium-arsenide detector, CaF_2 beamsplitter and a tungsten halogen lamp. The SWIR data were recorded with a spectral resolution of 4 cm^{-1} and a total of 1024 scans were averaged for each spectrum. The MIR spectra were obtained between 4000 cm^{-1} (2500 nm) and 600 cm^{-1} (16,700 nm) using a liquid-nitrogen cooled mercury-cadmium-telluride detector, KBr beamsplitter and a globar energy source. All MIR data were recorded with a spectral resolution of 4 cm^{-1} and a total of 512 scans were averaged for each spectrum. These high resolution spectral data were then down-sampled to simulate the ASTER responses.

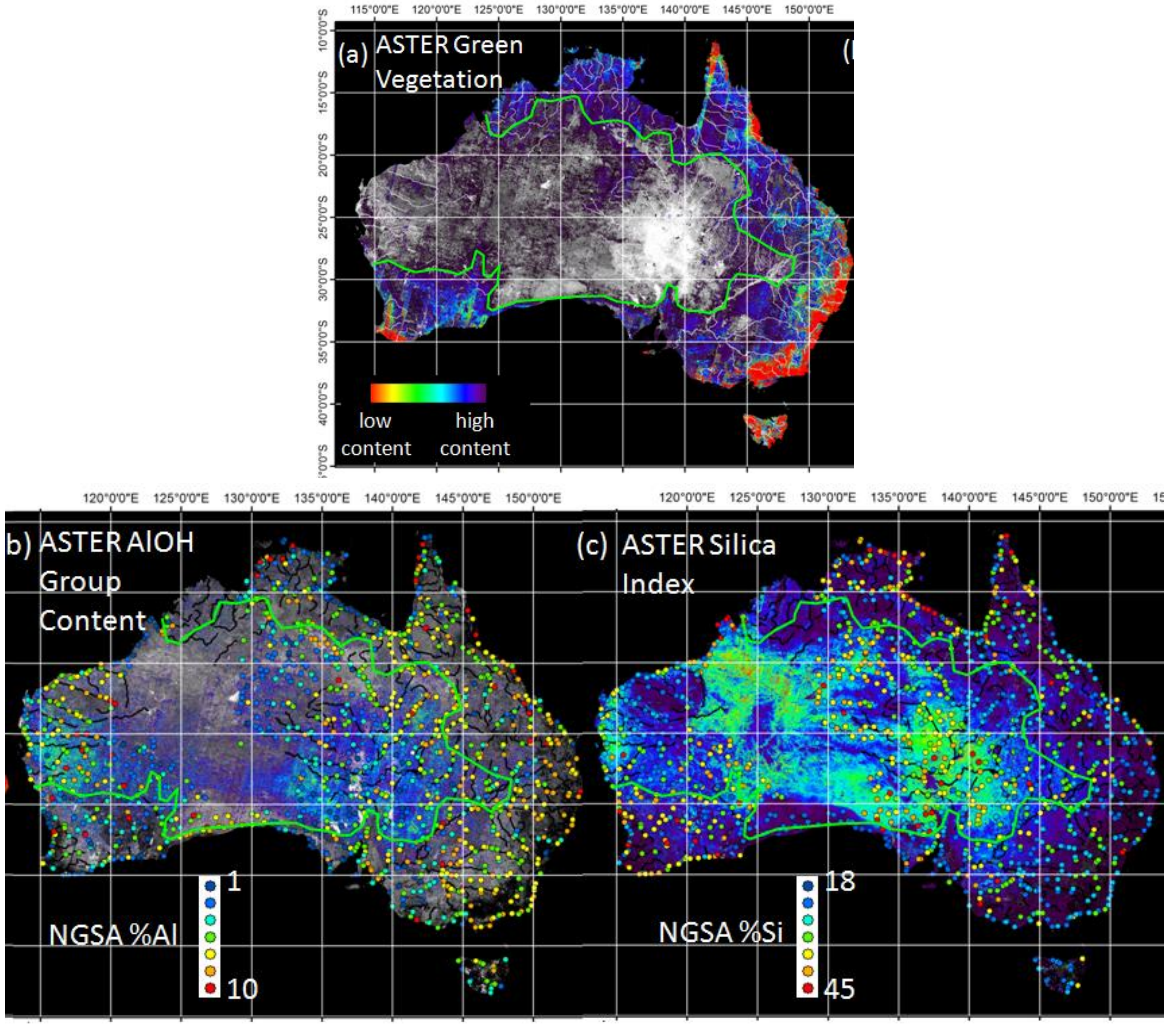

Figure 1. (a) ASTER green vegetation; (b) ASTER AlOH Group content and NGSA %Al; and (c) ASTER Silica Index and NGSA %Si. The green line shows the apparent boundary of abundant green vegetation from the ASTER product (a).

The results to date show significant correlations between the NGSA and simulated ASTER products measured from the 165 random samples, including: (i) ASTER Silica Index with NGSA %Si, %sand and inverse %clay; and (ii) ASTER AlOH Group composition with NGSA loss on ignition and a weathering index based on Si/(Si+Al+Ca+Mg+K+Na).

Figure 1 presents three of the National ASTER geoscience products together with point sample NGSA data. The current Version 1 ASTER geoscience products do not compensate fully for vegetation effects (Figure 1a), which can be improved through unmixing methods to more accurately map/measure the surface mineral information. This vegetation dilution effect is apparent in the Version 1 ASTER AlOH Group Content product (Figure 1b), where areas of high clay (%Al) content in the vegetated eastern part of Australia are under-predicted. In contrast, for Western Australia where vegetation is sparser, there is better correspondence between the NGSA and ASTER results. There is little, if any, apparent effect of vegetation on the ASTER Silica Index product (Figure 1c), which shows close spatial (and statistical) similarity with the NGSA %Si. This

particular ASTER geoscience product can be valuable for mapping the distribution of quartz sandy deserts (cover) across Australia, with possible implications for tracking the process of "desertification".

Mineralogy can also be used as a surrogate for mapping chemical parameters in the regolith, such as pH. For example, the Al-clay mineral montmorillonite is indicative of alkaline soils, while kaolinite is an indicator for more neutral to acidic soils. The ASTER geosciences map AlOH Group Composition was designed to map this clay compositional information (Figure 2), which shows spatial correlation with NGSA pH data for large parts of Australia, such as the Eucla and Lake Eyre Basins (montmorillonite and alkaline) versus tropical regions of northern Australia (kaolin and acidic).

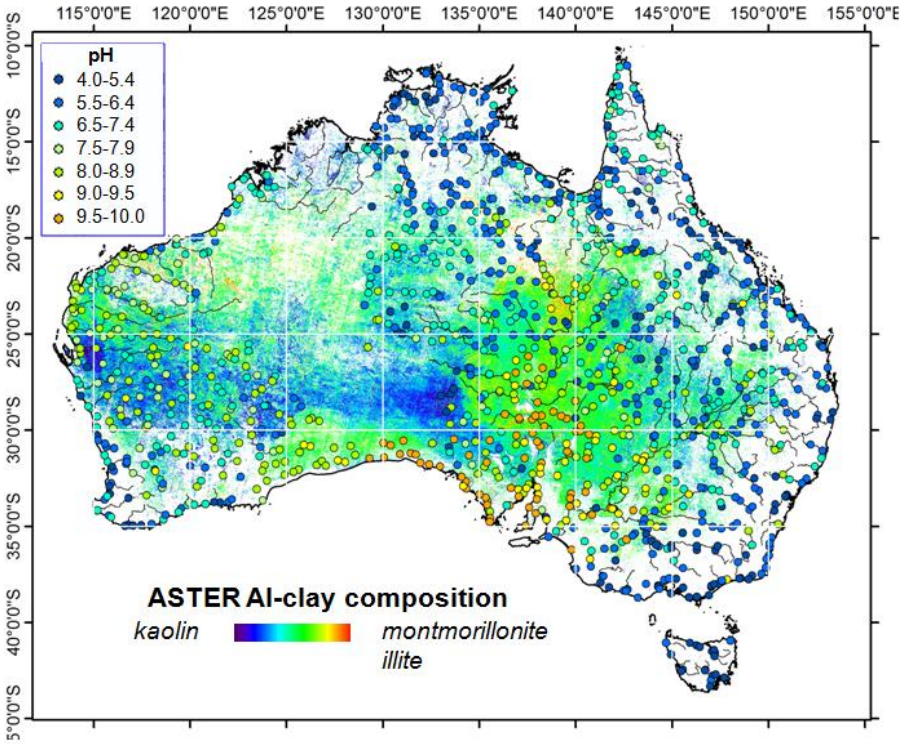

Figure 2. ASTER AlOH Group Composition and NGSA pH.

Additional correlations with these data, which have regolith implications on mapping/monitoring weathering intensity and erosion-deposition, are currently being prepared for publication.

Acknowledgements
Matilda Thomas and Patrice de Caritat publish with the permission of the CEO of Geoscience Australia.

References

Caritat, P. de, Cooper, M., 2011. National Geochemical Survey of Australia: The Geochemical Atlas of Australia. Geoscience Australia Record, 2011/20 (2 Volumes + Dataset), 557 pp. Available at: https://www.ga.gov.au/products/servlet/controller?event=GEOCAT_DETAILS&catno=71973

Cudahy, T., 2012. Satellite ASTER Geoscience Product Notes for Australia. CSIRO ePublish No. EP-30-07-12-44

Cudahy, T., Caccetta, M., Hewson, R., Collings, S., Thomas, M., Laukamp, C., Ong, C., Rodger, A., Lau, I., Chia, J., Woodcock, R., Fraser, R., Rankine, T, Vote, J., Warren, P., Abrams, M., Yamaguchi, Y., Kato, M., Ninomiya, Y., Doescher, C., Saxon, S., Meyer, D., Jones, M., Tyler, I., Mauger, A. and Close, D., (2012): Satellite ASTER Geoscience Map of Australia. v1. (DOI. 10.4225/08/51400D6F7B335).

Cudahy T , Jones, Thomas M, Cocks P, Agustin F, Caccetta M, Hewson, R, Verrall, M, and Rodger A (2010). Mapping soil surface mineralogy at Tick Hill, north-western Queensland, Australia, using airborne hyperspectral imagery In 'Proximal Soil Sensing', Progress in Soil Science, Vol. 1 Ed. R. Viscarra Rossel, A. McBratney, B. Minasny. Springer-Verlag.

Howard, F., Thomas, M. and English, P. 2012. A Preliminary Case Study in Characterising and Mapping Australian Salt Lakes. 15th ANZGG Conference, Bundanoon, 2012, Abstracts.

Thomas, M., Cudahy, T. and Caccetta, M. 2012. Recent developments in ASTER Geoscience products for Australia. 2012 Australian Regolith Geoscience Association (ARGA) Conference, Mildura.

Regolith and regolith geochemistry in several dimensions

P.A. Morris

Geological Survey of Western Australia, 100 Plain Street, East Perth, WA 6004

Introduction

With fewer mineral deposits found at or near to the surface, exploration for bedrock-hosted mineralization is being increasingly focused in areas of suspected but unproven mineral potential (greenfields areas). Typically, these areas have extensive and often thick regolith cover, although the exact thickness of regolith is usually unknown, due to the lack of exploration activity (e.g., drilling). As regolith is thick and transported (hence genetically unrelated to the underlying bedrock) it is viewed with little confidence in terms of a useful sample medium for regional geochemical programs. Other sample media have been used to 'see though' cover, such as termites (Petts et al., 2009), vegetation (Reid et al., 2010) or water (Gray et al., 2009). They have met with some success, but these media are not always suitable for grid-based surveys.

Although some doubt has been cast on the effectiveness of regolith as a sample medium in areas of thick and allochthonous cover (e.g., Anand et al., 2007), other studies have shown that mineralization buried beneath tens to hundreds of metres of such cover can be detected using soil as a sample medium (e.g. copper mineralization in Chile; Cameron et al., 2010). The approach taken by Cameron and co-workers was to focus on a soil fraction (particularly the fine fraction), which had the ability to sequester a component of the buried mineralization that had migrated sub vertically from its bedrock location. This exogenic component takes advantage of the elevated high cation exchange capacity of clay minerals to weakly bond or bind components. Combining this part of the sample medium with a suitable digest capable of stripping the exogenic component while ignoring the same component in the sample medium (the endogenic component) means that buried mineralization can be detected.

Regional regolith geochemistry in the east Wongatha area

The fine fraction exogenic/endogenic approach has been employed by GSWA in a regional regolith geochemistry program in the east Wongatha area on the eastern edge of the Archean Yilgarn Craton, where it abuts the Archean – Proterozoic Albany-Fraser Orogen. Both of these units are unconformably overlain by younger sedimentary rocks of the Gunbarrel Basin (Fig. 1). The Yilgarn Craton, and more recently the Albany-Fraser Orogen have documented bedrock-hosted mineralization, in particular gold. In the area of GSWA's program, rare earth element (REE; La – Lu), base metal and gold mineralization has been detected close to the Gunbarrel Basin margin at Mulga Rock (Energy and Minerals Australia, 2010). The east Wongatha area is dominated by regolith (about 3% outcrop; McGuinness, 2011), the majority of which is sandplain, occasionally supporting elongate dunes. Sparse and heterogeneously distributed drill hole information shows that regolith is between 5 and 121 m thick (average 55 m, n = 950; Morris, 2013).

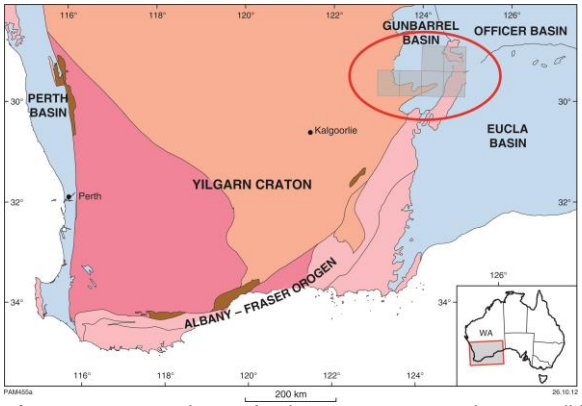

Figure 1. Location of the east Wongatha regolith geochemistry sampling program.

The GSWA program involved regolith sampling from 835 sites over an area of approximately 13 000 km^2. At each site, approximately 5 kg of unconsolidated regolith was collected at about 90 cm

depth using a power auger. Sufficient of the dry-screened <50 µm fraction of each sample was digested with aqua regia, then analysed for more than 50 elements largely by ICP.

The known association of gold mineralization and greenstones elsewhere in the Yilgarn Craton is evident in the distribution of fine-fraction gold from the east Wongatha area, where statistically anomalous Au concentrations (i.e., that above 9 ppb) are not only found on or close to greenstones (shown by aeromagnetic anomalies on MINIGWAL; Fig. 2) but also on aeromagnetic extensions of greenstones beneath the Gunbarrel Basin. However, some samples with anomalous concentrations found on the margins of the Gunbarrel Basin on NARNOO (Fig. 2) are not associated with greenstones, but instead could be indicative of unconformity-hosted mineralization typical of that found at Mulga Rock.

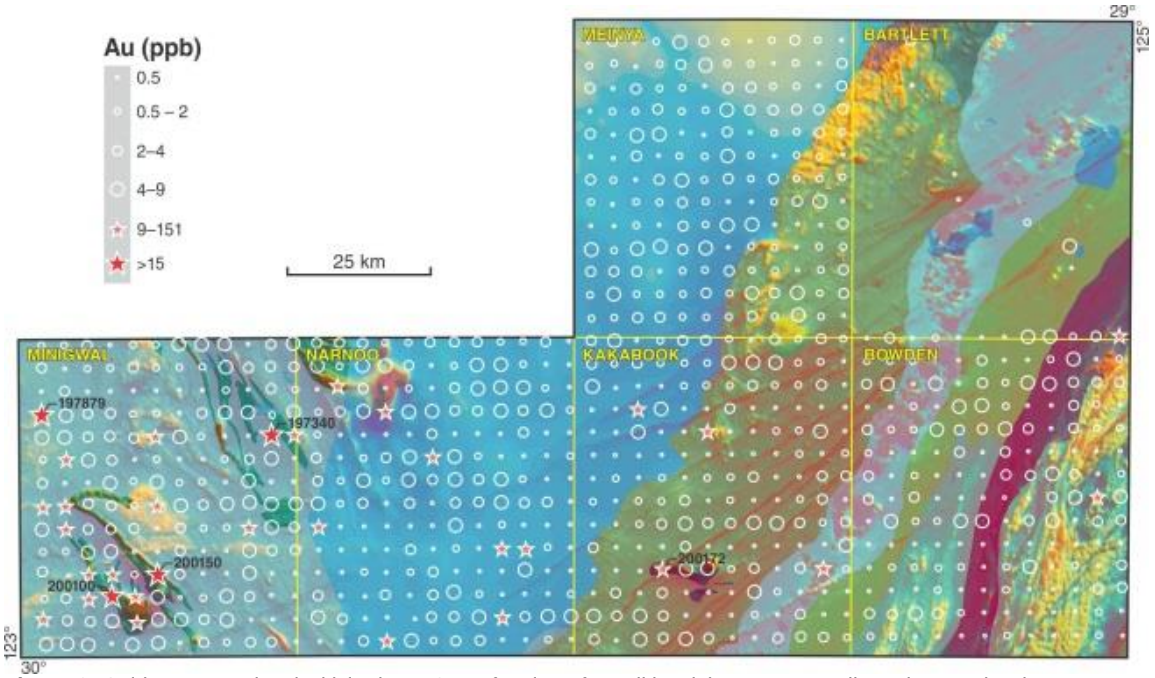

Figure 2. Gold concentration (ppb) in the <50 µm fraction of regolith. Pink stars are outlier values and red stars are extreme values. Note strong association of Au and greenstones (MINIGWAL), Au and aeromagnetic extensions of greenstones, and Au and the Gunbarrel Basin margin (NARNOO).

The established spatial relationship between known or suspected gold mineralization and either particular lithologies or structures gives some credence to the model of vertical migration through transported cover and sequestering of the exogenic mineralization signature in the fine fraction. A strong correlation of gold following both aqua regia and deionized water digestion (Morris, 2013) indicated that gold was not only fine grained but also water soluble. Further support for fine and ultrafine fraction gold came from reconnaissance work on gold in various size fractions of 14 regolith samples from the east Wongatha program (Noble et al., 2013), showing that the 2 – 0.2 µm fraction of one sample had more than 2 ppm gold.

Sandpit locality

Validation of the vertical migration model in the east Wongatha area required some knowledge of the third dimension ─ i.e., whether surface gold anomalies persisted at depth. To investigate this, a pit was excavated at a sandplain site with anomalous fine-fraction gold, and a series of samples were collected for analysis from the pit wall. During the regional program, a <50 µm fraction of regolith from this site produced a gold concentration of 14 ppb. The excavation also offered the opportunity to collect samples for optically stimulated luminescence (OSL) dating of quartz sand.

Figure 3a. Excavating at the Sandpit locality, east Wongatha area

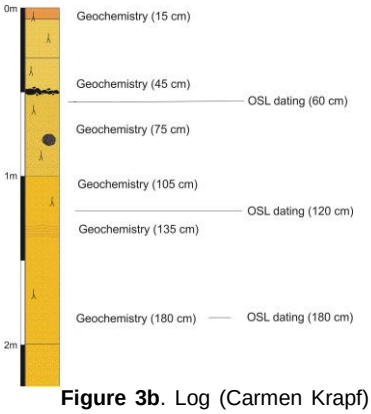

Figure 3b. Log (Carmen Krapf) and sample locations, Sandpit excavation.

The selected site is in the southern part of the NARNOO sheet (Fig. 2), close to the Gunbarrel Basin margin. The area is characterized by featureless sandplain with elongate dunes spaced at approximately 500 m intervals (Fig. 3a). The 1.8 m deep pit is characterized by broadly homogeneous quartz sand with localised cross-bedding. Root casts are found throughout and there are signs of bioturbation. Six samples were collected for geochemistry (Fig. 3b) and three samples for OSL dating. The fine-fraction chemistry shows that there is little variation in the Fe, As, Ca or Sr content of regolith with depth (Fig. 4), equating to limited ferruginisation, little sulphide, and minimal carbonate throughout.

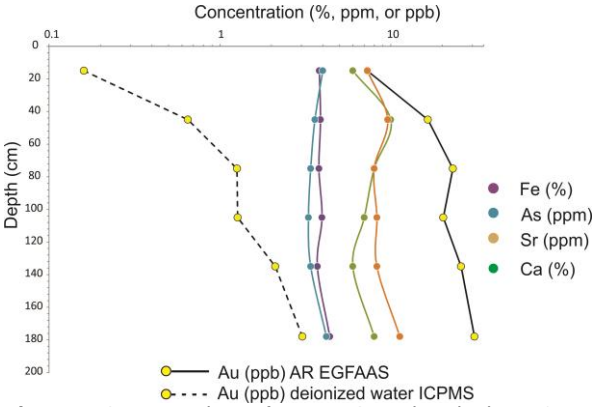

Figure 4. Concentrations of Fe, As, Sr and Au in the <50 µm fraction of regolith from the Sandpit location, and Au by aqua regia (AR) and deionized water digestion.

In contrast, fine-fraction gold following both aqua regia and deionized water digestion shows a consistent increase in concentration with depth. The OSL results show an increase in age from 6.7 ± 1.8 ka at 60 cm depth, to 90.9 ± 19.0 ka at 180 cm. These data indicate a sand accumulation rate of approximately 1 mm/70 years.

Additional samples collected within 20 m of the pit at a depth of approximately 90 cm have similar fine-fraction gold concentrations as the original sample i.e., 14 ppb. However, the shallowest sample in the pit, taken at 15 cm, contains 7 ppb gold, which is in the background range for the east Wongatha area. The implication is that samples collected at shallow depth are too young to have inherited an exogenic component from mineralization, which has implications for regional geochemical exploration programs.

The lack of drilling data means there is no information on the thickness of regolith cover at the Sandpit locality. In an attempt to gain such information GSWA has a program using passive seismic to estimate the thickness of both regolith and sedimentary rock sequences (Scheib and Morris, 2013). Passive seismic is a rapid non-invasive technique which estimates the depth of an impedance contrast between one or more units by measuring both the horizontal and vertical component of naturally-occurring seismic waves. The equipment is both cheap and portable, and each site reading takes about 15 – 20 minutes. The thickness of a unit is a function of the

frequency at which there is a notable change in the horizontal to vertical (H/V) signal of the ambient seismic 'noise'. The relationship is shown by:

$f_z = V_s/4h$

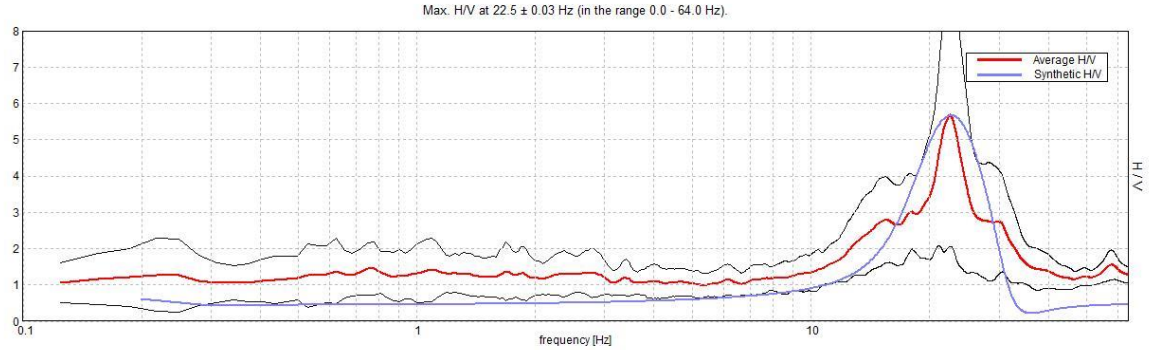

Figure 5. Passive seismic trace measured at the Sandpit locality, east Wongatha area, showing the ratio of the averaged horizontal to vertical change in seismic velocity (H/V) versus frequency as red line. Black lines are the 95% confidence limit. A peak in the trace occurs where there is a change in impedance, corresponding to a lithological boundary. The frequency at which this occurs can be related to depth according to $f_z = V_s/4h$ (see text). Blue line is the modelled trace using estimated V_s and h. At this location, regolith is modelled to be approximately 5 metres thick.

where f_z is the frequency at which there is a notable impedance change, V_s is the shear wave velocity, and h is the unit thickness. The frequency can be read from the passive seismic trace (Fig. 5), whereas V_s can be estimated from values documented from other similar units, or by knowing h from drilling data. Passive seismic data indicates a regolith cover thickness of 5 m at the Sandpit locality.

Conclusions

The GSWA program carried out in the east Wongatha area has shown that the fine fraction of regolith is useful in detecting mineralization buried beneath thick transported cover. At one locality, the concentration of anomalous fine-fraction gold at the surface increases with depth, and is not controlled by the amount of regolith carbonate or ferruginisation. The liberating of gold from the fine fraction by weak digests indicates gold is not only fine grained but also labile. The use of OSL to date regolith can impart useful information on the rate of accumulation of a buried mineralization signature in regolith, whereas passive seismic offers a relatively cheap, rapid and non-invasive method to investigate regolith thickness. The combination of these techniques provides useful information in terms of not only understanding regolith in four dimensions, but also some insight on how transported regolith can be used to detect bedrock-hosted mineralization.

References

Anand R.R., Cornelius M. and Phang C. 2007. Use of vegetation and soil in mineral exploration in areas of transported overburden, Yilgarn Craton, Western Australia: A contribution towards understanding metal transportation processes. *Geochemistry: Exploration, Environment, Analysis* **7**, 267-288.

Cameron E.M., Leybourne M.I., Reich M. and Palacios C. 2010. Geochemical anomalies in northern Chile as a surface expression of the extended supergene metallogenesis of buried copper deposits. *Geochemistry: Exploration, Environment, Analysis* **10**, 157-199.

Energy and Minerals Australia 2010. Mulga Rocks Ambassador deposit lignite uranium results and confirmation of polymetallic mineralisation. *Report to Australian Securities Exchange*, 10 May 2010.

Gray D.J., Noble R.R.P. and Reid N. 2009. Hydrogeochemical mapping of the northeast Yilgarn groundwater. *Geological Survey of Western Australia Record* **2009/21**, 78p.

McGuinness S.A. 2010. Regolith-landform mapping of the east Wongatha area. *In*: 1:100 000 Geological Information Series – East Yilgarn, 2010 update.

Morris, P.A. 2013. Fine fraction regolith chemistry from the East Wongatha area, Western Australia: tracing bedrock and mineralization through thick cover. *Geochemistry: Exploration, Environment, Analysis* **13**, 21-40.

Noble R.R.P., Cavalière M., Morris, P.A., Pinchand G.T. and Hough R.M.2013. Determination of micro and nanoparticulate fraction gold in regolith. *Explore* **159**, 1-13.

Petts A., Hill S.M. and Worrall L. 2009. Termite species variations and their importance for termitaria biogeochemistry: Towards a robust media approach for mineral exploration. *Geochemistry: Exploration, Environment, Analysis* **9**, 257-266.

Reid N., Lintern M., Anand R., Pinchand T., Gray D.J., Ryan R.P., Sutton G. and Jarrett R. 2010. North east Yilgarn biogeochemistry project (MERIWA). *Geological Survey of Western Australia Record* **2010/4**, 154p.

Scheib A. & Morris P.A. 2013. Passive seismic estimates of cover thickness – essential information for geochemical surveys in regolith-dominated terrains. *26th International Applied Geochemistry Symposium poster*, Rotorua, New Zealand.

The Loxton-Parilla Sands of the Western Murray Basin – From Macro to Micro Scale

S. M. McLennan[1,2], S. Hill[3], D. Giles[2], K. Barovich[1], & S. van der Wielen[2]

[1] University of Adelaide, School of Earth and Environmental Science, Mawson Building, North Tce, Adelaide SA 5005
[2] Deep Exploration Technologies Cooperative Research Centre, PO Box 66, Export Park Adelaide Airport SA 5950
[3] South Australian Geological Survey, GPO Box 1264, Adelaide SA 5001

Introduction

The Murray Basin covers some 300,000 km^2 of southeastern Australia, including large tracts of basement prospective for gold and other base metals. The sedimentology and hydrogeology of the basin is well understood however geochemical studies of the Cenozoic sediments are rare. This work is aimed at characterising the geochemistry of a portion of the Murray Basin, the Loxton-Parilla Sands, and linking it to the depositional environment and post-depositional conditions through the region. It seeks to understand how controls like parental lithology, climate, and landscape morphology influence the modern geochemistry of the formation and how it relates to the underlying basement geology and mineralisation.

The Loxton-Parilla Sands

The Loxton-Parilla Sands is a Late Miocene-Pliocene strandplain generally 15 – 60 m thick but up to 150 m thick in parts. The sediment package is comprised of shallow to marginal marine facies and minor estuarine and fluvial components (Brown & Stephenson 1991). Lithology and morphological expression of the Loxton-Parilla Sands and Karoonda Surface varies across its 135,000 km^2 distribution, mostly as a result of changing depositional environments and post-depositional weathering overprints. The undifferentiated Loxton-Parilla Sands are characterised by grey to yellow quartz sands, often iron stained to deep orange and red.

The lithology varies from silty sands to coarse sand and rare gravelly clay lenses. Sediments range from poorly consolidated “running sands” to sands strongly cemented with iron oxides, kaolin, or silica. Induration often increases up-sequence. The Loxton-Parilla Sands consists of clean quartz sand with little feldspar content and local heavy mineral concentrations. Heavy mineral assemblage of the Loxton-Parilla Sand includes zircon, ilmenite, leucoxene, rutile and minor monazite (Roy & Whitehouse 2003). Detrital muscovite is also present, especially in the lower sections of the unit. Thin goethitic horizons are common weathering overprints. Broad coarsening-upwards sequences are common. Broad scale cross-bedding (> 10 cm) is observed some outcrops but most of the sediments are either flat-lying or massive. Dissolution pipes occur in well-indurated parts of the formation. These features tend to be filled with nodular, reworked portions of the Loxton-Parilla Sands.

Groundwater in the unconfined to semi-confined Loxton-Parilla Sands aquifer is acidic (pH from 4.5 to <3.5), salty (over 50,000 mg/L TDS in some parts) and contains high soluble iron concentrations (Macumber 1991). Acidic groundwater is generally restricted to the upper reaches of the aquifer, to about 25 m below the water table (Macumber 1991). This more acidic groundwater also tends to be more oxidised than the water lower down (Macumber 1991). The major source of iron in groundwater in the Loxton-Parilla Sands aquifer is considered mobilisation of iron in recharging and through-flowing groundwater from the ferruginised Karoonda Surface.

Dune ridges of the Loxton-Parilla Sands are visible in elevation models and have also been mapped in considerable detail from remote imagery. The low feldspar and high quartz content on the sands shows up as dark bands on radiometric surveys, while the ferruginisation and magnetite content of the overlying Karoonda Surface is revealed as anomalous lines on magnetic datasets (Miranda 2007). Thermal night time imagery has also been successful in mapping the extent of preserved ridges (Kotsonis 1995).

Previous studies

Porosity of the sands and extensive post-depositional weathering has made it difficult to define the absolute timing of deposition of the Loxton-Parilla Sands. Most researchers have used correlations with units of known ages to constrain timing of deposition for the Loxton-Parilla Sands. Paine (2004), for example, places the start of deposition at 6.6 Ma as this was the time of the maximum extent of the Miocene-Pliocene transgression (Loutit & Kennett 1981, Brown 1983), while the youngest possible age of deposition is 4.0 Ma as basalts of this age cover ridges in the SW of the strandplain. Paleomagnetic dating of the overlying Blanchetown Clay by Zhisheng *et al*. (1986) gives an upper limit to deposition of the Loxton-Parilla Sands of 3.4 Ma but it is difficult to quantify the extent of erosion between the end of the regression and development of Lake Bungunnia. Miranda *et al*. (2009) used Sr isotopes recovered from unaltered molluscs, such as brachiopods, pectens, and bivalves. These results provide an absolute time constraint from within the Loxton-Parilla Sands, rather than correlations from other dated formations. From this, the period of deposition has been defined as starting at 7.2 Ma to somewhere between 5.0 – 4.5 Ma.

Current study

More than 800 samples have been taken from outcrop in cliffs, road cuttings, and gravel pits (Figure 1). These outcrops tend to only expose the top 4-18 m of the Loxton-Parilla Sands. Samples were also collected from stratigraphic and water bores and petroleum wells held by Geoscience Australia, Geological Survey of Victoria and Geological Survey of South Australia.

Prior to geochemical analysis samples were scanned using a HyLogger^{TM} core scanner at the South Australian Geological Survey Core Library. Samples were then analysed for bulk geochemistry by Acme Laboratories in Vancouver, Canada. For REE and refractory elements analysis was via ICP-MS with a lithium borate fusion and dilute acid digestion. Precious metals, base metals, and pathfinder elements were analysed via ICP-MS following aqua regia digestion. Oxides were analysed via XRF following fusion with lithium tetraborate/lithium metaborate flux. Microanalysis was performed on polished petrological thin sections with a Philips XL40 scanning electron microscope and Cameca SXFive electron microprobe at Adelaide Microscopy. Boreholes with formation information were sourced from the Murray Basin subsurface stratigraphic database (Brown & Stephenson 1986). Over 2000 drill holes intersecting the Loxton-Parilla Sands were digitised from printed microform records. This information was then imported into gOcad and used to produce a 3D geological map.

Discussion and conclusions

Microanalysis enables further resolution of bulk geochemistry to reveal some mineral speciation. Given the extensive acid sulphate weathering system that has been superimposed on the strandplain, sulphate minerals should also account for a proportion of the mineralogy. This is difficult to constrain in the bulk geochemistry without sulphate analysis. Preliminary scanning electron microscopy, however, shows barite and celestite phases in pore spaces, typical of acid sulphate weathering conditions. Integrating geochemistry, mineralogy, and sedimentology datasets into a single model allows for the visualisation of heterogeneity at the profile scale up to the basin scale while microanalytical techniques provide further information on weathering events and controls on geochemistry.

Acknowledgments

The authors would like to acknowledge the support of the Deep Exploration Technologies CRC in undertaking this research.

References

BROWN C. M. 1983. Discussion : A Cainozoic history of Australia's Southeast Highlands. *Journal of the Geological Society of Australia* **30**, 483-486.

BROWN C. M. & STEPHENSON A. E. 1986. Murray Basin, southeastern Australia: subsurface stratigraphic database. *Bureau of Mineral Resources Australia Report*.

BROWN C. M. & STEPHENSON A. E. 1991. Geology of the Murray Basin, southeastern Australia. *Bureau of Mineral Resources, Geology and Geophysics Australia. Bulletin.*

KOTSONIS A. 1995. Late Cainozoic Climatic and Eustatic Record from the Loxton-Parilla Sands, Murray Basin, Southeastern Australia. Master of Science thesis, School of Earth Sciences, University of Melbourne, Melbourne (unpubl.).

LOUTIT T. & KENNETT J. 1981. Australasian Cenozoic sedimentary cycles, global sea level changes and the deep sea sedimentary record. *Oceanologica Acta* **4**, 45-63.

MACUMBER P. G. 1991. *Interactions between groundwater and surface systems in northern Victoria*. Victorian Department of Conservation and Environment.

MIRANDA J. A. 2007. Late Neogene stratigraphy and sedimentation across the Murray Basin, southeastern Australia. PhD thesis, School of Earth Sciences, University of Melbourne (unpubl.).

MIRANDA J. A., WALLACE M. W. & MCLAREN S. 2009. Tectonism and eustacy across a Late Miocene strandplain: The Loxton-Parilla Sands, Murray Basin, southeastern Australia. *Sedimentary Geology* **219**, 24-43.

PAINE M. D. 2004. Distribution, Character and Provenance of Late Miocene to Pliocene Stranded Coastal Sediments in Southwestern Victoria. PhD thesis, Department of Applied Geology, Curtin University of Technology (unpubl.).

ROY P. S. & WHITEHOUSE J. 2003. Changing Pliocene Sea Levels and the Formation of Heavy Minerals Beach Placers in the Murray Basin, Southeastern Australia. *Economic Geology* **98**, 975-983.

ZHISHENG A., BOWLER J. M., OPDYKE N. D., MACUMBER P. G. & FIRMAN J. B. 1986. Palaeomagnetic stratigraphy of Lake Bungunnia: Plio-Pleistocene precursor of aridity in the Murray Basin, southeastern Australia. *Palaeogeography, Palaeoclimatology, Palaeoecology* **54**, 219-239.

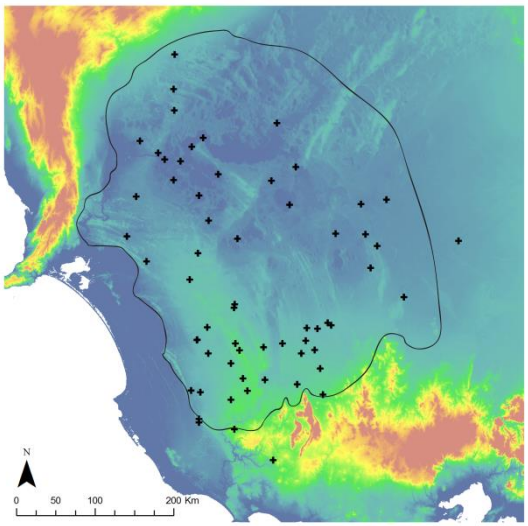

Figure 1: SRTM 3 second Digital Elevation Model (Geoscience Australia) with sample locations (crosses) and outline of the extent of the Loxton-Parilla Sands. Arcuate ridges trending NW-SE across the study area are the strandlines of the Loxton-Parilla Sands.

Hydrogeochemistry and other "aqueous phase" media in exploration

David J. Gray, Nathan Reid and Ryan R.P. Noble
CSIRO Earth Science and Resource Engineering, Kensington, WA 6151

Introduction

Groundwater sampling can represent an effective method for mineral exploration. As a media it is conceptually similar to partial extractions and biota sampling. The methods have advantages such as high signal-to-noise, although conversely there are batch effect and detection limit issues. We discuss the utility of groundwaters for geological sensing and mineral exploration in specific environments, as well as sensitivity to faults and other geological structures, with some generic ideas for geochemical exploration.

"Aqueous Phase" Exploration Methods

Despite some differences, groundwater, biota and selective extraction methods can conceptually be classed together. These techniques all involve dissolution of target elements into an aqueous phase, be they water, a biologically active fluid, or a chemical extractant in the field or laboratory. All these technologies are being actively investigated worldwide, for their potential to add value to "standard" geochemical and geophysical techniques. Understanding the robustness and comparative utility of these technologies is essential, as the usefulness of individual techniques will vary depending on area, lithology and geomorphology.

Exploration Issues

Use of Traverses

Numerous case studies for surface exploration methods involve single (or very few) traverse(s) across mineralisation, with varying depths of barren cover. "Success" can include an apical, "rabbit ear" or other shaped anomaly. The number of acceptable technical successes and potential for various natural (e.g., surface flow) or anthropogenic (e.g., drilling dust) effects means that "positive" results should be treated with scepticism. Given the traverses are commonly selected over previously identified ore bodies, they also represent severely biased data-sets.

Even if successful, this does not represent a direct exploration technique, as these technologies are more likely to add value for area selection or drilling targeting than for orebody resolution. As such, it is necessary that data values are "stand-alone", requiring good background data for differing rock types and geomorphological environments, and that batch-effects be minor, relative to thresholds. Good meta-data is essential to the success of any exploration method.

Scale Effects

Mineral systems concentrate various elements in particular zones and at various scales. For aqueous phase media, this is further complicated by the differing mobilities of various elements depending on the environment. In acidic groundwater environments, base metals may be highly mobile and give consistent haloes, although there are also high background concentrations due to acid attack on country rocks. In neutral groundwater environments, base metals commonly have low mobilities and oxy-anions (Mo, W, As) give larger and more consistent haloes.

At close scales (100 m spacing) sulfide ore bodies are clearly delineated by anomalous dissolved sulfate. Commonly this is enrichment due to sulfides fully oxidising, e.g.:

$$2FeS_2 + 3½O_2 + 7H_2O \rightarrow 2Fe(OH)_3 + 4SO_4^{2-} + 8H^+$$

However, in deeper groundwaters and/or eroded terrains (see below), groundwaters close to sulphide could (counter-intuitively) have lowered dissolved sulfate concentrations, e.g.:

$$5FeS + SO_4^{2-} + 2H_2O + 2H^+ \rightarrow 3FeS_2 + 2Fe(OH)3$$

By relating sulfate to conservative elements such as Cl or Br, a sulfate index can be calculated (Figure 1). At <500m scales, sulfate index anomalism can delineate sulfides. However, at the regional scale this effect is diluted, and instead S indices will pick up fluid mixing (Figure 2), and particularly the upwelling of deeper groundwater through fault systems.

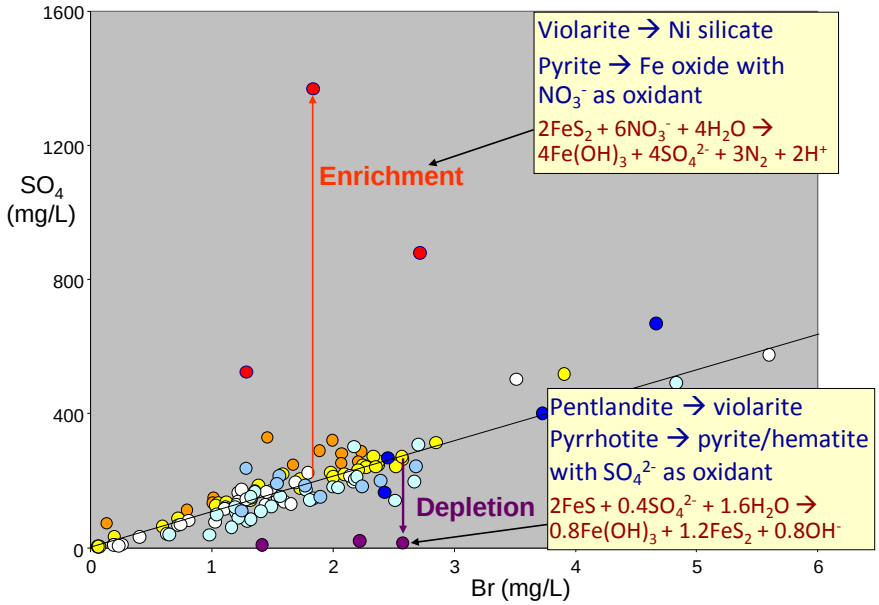

Figure 1: Dissolved sulfate vs Br for groundwaters from Ni sulfide ore bodies.

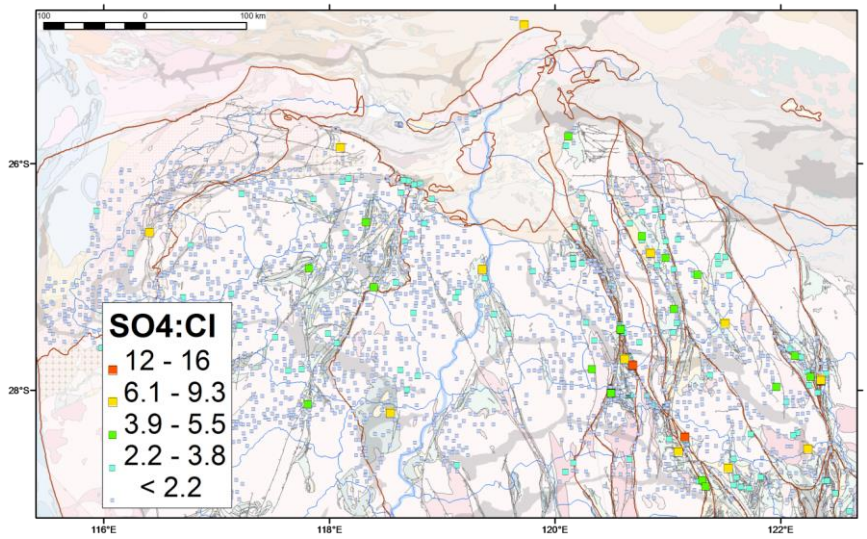

Figure 2: Dissolved sulfate enrichment in the northern Yilgarn Craton. Brown lines are crustal domain boundaries (Cassidy et al., 2006).

Sampling terrain

Despite various assertions in the literature, sample type and geomorphology can have a very strong effect on aqueous phase anomalies. Floodplain soils can give strong soil extraction anomalism, which can mimic buried mineralisation anomalism. Plants show much stronger base metal anomalism in eroded vs covered or deeply weathered terrains. In some terrains, particularly in southern regions of Australia (e.g., the southern half of the Yilgarn Craton), the upper 20 m of the water column can be 3 pH units lower than deeper groundwaters. In such a situation, mapping results for both shallow and deeper groundwaters will show highly erroneous spatial patterns.

Contamination

"Aqueous phase" extractions are generally only a small proportion of the element concentrations in the original rock. Site understanding and/or contamination indices are essential, as they are very sensitive to contamination sources, such as:

- Organic and other contaminants falling into groundwater bores;
- Drilling muds and additives
- Wind-blown soil or, more critically, drilling dust on plant surfaces
- Colluvial and/or alluvial mixing in soils from mineralised areas upgradient
- Drill-spoil contamination of soil

Case Studies

Continental-Scale Hydrogeochemistry

Interpreting groundwater or other geochemical data at the continental scale (Figure 3) requires resolving issues related to differing analytical quality, and sometimes differing sampling and analytical methods. At this level, this will enable discrimination of utility of these methods for varying terranes, e.g., from very acid/saline in the south of the continent, mostly fresh and neutral in the western 2/3, and sulfate-poor in the artesian dominated system of the NE (Figure 4). In each case, it is likely that differing element suites and indices will be valuable for exploration.

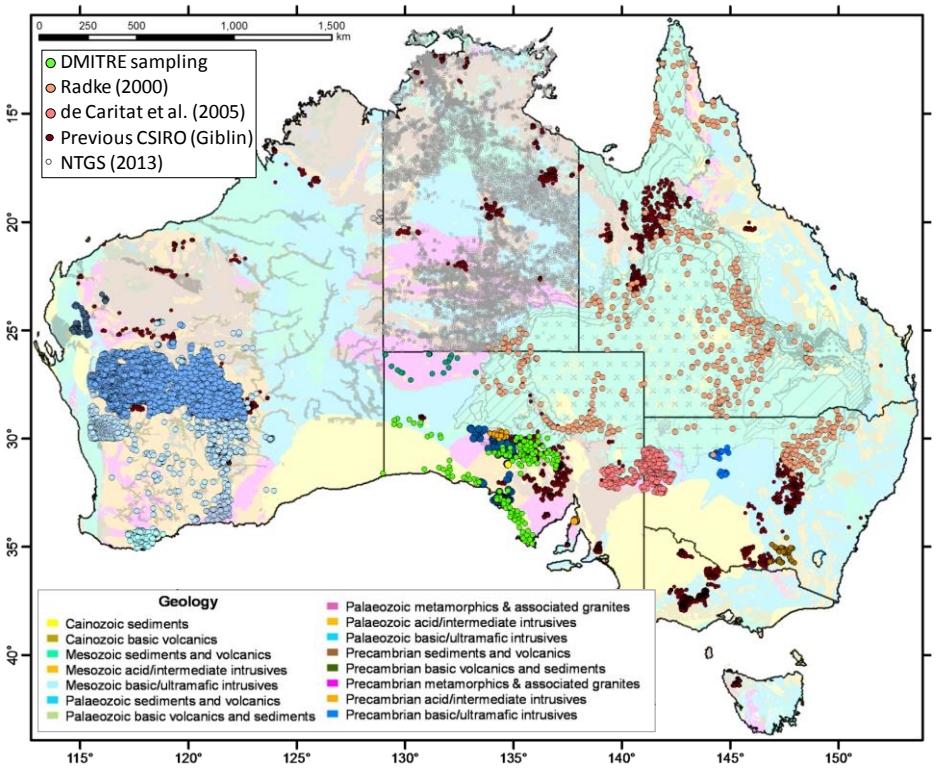

Figure 3. Progress towards a Continental-scale Hydrogeochemistry database. (Aside from those referenced in the top key, this data represents direct sampling by CSIRO Perth and/or collaboration with Geological Surveys or Explorers.)

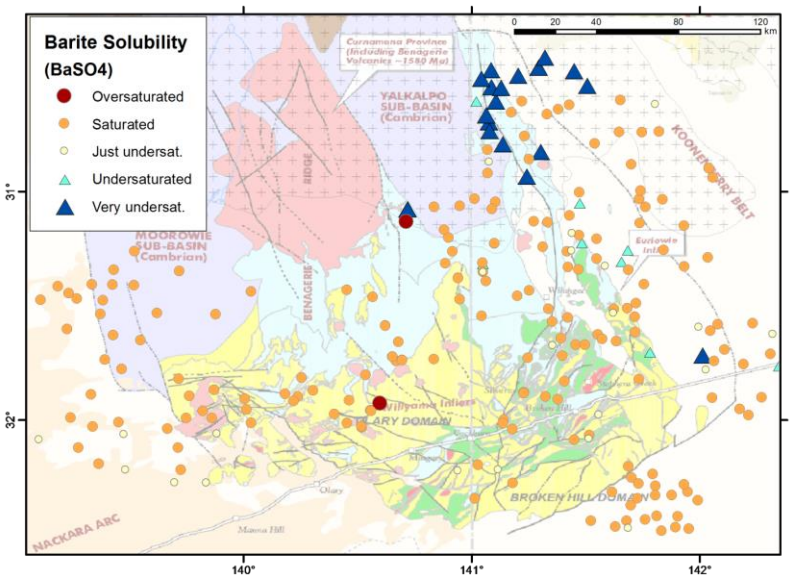

Figure 4: Abrupt change from sulfate-poor barite under-saturated groundwaters from the Great Artesian Basin (stippled area), to the sulfate-rich barite saturated groundwaters within the Curnamona Domain (de Caritat et al., 2005).

Terrain-Scale Hydrogeochemistry

At this scale (e.g., Figure 2), specific indices have value in delineating large scale lithological discrimination, and major mineral camps. Such a broad-scale approach does obscure camp scale-variation but does delineate major features, such as the Agnew and Granny Smith Gold camps. Other large systems, such as IOCG's or Cu Porphyries may also be observable.

Prospect-Scale Hydrogeochemistry

At this scale, indicator elements (e.g., Au, Ni, Cu, Zn, W, As) are commonly valuable. Geochemical Indices are developed for specific commodities, such as the AuMin (Figure 5) or NiS index (Figure 6). Combined with geophysics, this may assist in selecting drilling targets.

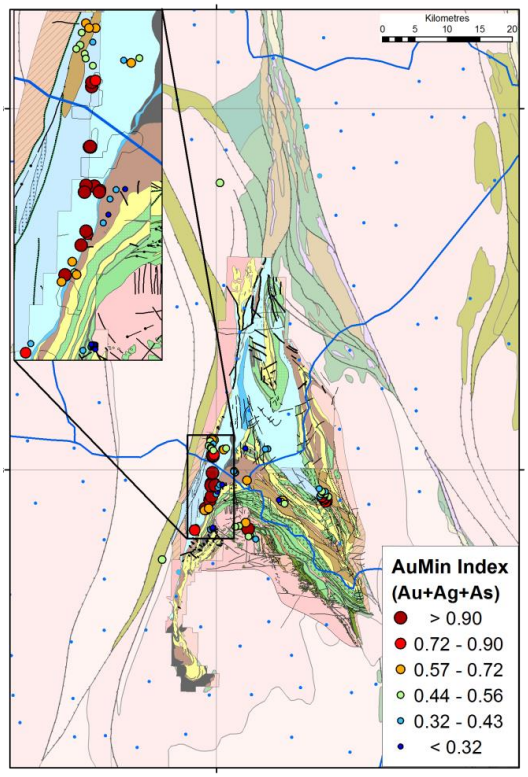

Figure 5. Spatial variation in AuMin Index (Au,Ag,As) in the Agnew region. AuMin values above 0.9 represent anomalism greater than for any of the regional samples.

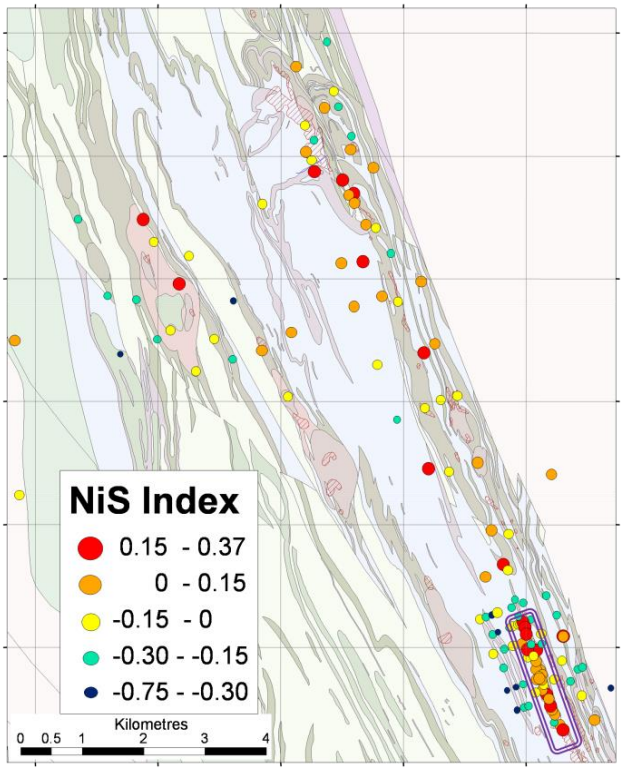

Figure 6. Spatial variation in NiS Index north of Leinster, exactly delineating the Harmony ore body (double purple line), and the line of potential mineralisation to the NNW.

Conclusions

Aqueous phase methods such as hydrogeochemistry have difficulties and advantages as exploration media. However, if combined with robust understanding of environmental factors, rock weathering and good quality analytical chemistry, these techniques can positively assist exploration at varying scales. This is particularly so when combined with robust geological modelling and geophysics. Continuing research and interaction with explorers should contribute to the next phase of economic mineral deposit discovery.

Acknowledgements

This presentation is partially based on a talk given at the 12th SGA Biennal Meeting 2013, August 11-15 2013, Uppsala, Sweden. The research was made possible through the support of CSIRO Minerals Down Under Flagship, and CRCLEME and DET CRC, funded by the Australian Government's Cooperative Research Centre Programme. There has also been substantial support through MERIWA, NSW Geological Survey, South Australian Geological Survey (DMITRE), as well as various Industry sponsors.

References

Cassidy, K.F., Champion, D.C., Krapez, B., Barley, M.E., Brown, S.J.A., Blewett, R.S., Groenewald, P.B. and Tyler, I.M., 2006. A revised geological framework of the Yilgarn Craton, Western Australia. Western Australia Geological Survey Record 2006/8. 8 p.

de Caritat, P., Kirste, D., Carr, G. and McCulloch, M., 2005. Ground water in the Broken Hill region, Australia; recognising interaction with bedrock and mineralization using S, Sr and Pb isotopes. Appl. Geochem. 20, 767-787.

NTGS, 2013. Data contributed to CSIRO. See http://www.lrm.nt.gov.au/water/water-data-portal

Radke, B.M. Ferguson, J. Cresswell, R.G. Ransley, T.R. Haberhehl, M.A., 2000, Hydrochemistry analysis of GAB bores and springs. http://www.ga.gov.au/meta/ANZCW0703015795.html

Regolith influences on surface water and groundwater composition at the Baldry dryland salinity management site, central west NSW

Tony Bernardi[1,2] and Leah Moore[2]

[1]Department of Primary Industries, P.O. Box 408, Queanbeyan, NSW 2620,
[2]Dryland Salinity Hazard Mitigation Program (DSHMP), University of Canberra, ACT 2601

Introduction

Baldry is an upland sub-catchment (260 ha) of the Little River catchment, in the greater Macquarie region; part of the Murray-Darling Basin (MDB) in central west NSW. The Baldry study site covers approximately 50 ha located near the catchment divide, upstream (south) of Dubbo (Figure 1) (Bernardi et al. 2012). The site is characterised by an open low hill and rise landscape with a northward flowing creek and gently inclined slopes (typically <10% gradient) with local geology mapped as deeply weathered early Devonian pink hornblende-biotite Kynuna Granite of the Yeoval Batholith (Wyborn et al. 1999; Raymond 1999).

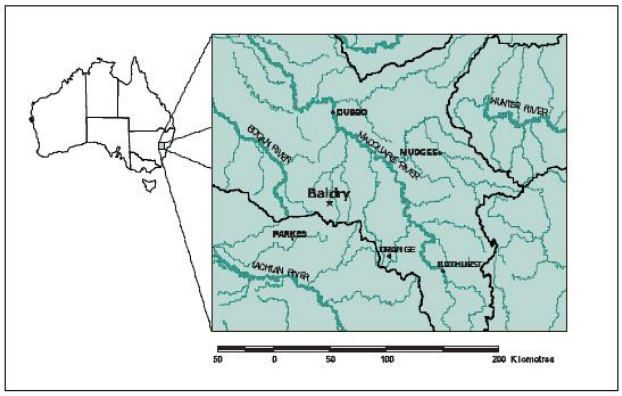

Figure 1. Location of the Baldry study site within the Little River Catchment, a tributary catchment of the Macquarie River in central west NSW.

The Baldry site is located on a high priority Groundwater Flow System (GFS) for salinity management. NSW Government initiatives targeted investment to reduce land salinity, salt loads and salt concentration to MDB tributaries. Salt expression in central NSW does not fit a simple classification model (Semple et al. 1994) because salt expression, mobilisation and transport mechanisms are highly variable and are commonly site specific (Wagner 2001). Monitoring of the stream at Baldry between 1996 and 2000 showed that the stream flowed for most of the year during the wet years of 1996 and 2000, and base flow occurred only in winter to early spring in lower rainfall years (A Nicholson pers. comm.). The EC measurements of the stream water were extremely high: ~7000 uS/cm during the wet years with spikes between 10,000-14,000 uS/cm in intervening years, particularly in late winter. Land salinisation manifested as devegetated scalds, with efflorescing halite crystals, at the break in slope and in footslope settings, particularly on the western side of the catchment. In September 2001 State Forests established 100 ha of *Eucalyptus camaldulensis* (River red gum) in lower slope settings and *Corymbia maculata* (Spotted gum) in upper mid-slope settings on the western side of the stream, from the break in slope (salt scald) to the ridge top. Land use on the eastern side of the creek is an ongoing fodder crop/pasture cycle.

Deep bore and shallow piezometer monitoring arrays were established in mid-2003 as part of a long-term approach to natural resource management at 'key sites' by the Department of Land & Water Conservation (in this case part of the Recharge Validation Project, funded by the NSW Salinity Strategy). Hydrologic research at the site focussed on the clarifying the processes of salt and water movement from the landscape into the stream, in this dry-upland setting at a time of transformational land use change. The patterns of land salinisation and water salinity differ from those studied at other key sites (Hughes et al. 2007; 2008 and Summerell et al. 2004; 2006) in this area. Original descriptions of materials at this site were limited to simple borehole and instrument pit logs, with the principle focus of early studies on water measurements. This study describes the underlying structure of catchment landforms, how the fractured rock and regolith regulates

subsurface fluid flow and influences the chemistry (salinity) of groundwater, and controls groundwater-surface water connectivity.

Preliminary detailed geological mapping of the site identified that the dominant rock type at the land surface was a jointed, indurated, fine-grained pink and grey crystalline rock, potentially a recrystallised volcaniclastic unit, forming rectangular to sub-spherical tors (<1.5m) at the land surface. On the hillcrest, high in the catchment in the stream bank, and in localised mid-slope areas, a coarsely crystalline biotite-bearing granitic rock, probably the Kynuna Granite, outcrops as corestones in saprolite in exposed faces, or forms rounded tors (<2m) at the land surface. A plot of the ratio of TiO_2 versus Zr (Hallberg 1984) and the consideration of fresh rock specimens in thin section, indicate the finer material is felsic (dacite/trachyte) and the coarser rock has a granodiorite-diorite composition. Volcanic rocks have not been mapped previously at this site, but in the greater region similar rock types are observed both in the Late Silurian-Early Devonian Cuga Burga Beds and the Devonian Dulladerry Volcanics.

Samples were taken at regular intervals from natural exposures in eroded stream banks and in excavations made during the installation of neutron moisture meter tubes. In order to establish mineral weathering pathways, samples were taken from the relatively unweathered core to the outer weathered 'onion skins' of corestones on both substrates, and then up through the regolith profile, including the soil zone, to the land surface. X-ray diffraction (XRD) analysis for mineralogical characterisation of soil/regolith samples was conducted (e.g. Moore and Reynolds 1989). X-ray fluorescence (XRF) was conducted for elemental analysis of the rock and soil/saprock samples (e.g. Norrish and Chappell 1977). Electromagnetic induction (EMI) profile data were compiled from previous work with colleagues in this area (Acworth et al. 2009).

Preliminary interpretation of the mapping and the geophysics is that there is a three-layer framework for groundwater modelling: fractured granitic rock with an irregular upper surface, finer-grained (volcanic) rock that has either mantled the older granite or has been intruded into, and a weathering profile developed in relation to the land surface. More careful interpretation of the intervals that shallow and deep piezometers and shallow and deep bores are sampling indicates that variability in water chemistry between holes can, in part, be explained because they are sampling different materials in the sub-surface geology/regolith geology.

Quartz is a relatively resistant phase throughout the profiles (Figure 2). For both substrates there is a decrease in the feldspar in increasingly weathered regolith materials, with a corresponding increase in kaolinite clay. There is increased homogenisation of the profile, and some horizonation due to pedogenic processes (e.g. bioturbation, illuviation of fines down profile) nearer the land surface. This results in a concentration of more resistant phases (quartz and remnant primary feldspar as sands) at the land surface over the granitic substrate, however kaolinite persists in the profile over the finer substrate. The presence of measurable ferruginous oxides and sesquioxides relates to localised percolation of oxidising fluids through the profiles. Understanding the configuration and composition of rocks and regolith materials in the Baldry catchment facilitates interpretation of observed patterns in hydrological analyses.

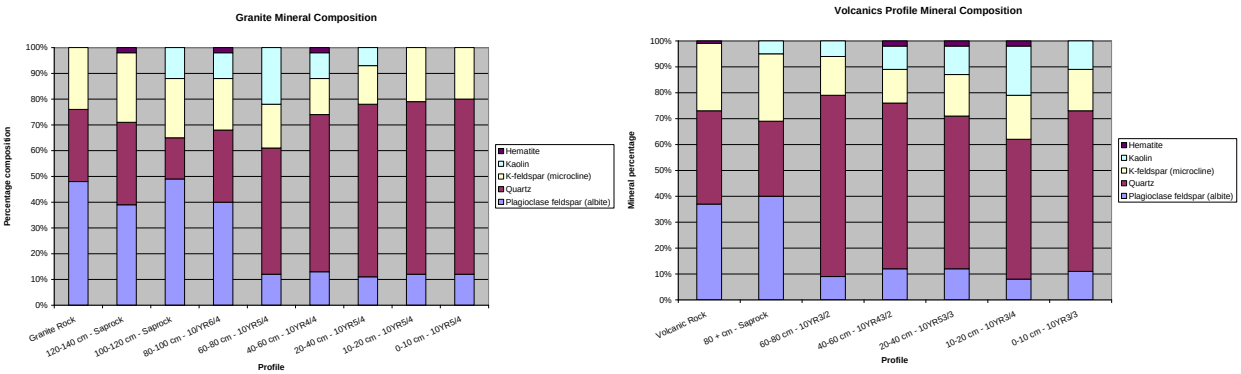

Figure 2. Percentage mineralogic composition for bulk X-ray diffraction analysis of (a) samples taken outward from a corestone and up through the regolith profile over a granitic substrate, and (b) samples taken outward from a corestone and up through the regolith profile over a fine-grained (volcanic) substrate.

References

Acworth RI, Timms WA and Bernardi T. 2009 Hydrogeological Study of the Baldry Site. UNSW Water Research Laboratory, Research Report **235**. University of New South Wales, Sydney, NSW.

Bernardi T, Moore L and Littleboy M (2012). Controls on land salinisation in the Baldry Catchment, central west NSW: influences of soil and regolith on fluid flow pathways. Soil solutions for diverse landscapes. Soil Science Australia/ New Zealand Soil Science Society: Hobart, Australia.

Hallbergh J.A. 1984. A geochemical aid to igneous rock identification in deeply weathered terrain. Journal of Geochemical Exploration **20**, 1-8.

Hughes J D, Khan S, Crosbie RS, Helliwell S and Michalk DL (2007). Runoff and solute mobilization processes in a semiarid headwater catchment. *Water Resources. Research* **43**, W09402, doi:10.1029/2006WR005465.

Hughes J D, Crosbie RS and van de Ven RJ (2008). Salt mobilisation processes from a salinised catchment featuring a perennial stream. *Journal of Hydrology* **362**, 308-319.

Moore D.M. and Reynolds R.C.J. (1989) X-ray diffraction and identification of clay minerals. Oxford University Press, Oxford UK.

Norrish. K and Chappell, B.W. 1977. X-ray fluorescence spectrometry. In: J. Zussman (Editor). *Physical mefhods* ill *defermill(l/il'e mineralogy, 2nd edition,* Academic Press. London. pp. 20 1-272.

Raymond OL. 1999. Dulladery Volcanics, 211-228. *In* Meakin NS and Morgan EJ (compilers). *Dubbo 1:250 000 Geological Sheet SI/55-4, 2nd edition. Explanatory Notes*. Geological Survey of New South Wales, Sydney, xvi + 504 pp

Semple, W.S., Wild, B.A., Nicholson, A.T., Craze, B., Koen, T.B., Waterhouse, D.B. & Williams. (1994) Physical, chemical and botanic data from 47 saline sites in the Central West of NSW. Department of Conservation and Land Management Technical Report No, 13

Summerell GK (2004). Understanding the processes of salt move-ment from the landscape to the stream in dryland catchments. PhD Thesis, The University of Melbourne

Summerell GK, Tuteja NK, Grayson RB, Hairsine PB, Leaney F (2006). Contrasting mechanisms of salt delivery to the stream from three different landforms in south eastern Australia. *Journal of Hydrology* **330,** 681–697.

Wagner R. (2001). Dryland Salinity in the South-East Region NSW, M.Sc. dissertation, Australian National University, Canberra.

Wyborn D., Warren AYE. and Meakin NS. 1999. Yeoval Batholith, 211-228. *In* Meakin NS and Morgan EJ (compilers). *Dubbo 1:250 000 Geological Sheet SI/55-4, 2nd edition. Explanatory Notes*. Geological Survey of New South Wales, Sydney, xvi + 504 pp.

Unravelling the regolith history and landscape evolution of the Eastern Musgrave, South Australia

Carmen Krapf, Mario Werner, Rian Dutch

Geological Survey of South Australia, GPO Box 1264, Adelaide SA

The Eastern Musgrave area is located at the intersection of two distinct geological provinces: the Proterozoic Musgrave Province and the Mesozoic Eromanga Basin. In addition, both provinces are partly overlain by palaeochannel sediments of the Neogene Hamilton Basin. Multiple phases of weathering, erosion and deposition lead to a complex regolith and landscape evolution history of the area. As one of the least understood and most underexplored areas in Australia it is crucial to understand and reconstruct the landscape evolution and regolith material dispersion for this area.

During the Mesozoic, the area formed part of the western margin of the Eromanga Basin. Deposition started in the late Jurassic with alluvial-fluvial sediments grading upward into fluvio-lacustrine sediments, which are today preserved as the Algebuckina Sandstone. These terrestrial sediments were deposited unconformably over a pre-existing basement topography, and were mainly sourced locally from deeply weathered and kaolinised Mesoproterozoic crystalline rocks. Continued basin subsidence enabled the westward transgression of a marine epicontinental seaway over the area in the early Cretaceous leading to the deposition of the marine Bulldog Shale, which is preserved in the far eastern part of the study area.

During the Cenozoic the climate changed being warm and wet to relatively arid. This resulted in a complex weathering and landscape evolution history of the area, which is dominated by polygenetic weathering profiles, palaeosurfaces and palaeochannels.

In the Tertiary, prior to the middle to late Eocene, intense chemical weathering resulted in a deep weathering profile of the underlying rocks that can reach up to 90m below the surface. The typically composite weathering profiles are characterised by kaolinisation and mottled or varicoloured, pallid, ferruginous or siliceous zones, capped by siliceous and ferruginous duricrusts.

The prominent silcretes and minor ferricretes on the top of many mesas have been correlated by Rogers (1986) with the late Eocene-Oligocene Cordillo Silcrete of Wopfner (1978). Krieg (1985) proposed that silcrete formation may have even started as early as early Eocene. The observations that the Algebuckina Sandstone and the Bulldog Shale have been silicified and ferruginised, and that the basement rocks of the Musgrave Province are deeply weathered at similar or higher topographic levels, implies that the silcrete developed at or near the top of an undulating palaeoweathering surface.

After duricrust formation in the Palaeogene the landscape underwent widespread erosion resulting in flat, silcrete- and ferricrete-capped mesas and associated colluvial slope and sand plains that were dominantly covered in siliceous, ferruginous or lithic lags. Prominent landslides, resulting from slope instability, have formed on many mesa slopes.

During the Neogene, rivers incised up to 70m into older cover sediments and basement rocks, discharging sediment into the Lake Eyre Basin. The fluvial channels were subsequently filled with clastic sediments during a warm and wet subtropical to tropical climate forming the infill of the Hamilton Basin. These Miocene to Pleistocene basin sediments comprise up to 80m of westward thickening floodplain and piedmont fan siliciclastics (Drexel & Preiss, 1995).

In the Quaternary the onset of aridity, with episodes of alluvial and aeolian activity, formed today's landscape with alluvial plains, sand plains and aeolian dunes and dunefields. Erosion led to widespread deposition of colluvium and sheetwash deposits around outcrops and adjacent uplands. Sand plains with thick mulga cover and distinct banded-mosaic (tiger-bush) pattern are occupying wide areas mirroring the extent of the Hamilton Basin. Sheetwash and sand plains are of residual origin when overlaying shallow weathered basement. The sand plains are overlain by isolated to widespread longitudinal aeolian dunes and dunefields of up to 15m height. Dune orientation is locally influenced by topography but is dominantly southwest-northeast. The main dune building event probably occurred about 18 kyr ago (Krieg, 1985) but there is also evidence for

both earlier and later dune-building episodes (Fitzsimmons, et al., 2013). Nodular pedogenic calcrete has locally formed within the sheetwash and sand plains.

The modern drainage appears to be controlled by the older palaeodrainage pattern, which are following older basement structures. Hamilton Creek, the largest river in the study area, occupies part of the old palaeodrainage of the Hamilton Basin.

Modern day geological processes are characterised by shallow dispersion of sediments throughout today's landscape.

References

Drexel, J. F. & Preiss, W. V. 1995. The Geology of South Australia. Vol. 2. The Phanerozoic. South Australia. Geological Survey. **Bulletin 54**, 347 pp.

Fitzsimmons, K. E., Cohen, T. J., Hesse, P. P., Jansen, J., Nanson, G. C., Mary, J. H., Barrows, T. T., Haberlah, D., Kelly, A., Larsen, J., Lomax, J. & Treble, P. 2013. Late Quaternary palaeoenvironmental change in the Australian drylands: a synthesis. Quaternary Science Reviews **74**, 78-96.

Kreig, G. W. 1985. DALHOUSIE, South Australia. Geological Atlas 1:250 000 Series - Explanatory Notes. Geological Survey of South Australia, SG53-11.

Rogers, P. A. 1986. ABMINGA, South Australia. Geological Atlas 1:250 000 Series - Explanatory Notes. Geological Survey of South Australia, SG 53-10.

Wopfner, H. 1978. Silcretes of northern South Australia and adjacent regions. In: Silcrete in Australia (ed. Langford-Smith, T.), Department of Geography, University of New England.

Rates of seismogenic landscape change in intraplate Australia

Dan Clark and Andrew McPherson

Geoscience Australia, GPO Box 378, Canberra ACT 2601

Australia is one of the lowest, flattest, most arid, and most slowly eroding continents on Earth (Quigley *et al.* 2010). The average elevation of the continent is ~330 m above sea level (asl), maximum local topographic relief is <1500 m (defined by elevation ranges with 100 km radii) and two-thirds of the continent is semi-arid to arid. With the exception of localized upland areas in the Flinders and Mt Lofty Ranges (Quigley *et al.* 2007a, Quigley *et al.* 2007b) and the Eastern Highlands (Chappell 2006, Tomkins *et al.* 2007), bedrock erosion rates are typically 1–10 m/Ma (Wellman & McDougall 1974, Bishop 1985, Young & MacDougall 1993, Bierman & Caffee 2002, Belton *et al.* 2004, Chappell 2006, Heimsath *et al.* 2010) (Fig. 1A). Despite this apparent geomorphological longevity (e.g. Fig. 1B), Australia has had a dynamic Neogene to Recent tectonic history.

In the past five decades seven locations in intraplate Australia are documented as having experienced earthquakes large enough to rupture the ground surface (Clark *et al.* 2013). These earthquakes produced scarps up to 2 m high and 37 km long. Several hundred features consistent in form with these historic ruptures have since been identified Australia-wide (Fig. 2), mainly through interrogation of digital elevation data (Clark *et al.* 2011, Clark *et al.* 2012). Palaeoseismic analysis of these features indicates that periods of earthquake activity comprising a finite number of large events are separated by much longer periods of seismic quiescence. While morphogenic earthquake events in an active period on a given fault may be separated by a few thousand years (≤0.4 mm/a uplift rates in an active period), active periods might be separated by a million years or more (long term uplift rates ≤0.001mm/a). A rupture sequence of this kind has the potential to have a dramatic effect on the landscape, especially in regions of low local topographic relief, such as the Murray Basin. For example, uplift across the Cadell Fault (Fig. 2) from 70 – 20 ka resulted in the formation of a 15 m high and 80 km long scarp which temporarily dammed, and ultimately diverted the Murray and Goulburn Rivers (McPherson *et al.* 2012). Even in upland regions, the effects can be marked, as demonstrated by the formation of Lake George over the last *ca.* 4 Ma as the result of uplift on the Lake George Fault (Pillans 2012). Over timescales of millions of years, such activity, in combination with mantle-related dynamic topographic effects (Sandiford 2007, Sandiford *et al.* 2009, Quigley *et al.* 2010), might be expected to have a significant influence on the distribution and thickness of regolith at regional-scales.

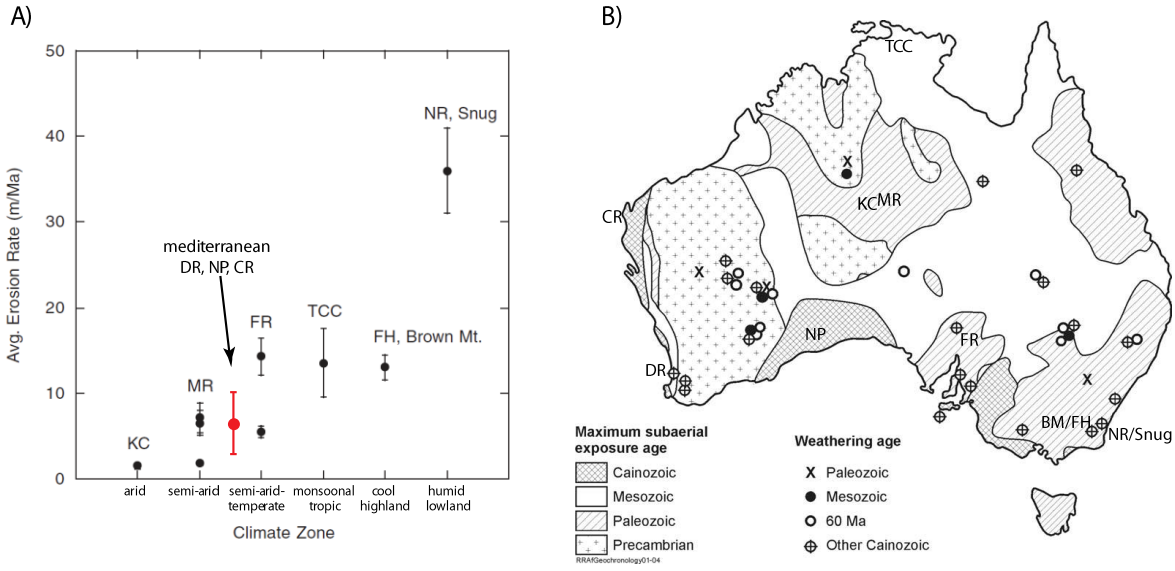

Figure 1: A) Bedrock erosion rate variation with climate. Modified after Heimsath et al (2010). Mediterranean climate zone includes NP=Nullarbor Plain (Stone *et al.* 1994), DR=Darling Range (Jakica *et al.* 2010), CR=Cape Range (Clark *et al.* 2011), B) Maximum subaerial exposure and weathering age distribution from Pillans (2004).

Given that the compressive nature of the Australian stress field (Hillis & Reynolds 2003) results in a predominance of dip-slip faulting (Leonard *et al.* 2002), long-term qualitative seismic activity rates across the continent can be assessed in terms of neotectonic uplift of the landscape. With respect to the morphogenic earthquake record, this is a function of neotectonic fault slip rate and density (with an appropriate modifier for destruction of relief according to local erosion rate, as mentioned above). In general, greater topographic expression associated with faults and fault systems occurring in extended crust relative to non-extended crust (cratonic and non-cratonic) suggests a higher rate of seismic activity in the extended setting (dark grey and stippled areas in Fig 2), consistent with observations worldwide (e.g., Johnston 1994, Cloetingh *et al.* 2008, Mooney *et al.* 2012). Under this rationale, non-cratonic crust is expected to have a higher rate of seismic activity than cratonic crust (white cf. pale grey colour in Fig. 2), due to minimal regional relief generation in cratonic crust. Such aneotectonic strain gradient has been documented between cratonic and extended crust in the central west of Western Australia (McPherson *et al.* 2013). Tools such as the weathering intensity index of Wilford (2012) might be used to provide additional constraints and as validation for this model, and aid initial interpretation.

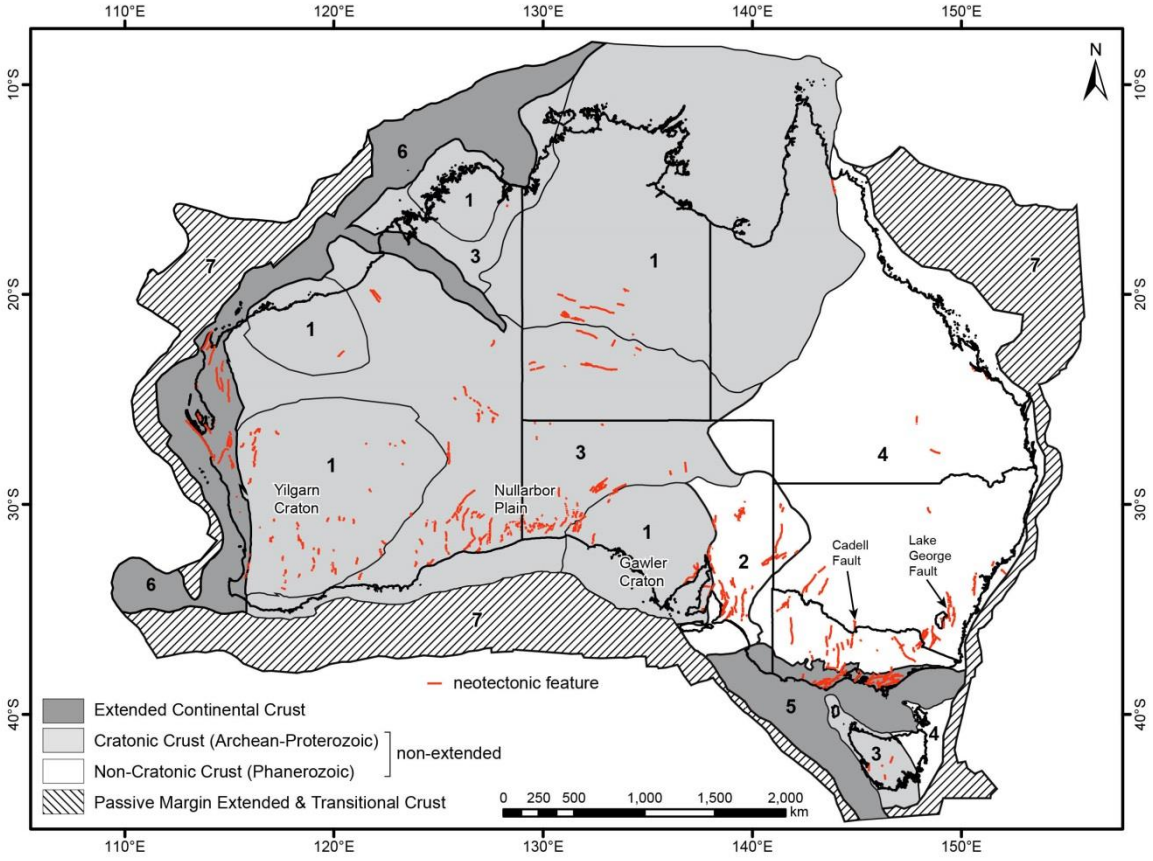

Figure 2: Neotectonics domains model of Clark et al. (2012), modified after Clark et al.(2014) to highlight extended, cratonic and non-cratonic crustal types. Numbers indicate neotectonic domains. Each neotectonic domain is characterised by a unique spatial arrangement of features (primarily faults and folds), reflecting the varying response of the crust to the imposed tectonic stresses.

References

BELTON D. X., BROWN R. W., KOHN B. P., FINK D. & FARLEY K. A. 2004. Quantitative resolution of the debate over antiquity of the central Australian landscape: implications for the tectonic and geomorphic stability of cratonic interiors. *Earth and Planetary Science Letters* **219**, 21-34.

BIERMAN P. R. & CAFFEE M. 2002. Cosmogenic exposure and erosion history of Australian bedrock landforms. *GSA Bulletin* **114**, 787-803.

BISHOP P. 1985. Southeast Australian late Mesozoic and Cenozoic denudation rates: A test for late Tertiary increases in continental denudation. *Geology* **13**, 479-482.

CHAPPELL J. 2006. Australian landscape processes measured with cosmogenic nuclides. *In:* Pillans B. ed., *Regolith Geochronology and Landscape Evolution*, pp 19-26, CRC LEME, Perth.

CLARK D., MCPHERSON A. & ALLEN T. 2014. Intraplate earthquakes in Australia. *In:* Talwani P. ed., *Intraplate Earthquakes*, pp 8-49, Cambridge University Press, New York.

CLARK D., MCPHERSON A., ALLEN T. & DE KOOL M. 2013. Co-seismic surface deformation relating to the March 23, 2012 MW 5.4 Ernabella (Pukatja) earthquake, central Australia: implications for cratonic fault scaling relations. *Bulletin of the Seismological Society of America* **104**.

CLARK D., MCPHERSON A. & COLLINS C. D. N. 2011. Australia's seismogenic neotectonic record: a case for heterogeneous intraplate deformation. *Geoscience Australia Record* **2011/11**, 95 p.

CLARK D., MCPHERSON A. & VAN DISSEN R. 2012. Long-term behaviour of Australian Stable Continental Region (SCR) faults. *Tectonophysics* **566-567**, 1-30.

CLOETINGH S., BEEKMAN F., ZIEGLER P. A., VAN WEES J.-D. & SOKOUTIS D. 2008. Post-rift compressional reactivation potential of passive margins and extensional basins. *In:* Johnson H., Dore´ A. G., Gatliff R. W., Holdsworth R., Lundin E. R. & Ritchie J. D. eds., *The Nature and Origin of Compression in Passive Margins*, Vol. 306, pp 27-70, Geological Society, London, Special Publications.

HEIMSATH A. M., CHAPPELL B. W. & FIFIELD K. 2010. Eroding Australia: rates and processes from Bega Valley to Arnhem Land. *Geological Society of London Special Publication* **346**, 225-242.

HILLIS R. R. & REYNOLDS S. D. 2003. In situ stress field of Australia. *In:* Hillis R. R. & Muller D. eds., *Evolution and dynamics of the Australian Plate* Vol. 22, pp 49-58.

JAKICA S., QUIGLEY M., SANDIFORD M., CLARK D., FIFIELD K. & ALIMANOVIC A. 2010. Geomorphic and cosmogenic nuclide constraints on escarpment evolution in an intraplate setting, Darling Escarpment, Western Australia. *Earth Surface Processes and Landforms* **DOI: 10.1002/esp.2058**.

JOHNSTON A. C. 1994. Seismotectonic interpretations and conclusions from the stable continental region seismicity database. *In:* Johnston A. C., Coppersmith K. J., Kanter L. R. & Cornell C. A. eds., *The earthquakes of stable continental regions-v. 1, Assessment of large earthquake potential*, pp 4-1-4-103, Electric Power Research Institute, Palo Alto, California.

LEONARD M., RIPPER I. D. & LI Y. 2002. Australian earthquake fault plane solutions. *Geoscience Australia Record* **2002/19**.

MCPHERSON A., CLARK D., CUPPER M., COLLINS C. D. N. & NELSON G. 2012. The Cadell Fault: a record of long-term fault behaviour in south-eastern Australia. *Second Australian Regolith Geoscientists Association Conference/22nd Australian Clay Minerals Society Conference, Mildura, Victoria* **7-9th February 2012**, 7-16.

MCPHERSON A., CLARK D. & WHITNEY B. 2013. Neotectonic evidence for a crustal strain gradient on the central-west Western Australian margin. Proceedings of the Western Australian Basins Symposium, 18-21 August 2013, Perth, WA (unpubl.).

MOONEY W. D., RITSEMA J. & HWANG Y. K. 2012. Crustal seismicity and the earthquake catalog maximum moment magnitude (Mcmax) in stable continental regions (SCRs):Correlation with the seismic velocity of the lithosphere. *Earth and Planetary Science Letters* **357-358**, 78-83.

PILLANS B. 2012. How old is Lake George? . *Australian and New Zealand Geomorphology Group 15th Conference, 2-7 December 2012, Bundanoon, New South Wales : Program and Abstracts*, 79.

QUIGLEY M., CLARK D. & SANDIFORD M. 2010. Late Cenozoic tectonic geomorphology of Australia. *Geological Society of London Special Publication* **346**, 243-265.

QUIGLEY M., SANDIFORD M., ALIMANOVIC A. & FIFIELD L. K. 2007a. Landscape responses to intraplate tectonism: quantitative constraints from 10Be abundances. *Earth and Planetary Science Letters* **261**, 120-133.

QUIGLEY M., SANDIFORD M., FIFIELD K. & ALIMANOVIC A. 2007b. Bedrock erosion and relief production in the northern Flinders Ranges, Australia. *Earth Surface Processes and Landforms* **32**, 929-944.

SANDIFORD M. 2007. The tilting continent: a new constraint on the dynamic topographic field from Australia. *Earth and Planetary Science Letters* **261**, 152-163.

SANDIFORD M., QUIGLEY M., DE BROEKERT P. & JAKICA S. 2009. Tectonic framework for the Cainozoic cratonic basins of Australia. *Australian Journal of Earth Sciences* **56**, s5-s18.

STONE J., ALLAN G. & FIFIELD L. K. 1994. Limestone erosion measurements with cosmogenic Cl-36 in Calcite - preliminary results from Australia. *Nuclear instruments and methods in physics research, section B - beam interactions with materials and atoms* **92**, 311-316.

TOMKINS K. M., HUMPHREYS G. S., WILKINSON M. T., FINK D., HESSE P. P., DOERR S. H., SHAKESBY R. A., WALLBRINK P. J. & BLAKE W. H. 2007. Contemporary versus long-term denudation along a passive plate margin: the role of extreme events. *Earth Surface Processes and Landforms* **32**, 1013-1031.

WELLMAN P. & MCDOUGALL I. 1974. Potassium-Argon ages on the Cainozoic volcanic rocks of New South Wales. *Journal of the Geological Society of Australia* **21**, 247–272.

WILFORD J. R. 2012. A weathering intensity index for the Australian continent using airborne gamma-ray spectrometry and digital terrain analysis. *Geoderma* **183-184**, 124-142.

YOUNG R. W. & MACDOUGALL I. 1993. Long-term landscape evolution: miocene and modern rivers in southern New South Wales. *Journal of Geology* **101**, 35-49.

Nickel laterites formed from the weathering of Tethyan ophiolites

Robert Thorne[1], Steve Roberts[2] and Richard Herrington[3]

[1]CSIRO Earth Science and Resource Engineering, Kensington, WA 6151
[2]School of Ocean and Earth Science, National Oceanography Centre, University of Southampton, SO14 3ZH, UK.
[3]Department of Earth Sciences Natural History Museum, Cromwell Road, London, SW7 5BD, UK.

Introduction

The closure of the Tethys Ocean during the Mesozoic resulted in the obduction of ophiolites that are today exposed in linear belts across much of Southeastern Europe. On exposure to the prevailing greenhouse climate of the Late Cretaceous the ultramafic rocks were subjected to intense weathering leading to the formation of Ni laterite deposits (Thorne et al 2012a).

During the weathering process nickel-bearing minerals, olivine and serpentine, are destroyed in an oxidising environment producing iron oxide dominated deposits containing residual concentrations of Ni. Secondary silicate deposits are created when Ni leached from the iron oxides reacts with the weathering products of primary silicates to form garnierite (Freyssinet, *et al.* 2005). Contemporary nickel laterite deposit formation is confined to low latitudes where temperature, rainfall and consequently ground water through-flow are high. Laterites located at higher latitudes and with cooler climatic regimes e.g. Greece and Turkey, are considered to be palaeodeposits that originally formed at lower latitudes during warmer climes (Freyssinet, *et al.* 2005). Complex interactions between the protolith, the water table, topography, climate and transportation mechanisms combine to produce oxide, clay or secondary silicate deposits of varying thickness. The variable role of these factors in the formation of a specific deposit is difficult to predict.

The Çaldağ deposit, Turkey

The Çaldağ nickel laterite deposit in the Aegean region of Turkey contains a reserve of 33 million tonnes of Ni ore with an average grade of 1.14% Ni. The deposit is developed on an ophiolitic serpentinite body that was obducted onto Triassic dolomites during the Late Cretaceous, and is overlain by Eocene sediments (Önen & Hall 2000; Çağatay et al., 1981). The weathering profile of the deposit is both laterally and vertically variable. An oxide zone, which is the main ore horizon, is located at the base of the profile. The contact between the oxide and saprolite represents a sharp physical (Fig. 1) and geochemical boundary. An electron microprobe profile across the saprolite-oxide boundary, which represents the weathering front, demonstrates a dramatic increase in FeO from 10% in the saprolite to 46% in the oxide, with decreases in SiO_2 from 20% to 7% and MgO from 13 to 1%. The change in MgO concentrations over a distance of 2 mm marks the “magnesium discontinuity”, above which the leaching process has removed Mg by the dissolution of silicate minerals. Nickel percentages are similar across the boundary (~2.2%) but are much more variable within the saprolite. Nickel concentrations within goethite, the main ore mineral, reach a maximum of ~3 wt% near the base of the oxide zone (Thorne et al., 2009). Nickel concentrations decrease as textures become more disaggregated. Variations within the weathering profile cannot be entirely attributed to the weathering history of the deposit. Much of the laterite is allocthonous with textures indicative of transportation. Faulting has lead to the erosion of *in-situ* laterite from the footwall and deposition of lateritic material onto hanging wall, forming profiles that are locally entirely disaggregated. Profiles with an *in-situ* base and transported upper horizons are indicative of pocket-type formation, which occurs where laterite in paleo-topographic lows has been covered by transported material from surrounding highs. Finally steeply dipping profiles contain localised disaggregated regions indicative of slumping. Each of the identified transportation mechanisms produces a contrasting set of textural and geochemical features (Thorne et al., 2009).

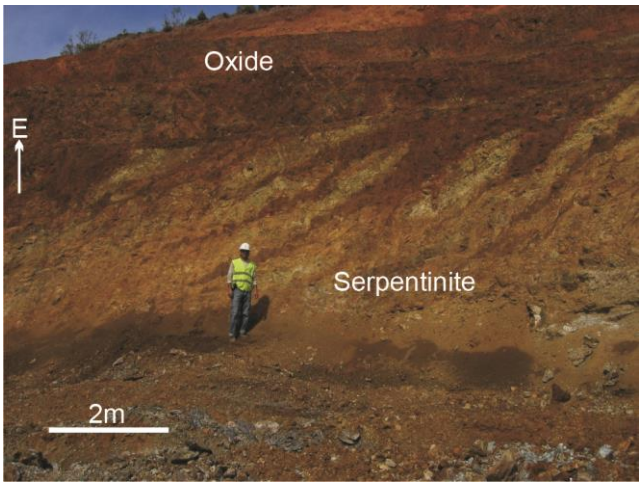

Figure 1. Interdigitation between serpentinite and the oxide zone at the base of the *in-situ* laterite profile

The Bitincke deposit, Albania

The Bitincke nickel laterite is located in the southeast of Albania close to the Greek border. The deposit has a JORC resource of 427,000 tonnes of contained Ni (35.6 million tonnes at 1.20% Ni). The laterite is situated on a fragment of ophiolite within the south of the Vardar zone (Bortolotti et al., 2004).

The Bitincke laterite deposit is composed of two distinct ore zones characterised by silicate nickel and iron oxide phases. The deposit developed over serpentinised peridotite and is overlain by conglomerates and limestones of Eocene age (Eliopoulos & Economou-Eliopoulos, 2000). The laterite is cross-cut by a number of normal faults with 10s to 100s of meters of displacement forming horst and graben structures with a N-S orientation. Faulting occurred both during and after deposit formation (Thorne et al. 2012b).

Original igneous textures are preserved within the saprolite and both layering and dunitic pods are observed. Serpentine is most obvious when found as a thin coating on fracture surfaces. The silicate zone is brown to red/grey and is highly veined and fractured and possesses a spheroidal weathering texture. Garnierite veins are rare but occur as thin veins near the contact with the iron nickel zone. Calcite veining is prolific, while silica and magnesite veins compose a minor proportion of the veins within this zone. Pyroxenes are only preserved in and near to the less altered saprolite. Chromite grains are observed throughout the zone but are more abundant than in the protolith. The reported nickel grade is on average highest close to the silicate - oxide contact, which is most frequently observed as a sharp linear boundary with little lateral variation. The oxide zone is massive and highly fractured, giving the horizon an angular blocky appearance. Manganese coatings are often found on fracture surfaces. Rare calcite veins within this horizon can cut across the silicate - oxide boundary. Nickel grade within this zone is highest nearest the contact with the silicate zone. A clast supported dominantly monomictic conglomerate is usually found directly above the oxide zone. Rare fine grained sands and mudstones containing fossils indicative of a warm, tropical climate are also present.

The profiles observed across the deposit are broadly similar but a combination of palaeotopography, erosion and faulting have combined to produce variations in profile thickness, morphology and nickel grade (Fig. 2). Profiles are thickest where they have been protected from erosion by the deposition of marls and limestones. This has occurred in small fault controlled basins that formed shortly after or during the weathering process. Unprotected laterite associated with palaeo-geographical highs has been eroded prior to the deposition of Eocene conglomerates (Fig. 2) (Thorne et al. 2012b).

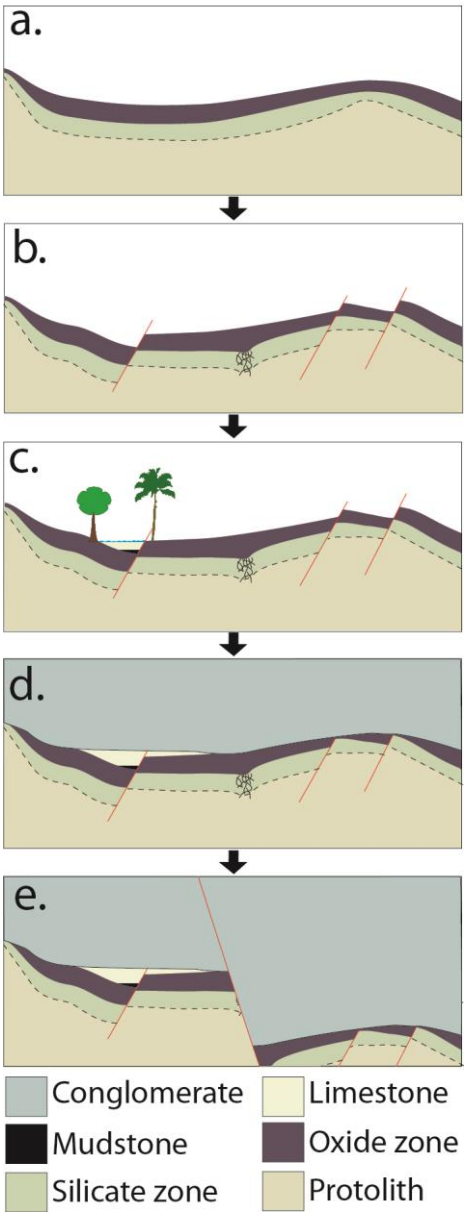

Figure 2. Evolution of the Bitincke laterite profile **a.** Formation of laterite profile with a secondary silicate and iron oxide zone. The laterite is developed from an ophiolitic serpentinite body, which was obducted in the Late Jurassic. Profile thickness is reduced on topographic highs **b.** The profile is thicker where fractures promote the through-flow of water. Normal faults cut across the laterite forming small fault controlled basins and a moderate topography. **c.** Transgressive mudstones and limestones are deposited in the basins, fossils suggest a deltaic environment with alternating marine and terrestrial conditions. **d.** Limestone conglomerates are deposited; laterite on topographic highs is eroded whereas laterite covered by mudstone and limestone is preserved. **e.** Normal faults cut across the area dividing the laterite into a number of separate fault blocks.

Discussion - Weathering History

The lack of a hydrous silicate zone in the Çaldağ deposit suggests that the leaching and transportation of nickel required to form secondary silicates has not occurred or has been interrupted. A high water table during laterite formation would prevent leached nickel from interacting with actively weathering primary silicates, resulting in little or no formation of nickel rich secondary silicates (Freyssinet, *et al.* 2005). The prevailing climate during laterite formation also plays an important role in the type of laterite deposit developed. Seasonality promotes the formation of secondary silicates. As humidity and rainfall increases the difference in the weathering rate of the framework minerals containing nickel (olivine and serpentine) decreases, leading to the formation of an oxide dominated deposit (Lelong *et al.* 1976; Trescases 1997). The degree of serpentinization of the protolith also affects the relative development of different horizons within the

laterite. Protolith dominated by serpentinite will normally weather directly into goethite. In contrast, the delay caused by the different weathering characteristics of olivine and serpentine together allows for the formation of a silicate layer at the base of the profile (Trescases, 1997). At Çaldağ the saprolite is composed almost entirely of serpentinite and the profile above contains significant amounts of silica. A combination of a serpentinized protolith, a high water table and a climate with little seasonality can account for the thickness of the oxide zone and the lack of secondary silicates at Çaldağ (Tavlan et al. 2011). The Bitincke nickel laterite was probably formed in a tropical seasonal environment in an area of moderate relief. The presence of secondary silicates suggests a seasonal climate and a relatively low water table with a high rate of water through-flow.

Acknowledgments

This work was funded by the National Environment Research council and the Natural History Museum. The access to deposits and assistance granted by European Nickel PLC is gratefully acknowledged.

References

Bortolotti V., Chiari M., Marcucci M., Marroni M., Pandolfi L., Principi G. & Saccani E. 2004. Comparison among the Albanian and Greek ophiolites: In search of constraints for the evolution of the Mesozoic Tethys Ocean. *Ofioliti*, **29(1)**, 19-35.

Çağatay A., Altun Y. & Arman B. 1981. The Mineralogy of the Çaldağ lateritic iron, nickel-cobalt deposits. MTA Maden Etut Dairesi **Report 1709**, Ankara

Freyssinet P., Butt C.R.M., Morris R.C. & Piantone P. 2005. Ore-Forming Processes Related to Lateritic Weathering. Economic Geolgy 100th anniversary volume pp. 681-722.

Eliopoulos D.G. & Economou-Eliopoulos 2000. Geochemical and mineralogical characteristics of Fe-Ni and bauxitic-laterite deposits of Greece. *Ore Geology Reviews,* **16**, 41-48.

Lelong F., Tardy Y., Grandin G., Trescase J.J. & Boulange B. 1976. Pedogenesis, chemical weathering and processes of formation of some supergene ore deposits. *In*: Wolf KH. ed. *Handbook of strata-bound and stratiform ore deposits*. pp 92-173 Elsevier.

Önen A.P. & Hall R. 2000 Sub-ophiolite metamorphic rocks from NW Anatolia, Turkey. *Journal of Metamorphic Geology* **18**, 483-495.

Tavlan M., Thorne R.L.T. & Herrington R. Uplift and lateritization history of the Çaldağ ophiolite in the context of Neo-Tehyan ophiolite obduction and uplift: implications for the Cenozoic weathering history of western Anatolia. *Journal of the Geological Society,* **168**, 927-940.

Thorne R.L.T., Herrington R. & Roberts S. 2009. Composition and origin of the Çaldağ nickel laterite, W. Turkey. *Mineralium Deposita*, **44**, 581-595.

Thorne R.L.T., Roberts S. & Herrington R. 2012a. Climate change and the formation of nickel laterites. *Geology*, **40**, 331-334.

Thorne R.L.T., Roberts S. & Herrington R. 2012b. The formation and evolution of the Bitincke nickel laterite deposit, Albania. *Mineralium Deposita*, **47**, 933-947.

Trescases J.J. 1997. The lateritic Nickel–Ore Deposits. *In*: Paquet H, Clauer N eds. *Soils and Sediments, Mineralogy and Geochemistry*, pp 125-138, Springer.

Unlocking the Southern Thomson's hidden mineral resource potential

Richard S Blewett

Regional Geology and Mineral Systems, Geoscience Australia (richard.blewett@ga.gov.au)

Due to extensive cover by Mesozoic and younger sedimentary basins and regolith, the geology of the southern Thomson Orogen is poorly understood. Small outcrops of the Thomson Orogen are exposed along the Eulo Ridge (Qld) and in the southwest around Tibooburra (NSW). Between these regions the thickness of cover averages ~200 m, which is within exploration and mining depths.

The southern Thomson Orogen is true 'greenfields' country. Although the mineral potential of the region is unknown, the northeastern Thomson Orogen is well mineralised (e.g., Thalanga, Charters Towers) and the similar-aged Lachlan Orogen to south is also well mineralised (e.g., Cadia, Cobar). In order to attract investment (exploration) into the southern Thomson Orogen, Geoscience Australia, the Geological Survey of Queensland and the Geological Survey of New South Wales have commenced a three-year collaborative project to collect new (and synthesise existing) pre-competitive data.

The first year and half of the project will synthesise existing datasets across the state borders to create a revised solid geology map. This map will form the basis of a 3D model (map), which will utilise pre-existing government and industry seismic and drilling data. In support of the 3D map, a programme of geophysical datasets will be acquired, processed and interpreted. These include: airborne electromagnetic (AEM), broad-band magnetotelluric (MT) and gravity data. In order to understand the nature of the cover rocks and their relationship to basement, a surface geochemical survey will also be acquired at a higher resolution infill of the National Geochemical Survey of Australia (NGSA).

In addition, the potential mineral systems of the region will be assessed and a gap analysis conducted, with these results and the 3D and cover maps informing a planned drilling programme to be conducted in 2014–15. The drilling methods will be informed by the results of a similar drilling project in the Stavely Zone of western Victoria. Prior to drilling, a series of geophysical experiments will be conducted in the vicinity of the proposed holes to aid selection and improve prediction of cover depths expected. The actual drill holes will test the predictive capacity of the various experiments – a useful outcome in its self. The recovered core will be analysed with a range of geochemical, geochronological, geophysical and geological techniques. The combined results will be synthesised and integrated into a pre-competitive geoscience data package for exploration investment.

Interim products and datasets will be released throughout the project, with the final results delivered to industry in mid-2016.

Provenance of zircon in high-zirconium heavy mineral sand deposits of the Eucla Basin, southern Australia

John Keeling, Anthony Reid and Baohong Hou

Geological Survey of South Australia, GPO Box 1264, Adelaide SA 5000

Introduction

The discovery by Iluka Resources in late 2004, of high-grade, zircon-dominant, heavy mineral (HM) sands along the north-eastern margin of the Cenozoic Eucla Basin in South Australia established the region as a world-class source of zircon in paleo-beach placer deposits. The Jacinth-Ambrosia deposit, ~100 km inland of the present-day coast, contains proved and probable reserves of 143 Mt grading 4.5% HM with zircon content averaging 50% (Iluka Resources 2011). At the time of discovery, demand for zircon was increasing, principally as a hardwearing, high-reflectance glaze for ceramic tiles, and prices had increased to more than twice that for titanium dioxide. The zircon-dominant discoveries in the Eucla Basin provided the opportunity to decouple zircon production from titanium minerals at a time when titanium dioxide prices were flat but demand for zircon was outstripping supply. Mining commenced in 2009 at Jacinth-Ambrosia, which rapidly developed as the largest zircon-dominant operation globally with capacity to produce 300,000 tonnes per annum of zircon, ~25% of annual global requirement.

The zircon to titanium dioxide ratio at Jacinth-Ambrosia is ~2.6, around 10 times the industry production average. Why the zircon content is so high is likely the culmination of many factors, including relative abundance of zircon in the source regions, mode of sedimentary transport and sorting, recycling through sedimentary basins, specifics of the trap sites, and post-depositional activity and zircon preservation. Dating the zircon population has proved useful in identifying the source regions and probable dispersion pathways to the Eucla Basin coastline, and ultimately to shore-face trap sites (Reid & Hou 2006, Hou et al. 2011, Reid et al. 2013b). The zircon age data from four sites along the Eucla Basin margin, described below, have modified our interpretation of the wider landscape processes that led ultimately to zircon placer deposits.

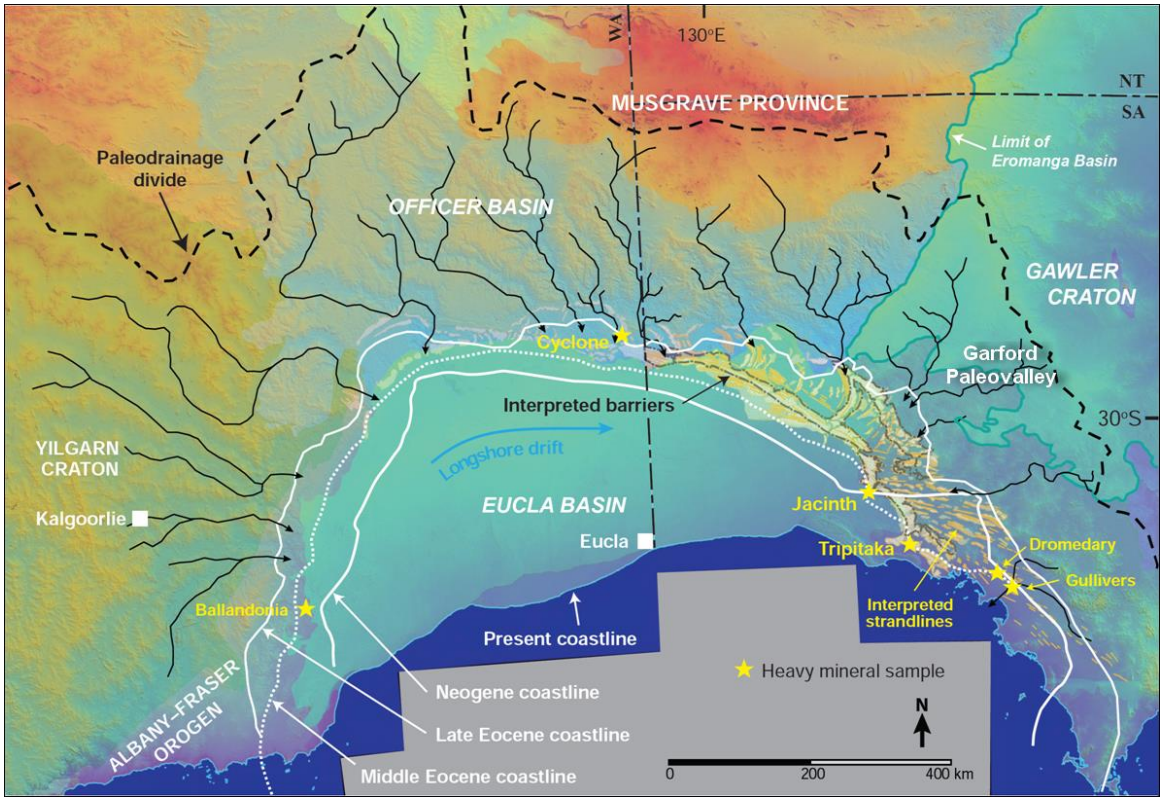

Figure 1: Eucla Basin with paleodrainage and crystalline basement/sedimentary basin zircon source areas within the basin catchment. Showing interpreted sea level highstands, strandlines and off-shore sand barriers. Sampled heavy mineral sand deposits and prospects are labelled (after Hou et al., 2008).

Zircon age data and provenance

Zircons from heavy mineral sites at Ballandonia, Cyclone, Jacinth and Tripitaka (Fig.1) all have dominant populations between 1300 and 1050 Ma (Reid et al., 2013b) (Table 1). This time interval is not represented in crystalline rocks of the Gawler Craton, where the last major igneous activity was ~1590 Ma with intrusion of Hiltaba Suite granite and associated Gawler Range Volcanics (GRV). Sediments from the Garford paleovalley on the Gawler Craton have a dominant zircon population between 1600-1550 Ma (~13%) and a cluster of zircons between 1300-1050 Ma (~9%), probably reworked Musgrave zircons from Cretaceous Eromanga Basin sediments (Reid et al., 2009). This compares with 1600-1550 Ma (2%) and 1300-1050 Ma (55%) for zircons analysed from Jacinth and Tripitaka (Table 1). Within the catchment, ~1100 Ma zircons formed during granitic intrusions and metamorphism of the Musgrave Orogeny (1220-1150 Ma) and Giles Event (1085-1040 Ma) in the Musgrave Province, and the Albany-Fraser Orogen (1345-1140 Ma) in the west.

Table 1: Eucla Basin heavy mineral sites – grade, zircon percentage of HM, dominant zircon age and εHf average.

Deposit	HM (%)	Zircon (%)	1300-1050 Ma (%)	1300-1050 Ma εHf average	1610-1550 Ma (%)
Ballandonia	~5	~1.5	55	-2.61	2
Cyclone	2.5	32	62	2.10	0
Jacinth 1688513	5.2	50	55	1.69	2
Tripitaka	2.4	65	55	0.2	2

The overlap of zircon ages for Albany-Fraser and Musgrave orogenic events is resoluble using hafnium (Hf) isotopic data for zircons from this time interval. Metamorphic and magmatic activity in Albany-Fraser Orogen reworked earlier Proterozoic rocks to give an evolved Hf isotopic signature with negative εHf values. By contrast, igneous activity in the Musgrave at that time had greater mantle input and more juvenile Hf isotopic signature and positive εHf values (Table 1, Fig. 2).

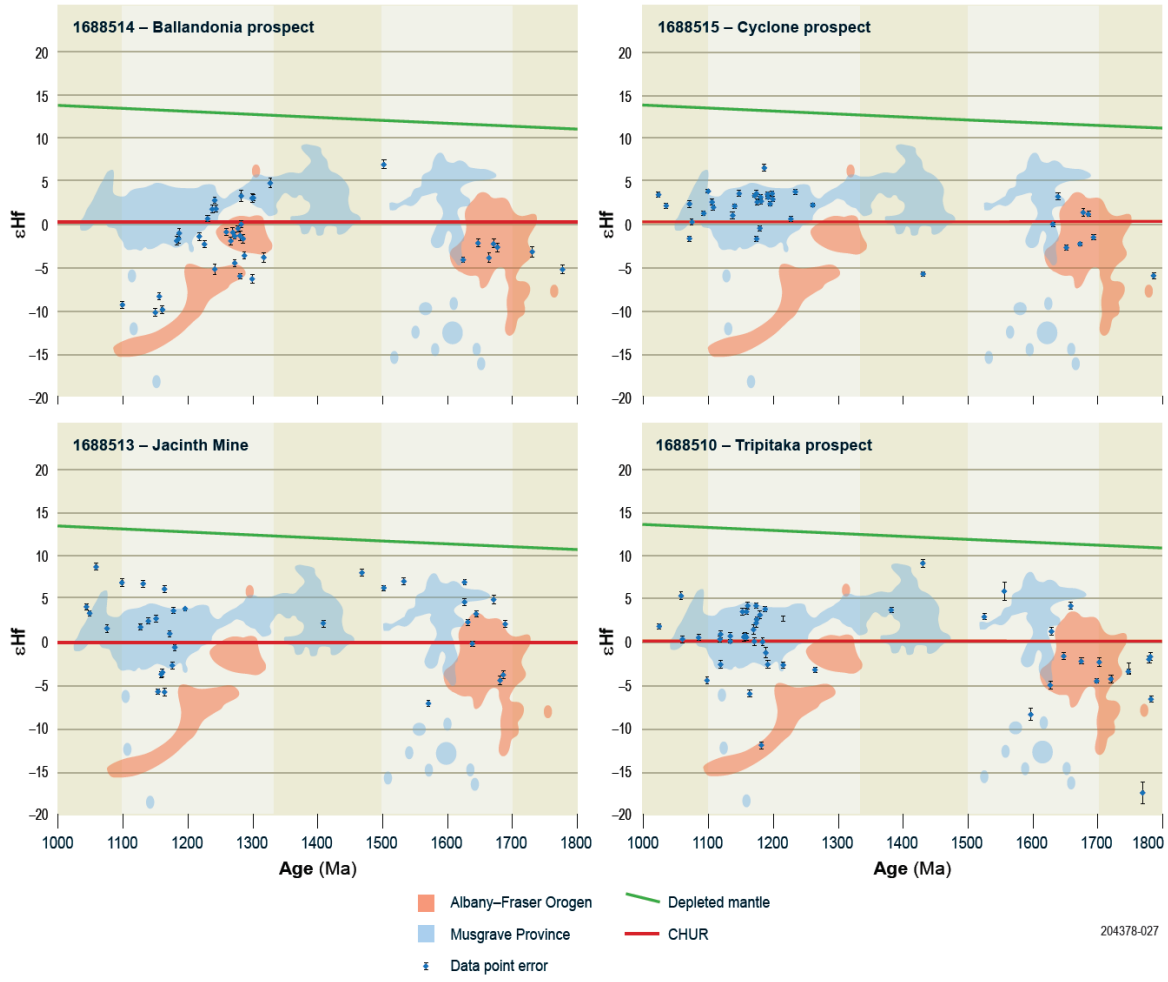

Figure 2: εHf vs Age plots for zircons from Eucla Basin HM sites compared with data fields for crystalline rocks from the Albany-Fraser Orogen and Musgrave Province (from Reid et al., 2013a).

As illustrated in Figure 2, Hf isotope data for Cyclone, Jacinth and Tripitaka show zircons formed between 1300-1050 Ma cluster more closely within and around the data field for the Musgrave Province. This compares with the sample from Ballandonia where zircons within this age bracket are somewhat older, overall, and plot within or close to the Albany-Fraser data fields. The result accords with the proximity of the Albany-Fraser Orogen to the Ballandonia site. The presence of a few Neoarchean age (c. 2800-2600 Ma) zircons in Jacinth and Tripitaka samples (not shown), and some ~1150 Ma zircons with negative εHf values indicate that a minor component of the zircon population in these deposits represents sources within the Yilgarn Craton and Albany-Fraser Orogen. These detrital zircons were transported possibly from the western margin of the Eucla Basin or were recycled from deposits in older sedimentary basins.

Landscape processes reflected in the zircon data

The Eucla Basin catchment extended across three cratons and several older sedimentary basins, and drained a multitude of potential zircon sources. Despite this, dating of zircon grains from heavy mineral sand placers along the Eucla margin, combined with Hf isotope data, gives a population distribution that indicates the Musgrave Province was the ultimate source region for a majority of zircons found in zircon-dominant deposits along the eastern basin margin. These results, when combined with reconstructed paleodrainage and paleoshorelines, provide insights into the dominant landscape processes operating at the time of zircon transport and deposition. Key indications include:

- During middle Eocene marine transgression, flooding was comparatively rapid across a gently sloping fluvial plain, with minimal reworking of earlier fluvial sediments into coastal deposits.
- Rivers to the north of the basin were the primary source of sand that built coastal beach and dune deposits along the northern and eastern basin margins. Longshore drift with eastward migration of sand under prevailing westerly winds was the dominant mode of beach sand transport.
- Early Cenozoic river networks draining the Gawler Craton, westward toward the Eucla Basin, were swamped during marine transgressions, and outflows were impeded by build up of coastal sediments derived from the west and north. These rivers deposited mostly fine-grained sediment in backshore lagoons and swamps. By the time of marine transgression, topographic relief across the Gawler was likely much less than in the north, with rivers occupying broad valleys with low channel gradients and low energy flows.
- Erosion of Musgrave crystalline basement in upland regions of the north probably contributed significant detritus to fluvial systems, but much of the drainage network was incised also into flat-lying Cambrian sandstones of the Officer Basin. Zircon in the sandstones mostly originated from the Musgrave Province (Reid et al. 2013b). The sandstones were exposed to glacial conditions during Permian time and deep weathering during the Cretaceous and early Paleogene; these conditions would have favoured preservation of resistant zircon over other heavy minerals, in particular iron-rich ilmenite.

Long fluvial transport from the Musgrave Province, combined with recycling zircon through Officer Basin sandstones, followed by reworking and sorting via longshore drift over tens to hundreds of kilometres were likely important preconditions for the subsequent formation of large, zircon-dominant placer deposits at suitable trap sites on the eastern Eucla Basin coastline.

References

Hou B., Frakes L., Sandiford M., Worrall L., Keeling J. and Alley, N.F. 2008. Cenozoic Eucla Basin and associated palaeovalleys, southern Australia — climatic and tectonic influences on landscape evolution, sedimentation and heavy mineral accumulation. *Sedimentary Geology* **203**, 112–130.

Hou B., Keeling J., Reid A.J., Warland I., Belousova E., Frakes L., Hocking R. and Fairclough M. 2011. Heavy mineral sands in the Eucla Basin, Southern Australia: deposition and province-scale prospectivity. *Economic Geology* **106**, 687–712.

Iluka Resources 2011. Iluka annual review 2011, viewed February 2013 <http://www.iluka.com/ annualreport2011/#>.

Reid A.J. and Hou B. 2006. Source of heavy minerals in the Eucla Basin paleobeach placer province, South Australia: Age data from detrital zircons. *MESA Journal* **42**, 10-14.

Reid A.J., Keeling J.L. and Belousova E.A. 2013a. Hf isotope investigation into provenance of zircons in heavy mineral sands of the Eucla Basin. *MESA Journal* **68**, 17-24.

Reid A., Keeling J., Boyd D., Belousova E. and Hou B. 2013b. Source of zircon in world-class heavy mineral placer deposits in Cenozoic Eucla Basin, southern Australia from LA-ICPMS U-Pb geochronology. *Sedimentary Geology* **286-287**, 1-19.

Reid A., Korsch R.J., Hou B. and Black L.P. 2009. Sources of sediment within the Eocene Garford Palaeovalley, South Australia, from detrital zircon geochronology. *Australian Journal of Earth Sciences* **56**, S125–S137.

Biomineralisation in the sulfur hyperaccumulator *Acacia bivenosa*

Nathan Reid[1] and Thomas Robson[1]

[1]CSIRO Earth Science and Resource Engineering, Kensington, WA 6151

Hyperaccumulator plants are able to take up elements from soils to levels far above that for “normal" plants. They are potentially useful in cleaning contaminated soils (phyto-remediation) or for mining metals (phyto-mining). *Acacia bivenosa* is able to hyperaccumulate sulfur and deposit it as gypsum within dry phyllode (leaf) cells.

Acacia bivenosa

Acacia bivenosa (two-nerved wattle) has a widespread distribution across much of northern Australia (Figure 1). It is a dense, glabrous shrub, 1-2 m high, 1-2 m diameter, with deep golden, spherical flowers that cover the shrub following the wet season in summer. *Acacia bivenosa* grows on a variety of soils, though mostly sandy and in areas of seasonal surface water accumulation (Moore 2005). The plant has a series of shallow lateral roots and a single thicker sinker root to depth. This species was sampled at the Oberon Au Prospect in the Tanami Desert, Northern Territory (Reid et al. 2009) in order to test its potential as a mineral exploration tool.

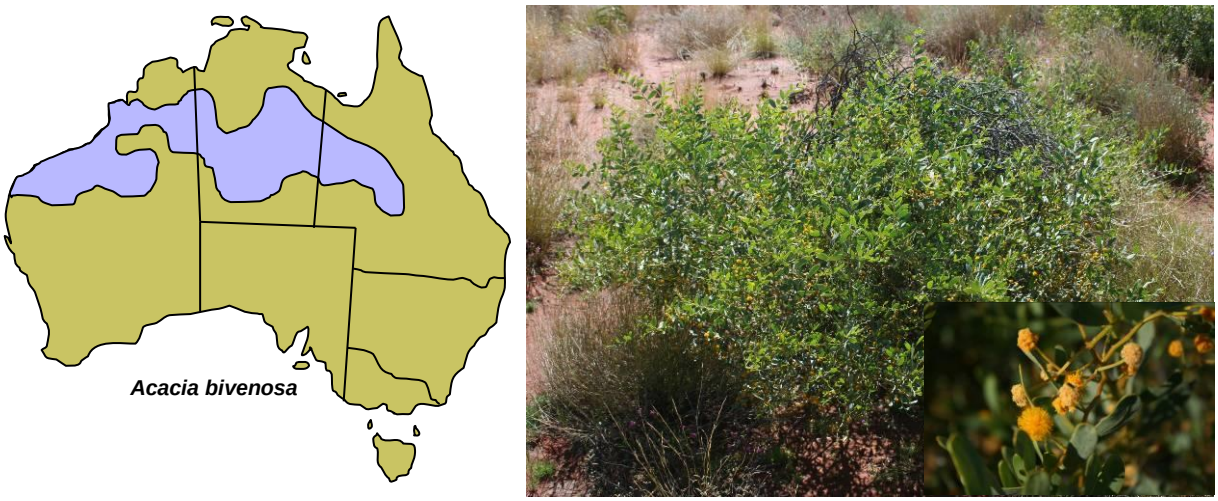

Figure 1: *Acacia bivenosa* form, flowers and distribution, adapted from Moore 2005

Sulfur accumulation

Acacia bivenosa has much greater (3 - 10 times) concentrations of S than the other plant species (Figure 2) at the Oberon prospect in the Tanami Desert, Northern Territory. Sulfur concentrations in the plant do not spatially correlate to the underlying sulfide mineralisation at this site (Figure 3). The plant could be sourcing S from carbonates and/or gypsum at or near the surface, . There is also the possibility for sourcing of S from the atmosphere but this is yet to be tested.

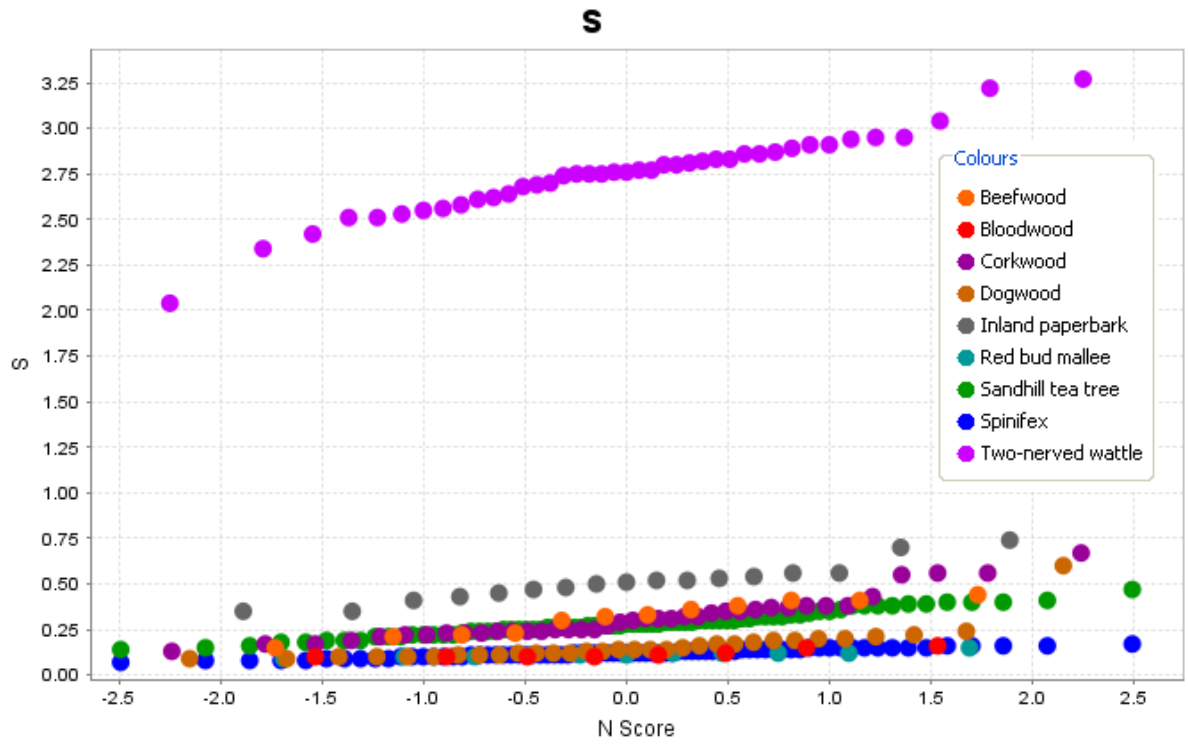

Figure 2: Sulfur (wt%) results for various plant species at the Oberon Prospect.

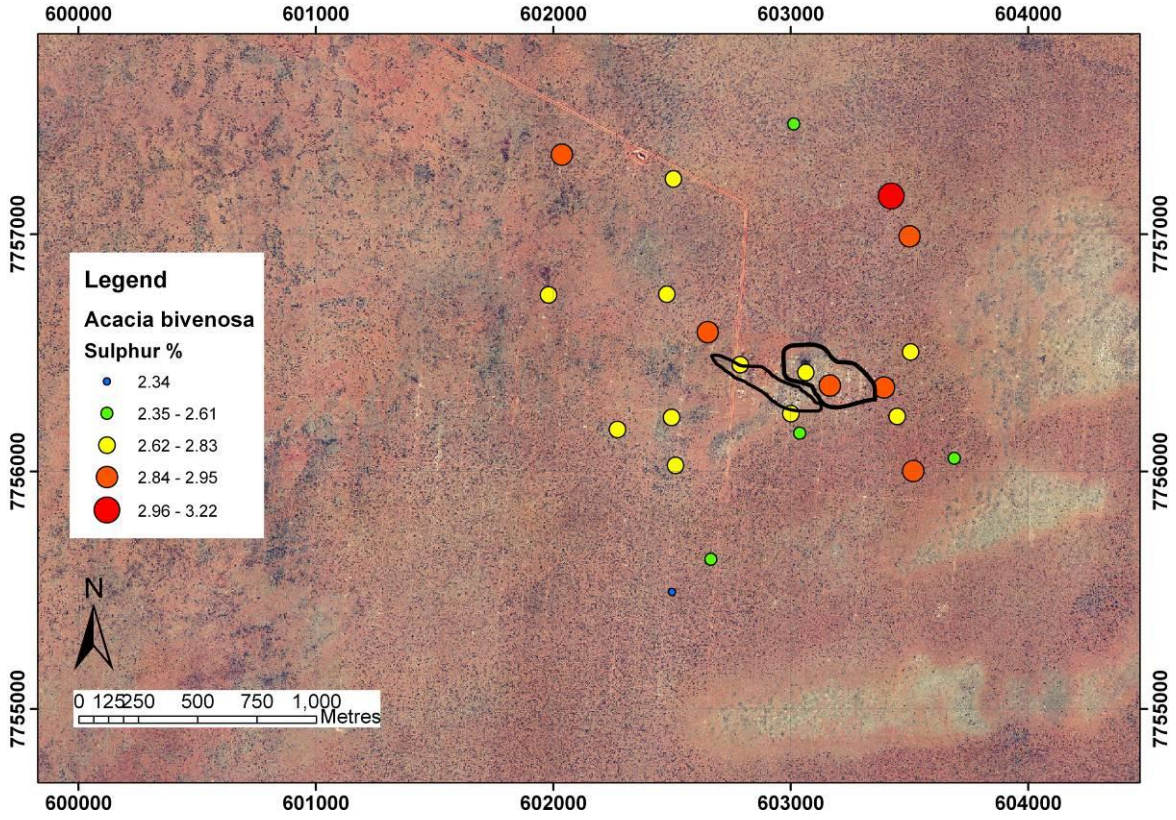

Figure 3: Plots of S concentration for *Acacia bivenosa* overlying the orthophoto of the Oberon Prospect, black lines are the projected outline of Au mineralisation.

Polished sections of *Acacia bivenosa* were examined under a scanning electron microscope (SEM). Crystals were found within the veins and vacuoles of the phyllodes (Figure 4). These crystals had a predominant spectral signature of Ca, S and O from energy dispersive X-ray spectrometry (EDS) analysis. SEM, combined with EDS, identified the same crystals within phyllode samples from various locations and soil types. X-ray diffraction showed that the crystals were gypsum within dried material.

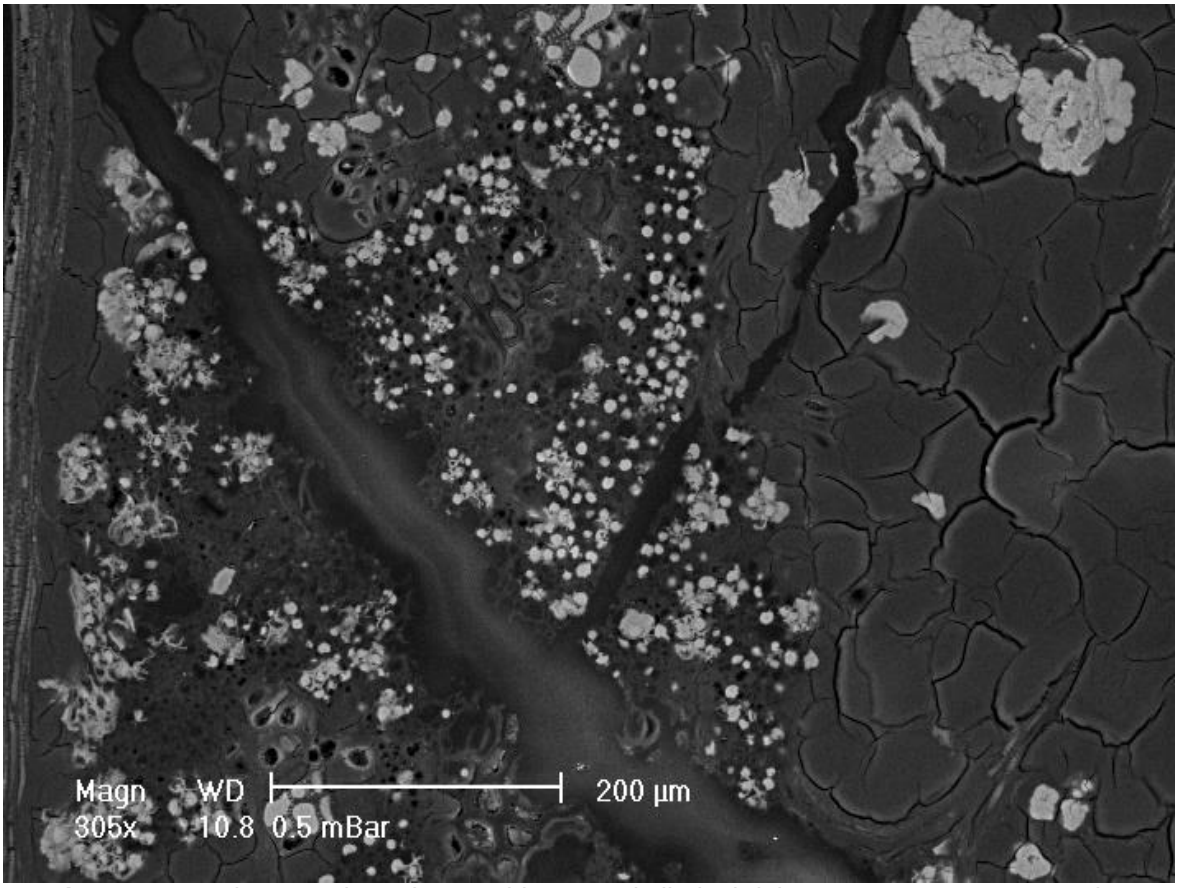

Figure 4: SEM imagery through an *A. bivenosa* phyllode, bright spots are gypsum crystals.

The physiological function for this biomineralisation is still being tested but we hypothesise that S accumulation may convey drought tolerance and/or providing a higher ionic potential within the plant for greater salt tolerance. The hyperaccumulation of S makes these species unsuited for mineral exploration purposes but potentially suitable for phyto-remediation, which is the subject of further research in this area.

References

Moore, P., (2005). A Guide to Plants of Inland Australia. New Holland Publishers (Australia) Pty Ltd

Reid, N., Hill, S. M., Lewis, D. M., (2009). Biogeochemical expression of buried Au-mineralisation in semi-arid northern Australia: Penetration of transported cover at the Titania Gold Prospect, Tanami Desert Australia. Geochemistry: Exploration, Environment, Analysis **9**, 267-273.

Forming an artificial soil from waste materials for mine site rehabilitation

Mohan Yellishetty[1], Vanessa Wong[2], Michael Taylor[1], Johnson Li[1],

[1]Division of Mining and Resources Engineering, Department of Civil Engineering, Monash University, Wellington Rd, Clayton VIC 3800
[2]School of Geography and Environmental Science, Monash University, Wellington Rd, Clayton VIC 3800

Introduction

Surface mining activities of brown coal in the La Trobe Valley often produce large volumes of solid waste which requires the removal of significant quantities of overburden. This waste material can contain significant amounts of sulfide minerals such as pyrite, which produces sulfuric acid following oxidation, commonly known as acid mine drainage (AMD; Evangelou and Zhang 1995). Acid generation lowers the pH of sediment and water and can mobilise large quantities of trace metals (Elders 2001; Taylor et al. 2013). As mines expand, larger volumes of waste rock need to be moved which also require extensive areas for their safe disposal and containment. The erosion of these dumps may result in landform instability, which, in turn, may result in further exposure of sulfidic materials, mobilisation of trace metals, elevated sediment delivery to adjacent waterways, and the subsequent degradation of downstream water quality.

The Yallourn Brown Coal Mine is an open cut mine with approximately 18 000 000 t of high moisture brown coal mined annually. This results in roughly 6 000 000 m^3 of overburden being removed and displaced annually to expose the extractable coal. The area of influence, including the Power Station, mine and buffer zones, covers approximately 5500 ha. In addition to large volumes of overburden, power generation also produces alkaline combined ash (CA). Therefore, there is a substantial volume of waste material produced and a large area to rehabilitate. However, the brown coal mines of the La Trobe Valley do not have sufficient natural soil suitable for progressive rehabilitation following mining activities. Furthermore, the low soil pH, high trace metal concentrations and low nutrient concentrations poses a serious challenge for successful site remediation for vegetation establishment and growth.

There are a number of industries located in close proximity in the La Trobe Valley in addition to Yallourn Mine. Gippsland Soil and Water Organic Recycling Facility (SORF) receive and treat domestic and industrial wastewater and other solid and liquid wastes. Waste material from the SORF is processed to form a high quality compost which is compliant with Australian standards.

Regulations for deposition of material in to landfill are becoming increasingly more stringent with increasingly higher associated costs. Therefore, the reuse of waste materials from industrial processes is becoming increasingly more important. This paper presents results from two pilot studies which aimed to create artificial soils from waste materials derived from mining, power generation and wastewater industries with sufficient buffering capacity to remediate acidity, and with sufficient nutrients for plant establishment and growth.

Methods

Twelve (grab) samples of the raw materials (overburden (OB) waste from brown coal mines, power station Combined Ash (CA), brown coal (BC) and composted sewage sludge (SS)) were oven-dried to determine the moisture content. To determine the appropriate mixing ratios for each waste stream, Acid Neutralisation Capacity (ANC) and Net Acid Generation (NAG) were determined. The Net Acid Producing Potential (NAPP) of each sample was calculated based on the ANC and NAG results. An estimated mixing ratio was estimated from the NAPP results, which was then used to form a range of artificial soils. Compost was treated as an additive.

The artificial soils were formed by combining OB waste from brown coal mines, power station CA, BC and composted SS to assess the potential for plant growth in a pot trial. These were combined according to the following ratios (dry mass): 1 part OB, 1.23 part CA, with 3 ratios of composted sludge (0.5, 1 and 1.5) and 3 ratios of brown coal (0.5, 1 and 1.5) in a factorial design. The artificial soils were termed according to the following ratios:

- AF1/1 – SS (0.5):BC (0.5):OB (1):CA (1.23)
- AF2/1 – SS (0.5):BC (1):OB (1):CA (1.23)
- AF3/1 – SS (0.5):BC (1.5):OB (1):CA (1.23)

- AF1/2 – SS (1):BC (0.5):OB (1) CA (1.23)
- AF2/2 – SS (1):BC (1):OB (1):CA (1.23)
- AF3/2 – SS (1):BC (1.5):OB (1):CA (1.23)
- AF1/3 – SS (1.5):BC (0.5):OB (1):CA (1.23)
- AF2/3 – SS (1.5):BC (1):OB (1) CA (1.23)
- AF3/3 – SS (1.5):BC (1.5):OB (1):CA (1.23)

Approximately 50 g of Rye grass seed, available from local nurseries, was sown in to each pot to assess the suitability for vegetative growth over a six week period. The plots were watered with 450 mL every day. Water was not applied following rainfall to avoid the excessive leaching of nutrients in the test plots. The height of the grass was measured weekly over a period of 6 weeks.

The pH was determined in duplicate for each raw material and mixture in a 1:1 extract at the end of the experimental period. The electrical conductivity (EC) of each raw material and mixture was also determined in duplicate in a 1:5 soil to water suspension. Particle size analysis was undertaken using the hydrometer method and Atterberg limits were also determined (data not shown).

Results and Discussion

The combination of solid waste, sourced from mines, which are frequently nutrient poor and acidic, with nutrient-rich composted material produced from sewage treatment and alkaline combined ash has the potential to lead to a soil suitable for mine rehabilitation and successful seed germination and plant growth.

We found that pH generally increased in the artificial soil mixtures (Table 1) and was able to support plant establishment compared to the OB and BC. EC also increased in the artificial soil mixtures relative to the OB with the addition of the other waste streams (Table 1).

Table 1. pH and EC of the raw waste materials and artificial soils

Sample	pH	EC (mS/cm)
CA	8.30	0.33
OB	6.50	0.01
SORF	6.92	1.11
BC	3.51	0.18
AF1/1	7.32	0.78
AF2/1	7.28	0.85
AF3/1	6.77	0.96
AF2/1	7.19	1.11
AF2/2	6.88	1.40
AF2/3	7.07	1.14
AF3/1	7.13	1.08
AF3/2	6.74	1.19
AF3/3	6.43	0.85

Plant growth was greatest in those soils with the greatest proportion of compost, most likely due to the higher nutrient concentration provided by the compos (Figure 1). These pot trials suggest that the use of different waste streams to form an artificial soil can potentially be used in mine site rehabilitation where there is a nutrient-rich source of waste.

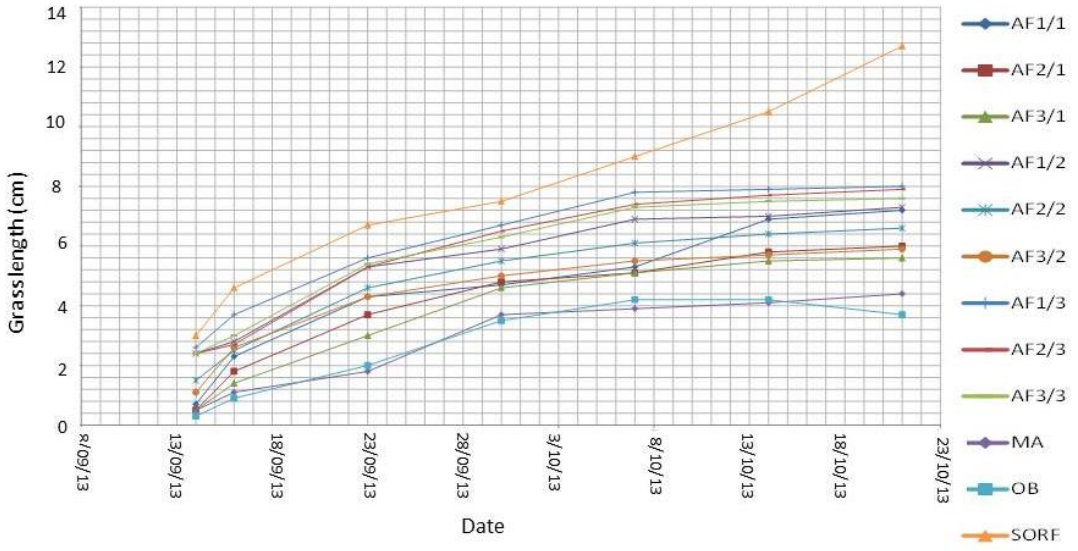

Figure 1: Grass growth in each artificial soil and raw waste material over 6 weeks.

Conclusions

A range of mixtures of OB, CA, SS and BC were created, which beneficially altered soil characteristics such as pH, EC and plant growth. In many cases, the highly acidic soils that originally could not support vegetation were successfully remediated. Although all samples supported grass growth, a number of issues were identified requiring further consideration. Leachate from mixtures showed an increase in EC, which may indicate potential leaching issues when used in the environment. This illustrates the great variability in overburden composition throughout an OB dump and needs to be considered when creating artificial soils on a large scale.

Further studies are required to characterise the waste materials and artificial soils in greater detail. An understanding of the geochemical properties and nutrient concentrations of each waste stream will assist in creating an optimal artificial soil which is physically stable and can support plant growth for a resilient ecosystem in the longer term.

References

ELDERS, JA (2001) Hydrogeochemical and Geophysical Investigations into the Environmental Impact of the Overburden Pile at Loy Yang Coal Mine, Australia, Monash University, Clayton.

EVANGELOU VP and ZHANG YL (1995) A Review - Pyrite Oxidation Mechanisms and Acid-Mine Drainage Prevention. *Critical Reviews in Environmental Science and Technology*, 25. 141-199

TAYLOR M, YELLISHETTY M and PANTHER B (2013) Geotechnical and hydrogeological evaluation of artificial soils to remediate acid mine drainage and improve mine rehabilitation – an Australian case study. In Proceedings of the 22nd MPES conference, C Drebenstedt and R Singhal (Eds), pp. 855-865.

Author Index